Desease models in vertebrates : from hypoxia to cancer

Santos Marques, I.J. dos

DISEASE MODELS IN VERTEBRATES:

FROM HYPOXIA TO CANCER

Inês João dos Santos Marques

Cover: fli1(egfp) zebrafish larva (5dpf)

Layout: Ines Marques

Printed by: GVO drukkers & vormgevers B.V. | Ponsen & Looijen

Disease Models in Vertebrates: From Hypoxia to Cancer

PROEFSCHRIFT

ter verkrijging van

de graad van Doctor aan de Universiteit Leiden,

op gezag van Rector Magnificus prof. mr.

volgens besluit van het College voor Promoties

te verdedigen op woensdag 29 Juni 2011

klokke 11:15 uur

door

Inês João dos Santos Marques

geboren te Lisboa, Portugal

in 1980

Promotiecomissie

Promotors:	Prof. Dr. Michael K. Richardson
	Prof. Dr. Herman P. Spaink
Overige leden:	Prof. Dr. Carol J. ten Cate
	Prof. Dr. Jeroen den Hertog
	Prof. Dr. Bob van de Water
	Dr. André Ribeiro (Tampere University of Technology, Finland

The work described in this thesis was supported by a grant from the Portuguese Foundation for Science and Technology (FCT), reference SFRH/BD/27262/2006, financed by the POHP-QREN- tipology 4.1- Advanced Formation, and co-funded by the European Social Fund and national funds from the MCTES

Para os homens da minha vida:

João, Miguel e Tomás

Contents

CHAPTER 1 GENERAL INTRODUCTION AND THESIS OUTLINE 9

CHAPTER 2 TRANSCRIPTOME ANALYSIS OF THE RESPONSE TO CHRONIC CONSTANT HYPOXIA (CCH) IN ZEBRAFISH HEARTS 33

CHAPTER 3 METASTATIC BEHAVIOR OF PRIMARY HUMAN TUMORS IN A ZEBRAFISH XENOTRANSPLANTATION MODEL 79

CHAPTER 4 RETINOIC ACID RECEPTOR (RAR) ANTAGONISTS INHIBIT MIR-10A EXPRESSION AND BLOCK METASTATIC BEHAVIOR OF PANCREATIC CANCER 113

CHAPTER 5 SUMMARY AND DISCUSSION 145

CHAPTER 6 SAMMENVATING 153

PUBLICATIONS AND CURRICULUM VITAE 161

CHAPTER 1

GENERAL INTRODUCTION AND THESIS OUTLINE

Cancer is probably the biggest epidemic of the 21st century (Figure 1). Despite considerable resources spent on cancer research and the better and marked improvement of cancer therapies, cancer is still one of the leading causes of death worldwide. According to the World Health Organization (WHO), cancer-associated mortality is predicted to continue rising, with an estimated 12 million yearly deaths by 2030 (WHO, 2011). Lifestyle changes and early detection are still the best way to prevent and treat cancer.

In 2000, Hanahan and Weinberg foresaw that a more logical approach should be followed in cancer research, in order to better understand the complexities of the disease in terms of a small number of underlying principles. In their review article they summarized the six alterations that most, if not all, cancers must have undergone (Figure 2): the ability to control its own growth (self-sufficiency of growth signals); resistance to anti-growth signals; evasion of programed cell-death (no apoptosis); unlimited replication; the ability to form new blood vessels around it, (angiogenesis); the ability to invade other tissues and metastasize to different areas of the body (Hanahan, et al., 2000). Nonetheless, metastasis is a very complex process in which primary tumor cells must first invade the neighboring tissues; then intravasate into the circulation; translocate through the vasculature until they arrest in distant capillaries; extravasate into the perivasculature; and finally proliferate from micrometastasis into macroscopic secondary tumors (Fidler, 2003). And, in order for us to fight this deadliest aspect of cancer, we must understand and find a way to prevent each of the steps required for a cancer to metastasize.

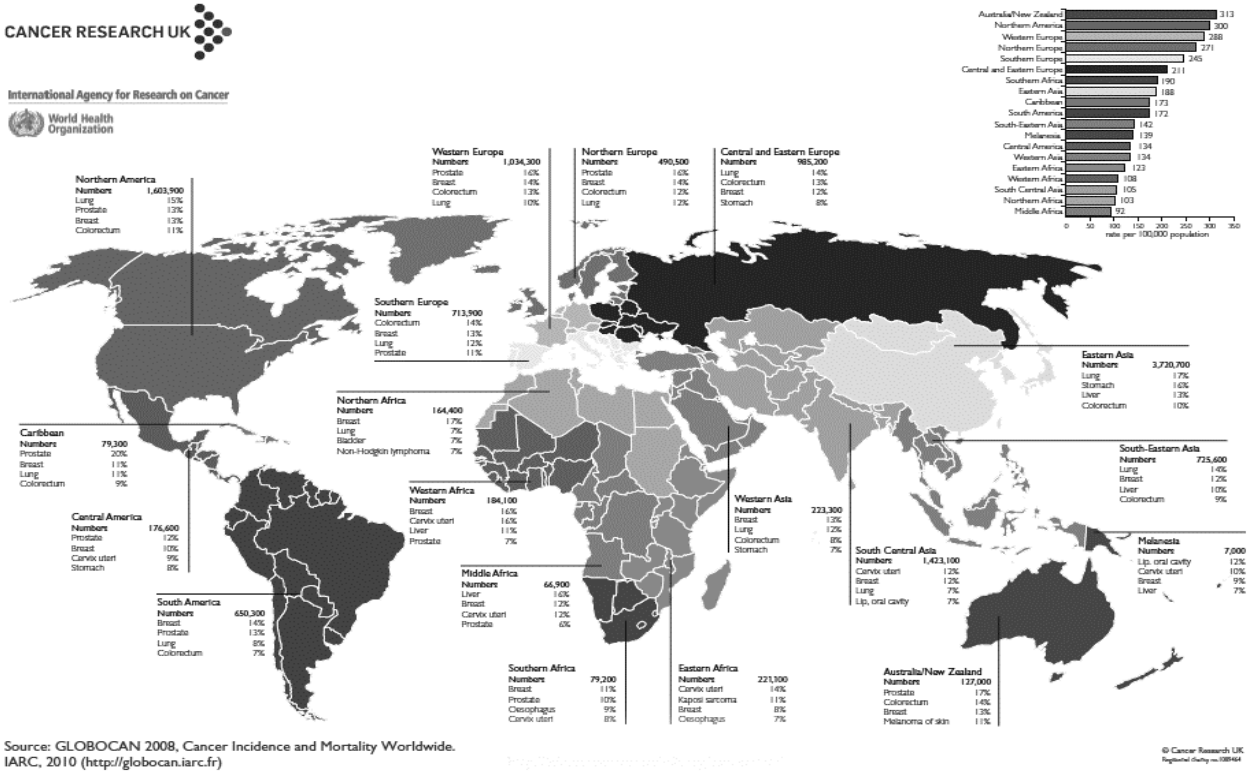

Figure 1 Cancer Incidence Worldwide: this map illustrates cancer incidence worldwide, standardized by age and the most commonly diagnosed cancers. (Source: GLOBOCAN 2008 (Cancer Research UK).)

Nowadays pancreatic cancer is considered one of the deadliest forms of cancer. Patients diagnosed with this type of cancer have usually a very poor prognosis, mainly due to the late detection of the tumor. This delay in diagnosis is largely attributable to the absence of symptoms and early stages of the disease can often be mistaken for chronic pancreatitis. Additionally, resistance to conventional treatments, like chemotherapy and radiation, also contributes to the high mortality rate. Survival after diagnosis is usually three to six months, and the 5-year survival is only 5% (WHO, 2011). The best way to increase early detection of pancreatic cancer is to find specific biomarkers for this type of cancer, which still do not exist. Novel biomarkers should be able to distinguish between chronic pancreatitis and pancreatic cancer. A review of literature reveals several other biomarkers that can be used to identify pancreatic cancer in early stages (Tanase, et al., 2010)

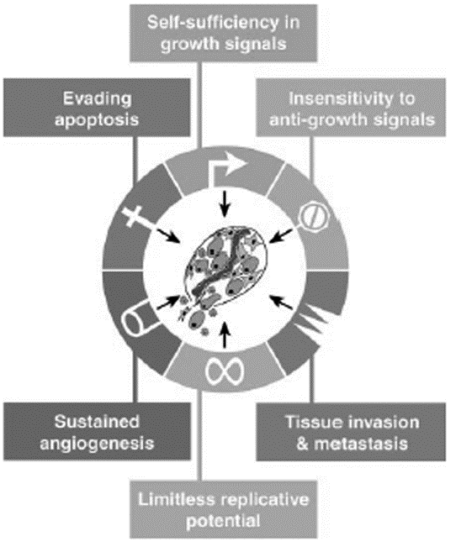

Figure 2 Summary of the mutations a normal cell must undergo in order to become a cancer cell (Hanahan, et al., 2000)

The Zebrafish as a vertebrate disease model

The use of zebrafish as a model system is first mentioned in the literature in 1958, (coincidentally this was in the context of cancer research). KK Hisaoka (1958) describes the effects of the carcinogen 2-acetylaminofluorene in the embryonic development of the zebrafish. Since then it has been mentioned in over thirteen thousand articles. Although evolution has placed some distance between humans and zebrafish, many signaling pathways have been conserved. These include pathways involved in development, proliferation, cell movements, apoptosis, etc. (Amatruda, et al., 2008), as well as, cell-cycle genes, tumor suppressor genes and oncogenes (Amatruda, et al., 2002). The low maintenance costs, fecundity, transparency of the embryos and fast development make the zebrafish a very versatile animal model that can be used in a broad array of research studies. Also, the genetic manipulation to create fish lines with specific genetic characteristics, such as the fli1::egfp line that develops GFP-labeled vasculature (Lawson, et al., 2002) or the *casper* line which is characterized by transparent adult fish (White, et al., 2008), makes it a very amenable model for developmental and cancer studies. Zebrafish are also very easy to use in forward genetic screening and reverse genetics techniques, such as morpholino injections (inhibitory of mRNA translation). Furthermore, they have a developed innate and adaptive immune system (the last one appearing only in later stages of development, around 4-6 weeks). The late development of adaptive immunity has allowed us to carry out successful xenotransplantation experiments of human pancreatic cancer cells and implantation of primary tumor tissue, in embryonic stages (Chapter 3 of this thesis).

The zebrafish was the first fish model to be used for carcinogenesis studies (Stanton, 1965). In his research Stanton describes how he chemically induced

hepatic degeneration and neoplasia in the zebrafish. In the last decade several advances were made in the cancer research field using this model. In 2000 Spitsbergen demonstrated that the zebrafish responds in a similar way to mammals to carcinogens, and develop tumors that are histopathologically similar to their human counterparts (Spitsbergen, et al., 2000a; Spitsbergen, et al., 2000b). Subsequently Lee *et al* (2005) and Topczewska *et al* (2006) showed that human tumor cells can be easily injected into zebrafish embryos and survive through to adulthood. Since then, several xenotransplantation studies of human and mouse tumors into zebrafish embryos and larvae have been published, proving that these cells were able to proliferate, invade and form tumor masses in zebrafish embryos (Lee, et al., 2006; Nicoli, et al., 2007; Stoletov, et al., 2007; Hendrix, et al., 2007). The use of zebrafish allows for a very simple monitoring of cancer formation and progression. They also allow fast genetic screening as well as rapid tests to evaluate new anti-cancer drugs and small molecule compounds that selectively target tumor tissue and cells (L.I., et al., 2005; den Hertog, 2005; Kari, et al., 2007; Lally, et al., 2007; Geiger, et al., 2008). The incorporation of such compounds into the zebrafish is done simply by adding them to the water where the embryos are swimming, so that they are absorbed by the organism through the skin or ingested.

In conclusion, the use of the zebrafish in cancer research is a major catch, presenting a number of advantages over the mouse model. For example, it avoids time-consuming transplantation studies, which require large numbers of cells, and which require the sacrifice of the animal; it also allows cancer formation and development to be followed *in vivo.* Finally, it provides a rapid screen for new anti-cancer therapies.

From hypoxia to cancer

Hypoxia, or a low level of oxygen, has been recognized as playing a key role in several cellular physiological processes, from cell proliferation, to cell survival, angiogenesis, metabolism and tumor progression and metastasis. Hypoxia can be divided into acute and chronic hypoxia. The acute variant is usually caused by a temporary disruption to the blood flow and does not last long. On the other hand chronic hypoxia is durable and can have lasting effects (Dewhirst, 1998).

Besides the epigenetic, genetic and somatic changes that occur in cancer, it is also important to understand the tumor microenvironment, since it may also play a significant role in tumor progression and metastasis and influence the response to conventional cancer treatments, like chemo- and radiotherapy. One of the micro environmental stresses that play a role in cancer is hypoxia. Hypoxic cells have been shown to be more resistant to radiotherapy and chemotherapy, and they usually originate more unstable and aggressive phenotypes (Rademakers, et al., 2008).

Adaptation of cancer cells to low oxygen levels has been shown to be dependent on the expression of HIF-1 (hypoxia inducible factor 1 (Semenza, et al., 1992)). HIFs are transcription factors that play a key role in the regulation of oxygen homeostasis and the response of cells to hypoxia. They are comprised of an α and a β subunit. Of the three known HIFs, HIF-1 has been recognized as the main regulator of oxygen homeostasis, and it has been shown to be over-expressed in the several human cancers (Zhong, et al., 1999). Under hypoxic conditions, molecular O2 is unavailable, and HIF-1α is up regulated and dimerizes with HIF-1β. This heterodimer then migrates to the cell nucleus, where it binds to specific DNA sequences and activates the genes necessary for the adaptation of the cell to hypoxia. These genes then regulate pathways linked to cell survival (e.g. GUT-

1 – glucose transporter 1), angiogenesis (e.g. VEGF – vascular endothelial factor) and metastasis (e.g. TGF-α), which are well known to be involved in tumor development and aggressiveness (Melillo, 2006) (Figure 3).

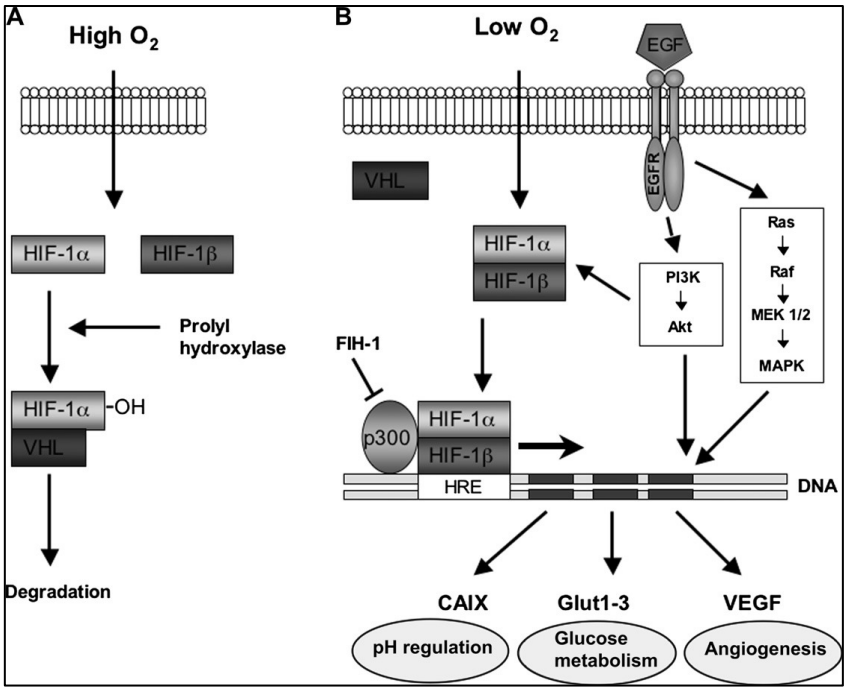

Figure 3 Schematic representation of the HIF-1 pathway. Under normoxic conditions HIF-1α is hydroxilated and rapidly degraded (A). Under hypoxia HIF-1α dimerizes with HIF-1β, becoming a stable complex, which then initiates the transcription of its target genes (adapted from (Rademakers, et al., 2008)).

Ruan and colleagues (2009) wrote a short review where they analyze how hypoxia mediates and regulates each of the hallmarks of cancer (Figure 4). Intra-tumor hypoxia has been demonstrated to be a key factor for the poor prognosis observed in several types of cancer, such as prostate, breast or cervical cancer (Chan, et al., 2007; Vaupel, et al., 2007). It occurs when cancer cells are located

at such a distance from functional blood vessels that they no longer get the necessary oxygen levels. So in order to survive the hypoxic environment, cancer cells must adapt.

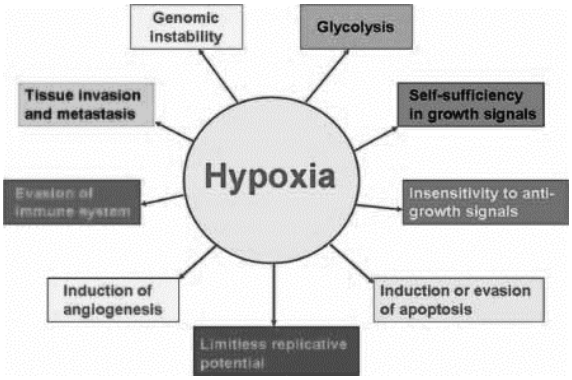

Figure 4 Role of hypoxia in the hallmarks of cancer (adapted from Ruan *et al* l., 2009)

Under hypoxia, cancer cells must first overcome anti-proliferative signals. In order to achieve this, hypoxia induces not only expression of several growth factors that promote cell proliferation (e.g. EGF, insulin, IGFs) (Maxwell, et al., 2001), but can also adapt growth-inhibitory signals. An example is the case of the PTEN gene, which regulates hypoxia and IGF-1 induced angiogenic expression. Knocking-down PTEN promotes tumor growth through the deregulation of Akt activity and HIF-1 regulated gene expression (Zundel, et al., 2000).

Secondly, hypoxic microenvironments induce apoptosis, which at least some cancer cells must avert. Tumor cells have developed several mechanisms to avoid HIF-1 mediated apoptosis. For example, in KHT cells it has been demonstrated that hypoxia up-regulates Mdm2, via the p53 pathway, and this way increases cell resistance to apoptosis (Zhang, et al., 2004). Hypoxia also mediates the selection of p53 mutant cells which have a reduced apoptotic potential (Graeber, et al., 1996).

Thirdly, hypoxic microenvironments potentiate angiogenesis which is favorable for cancer cell survival. They either directly stimulate the expression of angiogenic factors involved in the development of endothelial cells, or they induce a favorable microenvironment for endothelial cells and consequently for cancer cell survival, migration and invasion (Ruan, et al., 2009).

Hypoxia can thus be considered a very important microenvironmental factor in tumor invasion and metastasis as demonstrated by several studies (Gatenby, et al., 2007; Liao, et al., 2007; Chang, et al., 2006). Furthermore, a strong correlation between hypoxia and HIF-1 production, and consequent prolonged cell survival, has been demonstrated, suggesting the possibility of HIF-1 being targeted for a possible therapeutic strategy (Ruan, et al., 2009; Fraga, et al., 2009).

The role of microRNAs in cancer

Micro RNAs (miRNAs) are small non-coding RNAs, 20-23 nucleotides long, expressed in a tissue- and development-specific manner (Ambros, 2008). They were first identified in *Caenorhabditis elegans* where they were shown to play a role in regulating larval development (Lee, et al., 1993). Since their discovery they have been associated with the regulation of several biological functions, from cellular development, to apoptosis, metabolism, and have more recently been linked to cancer.

MicroRNAs are produced in the cell nucleus. They are excised from a primary harpin precursor RNA structure (pre-miR) which has first been transcribed from a larger Pol II primary transcript (pri-miR). Pre-miRs are then exported to the cytoplasm, where they are processed by Dicer to become the 20-23 nucleotide mature single-stranded microRNA. Finally the single-stranded miRNA is

incorporated into the RISC complex which will bind to their target mRNAs, regulating mRNA degradation and translational repression (Figure 5).

The first association of micro RNAs with cancer was made by Calin *et al* (2002). They showed that miR15 and miR16 were frequently down-regulated in more than half of the patients with B cell chronic lymphocytic leukemia. Later several more studies surfaced linking microRNAs with cancer. The majority of cancer-associated miRs have been located downstream of oncogenes and tumor suppressors that act as transcription factors; as such, miRNAs can either act as oncogenes or as tumor suppressor genes. Micro RNAs play several roles in regulating the hallmarks of cancer (Hanahan, et al., 2000) and their expression in cancer is tissue- and tumor-specific (Santarpia, et al., 2010).

First, some miRs have been shown to help cancer cells to become self-sufficient in growth signals. For example, mir-205 has been demonstrated to act as an onco-suppressor gene in breast cancer, by interfering with the proliferative pathway mediated by HER receptor family (Iorio, et al., 2009). Another study reveals that miR-210 expression progressively increased under hypoxia. This microRNA was necessary and sufficient to down-modulate the expression of Ephrin-A3, which had significant functional consequences: it affected the endothelial cell response to hypoxia, affecting cell survival, migration, and differentiation (Fasanaro, et al., 2008).

Second, cancer cells can become insensitive to antigrowth signals. There are miRs that interfere with the components that manage the transit of the cells through the G1 phase of the cell cycle. For instance, miR-34 induces cell cycle arrest in both primary and tumor-derived cell lines, in response to p53 activation, mediating G1 arrest by down regulating several cell cycle related transcripts (He, et al., 2007).

Third, some miRs also interfere in cancer cells acquired resistance to PDCD (apoptosis). For example, over-expression of miR-330 in PC-3 cells resulted in cell growth suppression by reducing E2F1-mediated Akt phosphorylation and thus inducing apoptosis (Lee, et al., 2009). In another study, miR-21 has been demonstrated to act as an anti-apoptotic factor in human glioblastoma cells, by blocking the expression of critical apoptosis-related genes (Chan, et al., 2005).

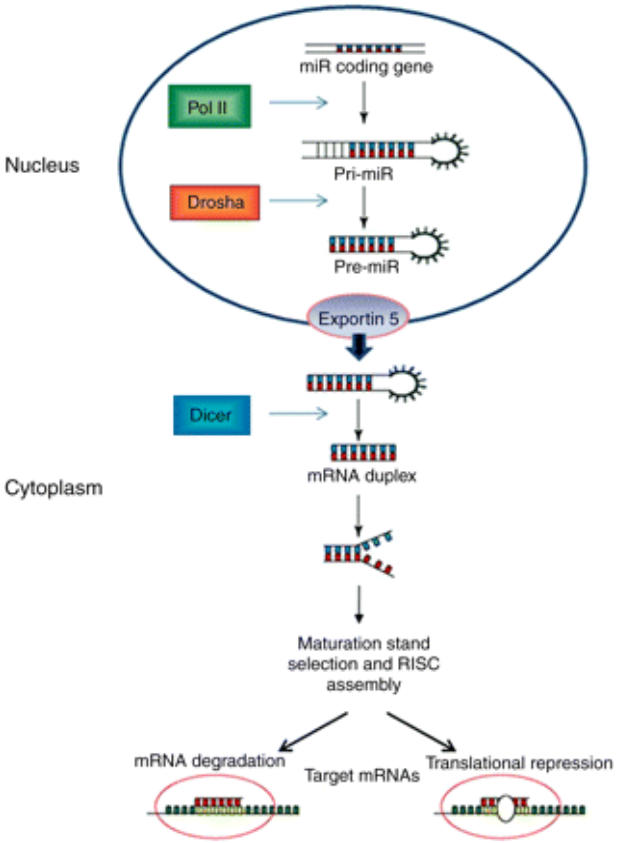

Figure 5 MicroRNA regulatory pathway (adapted from Santarpia *et al, 2010*). In the nucleus, Pol II transcribes the pri-miR from the miR coding gene, and then is processed by Drosha into the pre-miR. The pre-miR is exported from the nucleus to the cytoplasm, where Dicer processed it into the 20-23 nucleotide single-stranded, mature microRNA. Finally, the mature microRNA is incorporated into the RISC complex. This complex then recognizes the miRs multiple targets.

Fourth, miRs have been validated as playing and important role in diverting oncogene-induced senescence, thus helping cancer cells to gain a limitless replicative potential. Examples are miR-372 and miR-373 which neutralize p53-mediated CDK inhibition through suppression of LATS2, thus allowing tumorigenic growth in the presence of wild-type p53 (Voorhoeve, et al., 2006).

Finally, cancer cells must overcome the hypoxic environment that their rapid expansion causes, and also be able to invade and metastasize to distant tissues. Several miRs have been established as a key factor in tumor hypoxia. Microarray-based expression profiles revealed that there are several microRNAs that are induced in response to low oxygen, some of them via the HIF pathway, and that the vast majority of these hypoxia-induced micro RNAs are also over-expressed in human tumors (Kulshreshtha, et al., 2007). Many of these miRs play a role in the angiogenic process by, for example, regulating VEGF and other angiogenic factors under hypoxic conditions (Hua, et al., 2006). Hua *et al* (2006) used CNE cells to investigate microRNA-directed regulation of VEGF under hypoxia. They found that VEGF could be regulated by different miRs in different cells and also that VEGF was regulated by multiple miRNAs using different combinations. And, at last, numerous studies have demonstrated that the targets of the metastasis associated micro RNAs are proteins that participate in the regulation of cell motility, cell-cell adhesion and cell-matrix interactions (Santarpia, et al., 2010). One such case is micro RNA 10a (miR-10a) that, as described in chapter 4 of this thesis, by down regulating HOXB3 and HOXB4 promotes invasion and metastasis. We demonstrated that miR-10a regulates the expression of proteins of the cadherin catenin complex (Weiss, et al., 2009). The role of several other microRNAs in tumor invasion and metastasis can be red in the review written by Santarpia *et al* (2010).

Taking into consideration the different roles played by microRNAs in the hallmarks of cancer, it is only natural that miRs are currently being considered as important biomarkers for the prognosis of cancer (for instance, several studies reported that a number of miRs are upregulated in pancreatic cancer and chronic pancreatitis, as it is the case miR-10a (Weiss, et al., 2009), as well as targets for the treatment of the disease. For example, Kota *et al* (2009) established that delivering miR-26 in a mouse model of hepatocellular carcinoma reduced liver tumor size, suggesting that delivery of microRNAs that are highly expressed and tolerated in normal tissue, but absent in cancer cells might provide a strategy for miRNA replacement therapies (Kota, et al., 2009).

Conclusion

Cancer is one of the deadliest diseases of the developed world. Understanding the pathogenesis of a disease is perhaps the most effective way to prevent and treat it. To do so, we must find which genes regulate cancer and its microenvironment.

Although other animal models have a longer tradition in cancer research, the zebrafish as a vertebrate model is becoming ever more relevant for these studies. Its specific characteristics, such has transparency, fast development, gene conservation when compared to humans, makes it an ideal model to study many human diseases, including cancer. We have used this model to better understand hypoxia, a relevant aspect of the microenvironment in which tumors develop. Using also this animal model, we analyzed the role of miR-10a and developed a hypothetical model for the regulation of miR10a in pancreatic cancer

Thesis outline

Cancer is the epidemic of the 21st century. Every year sees an increase in its global health burden, but developed countries are the most affected by this disease. Stress, diet and tobacco are among the most common causes of cancer. Lifestyles factors together with late diagnosis and hereditary traits are the principle causes of cancer associated deaths. Cancer research now takes a more logical approach focusing on what mutations occur within a cell to make it a cancer cell. Which (onco-)genes are (de-)activated, and how. How are tumor suppressor genes suppressed? How do we prevent these mutations from occurring? Can we reverse these mutations? How does the cell microenvironment affect the development of a cancer? These and many other lines of investigation are nowadays followed on cancer research.

In this thesis we show that an animal model with a relatively recent history, the zebrafish, can be useful in human disease studies, more specifically for hypoxia and cancer research. In the case of hypoxia, understanding how the fish adapts and survives under low oxygen levels may prove very useful to fight human diseases caused by ischemia and low oxygen. In cancer studies the focus of our work was the case of pancreatic cancer, where we demonstrated that the zebrafish can be used as a tool to quickly determine genes involved in formation and development of this type of cancer.

Chapter 2 shows how the zebrafish is a versatile and resilient model. Not many animals can survive for long periods under constant chronic hypoxia. Our research demonstrated that zebrafish under these stressful conditions can adapt and survive. This results in the up- and down-regulation of several genes, as well as physiological and morphological changes. Understanding how organisms adapt to hypoxia can be fundamental in cancer research. Cancer cells are capable

of withstanding and surviving in very stressful conditions, including low oxygen levels. Matching genes that are regulated under hypoxia can be a new strategy to fight and cure cancer.

Chapter 3 demonstrates how the zebrafish can be used as an animal model for cancer studies. Zebrafish embryos can be obtained in large numbers and can be used for a rapid analysis of metastasis. We showed, in this publication, that human cancer cells are capable of invading new tissues and forming micro metastasis in zebrafish embryos. The quick results that we can obtain by using this model can expedite preliminary analysis of metastatic properties of cells, test gene regulation in cancer cells or evaluate potential anti-cancer drugs.

Chapter 4 is a research study on the role of retinoic acid receptors (RAR) and miR-10a in pancreatic cancer. Using the zebrafish as a model and human pancreatic cancer cells and tissue from primary pancreatic tumors we demonstrate the role of retinoic acid receptor (RAR) antagonists in pancreatic cancer. Our model proposes that retinoic acid stimulates the dimerization of retinoic acid receptors, which in turn bind to retinoic acid elements and trigger increased miR-10a expression. This up-regulation of miR-10a, in turn suppresses HoxB1 and HoxB3, promoting invasion and metastasis.

References

Amatruda, J. F., J. L. Shepard, H. M. Stern, e L. I. Zon. (2002) *Zebrafish as a Cancer Model System.* Cancer Cell; 1(3): 229-231.

Amatruda, J.F., e E.E. Patton. (2008) *Genetic Models of Cancer in Zebrafish.* International Review of Cell and Molecular Biology; 271: 1-28.

Ambros, V. (2008) *The evolution of our thinking about microRNAs.* Nature Medicine; 14(10): 1036-1040.

Calin GA, Dumitru CD, Shimizu M, Bichi R, Zupo S, Noch E, Aldler H, Rattan S, Keating M, Rai K, Rassenti L, Kipps T, Negrini M, Bullrich F, Croce CM. *Frequent deletions and down-regulation of micro- RNA genes miR15 and miR16 at 13q14 in chronic lymphocytic leukemia.* Proceedings of the National Academy of Sciences of the United Sattes of America; 99(24): 15524-15529.

Cancer Research UK.

http://info.cancerresearchuk.org/cancerstats/world/commoncancers/index.htm. s.d.

Chan JA, Krichevsky AM, Kosik KS. (2005) *MicroRNA-21 is an antiapoptotic factor in human glioblastoma cells.* Cancer Research; 65(14): 6029-6033.

Chan, N., M. Milosevic, e R. G. Bristow. (2007) *Tumor hypoxia, DNA repair and prostate cancer progression: new targets and new therapies.* Future Oncology; 3(3): 329-341.

Chang, Q., R. Qin, T. Huang, J. Gao, e Y. Feng. (2006) *Effect of antisense hypoxia-inducible factor 1alpha on progression, metastasis, and chemosensitivity of pancreatic cancer.* Pancreas; 32: 297-305.

den Hertog, J. (2005)*Chemical Genetics: Drug Screens in Zebrafish*. Bioscience Reports; 25(5): 289-297.

Dewhirst, M.W. (1998) *Concepts of oxygen transport at the.* Seminars in Radiation Oncology; 8(3): 143-150.

Fasanaro P, D'Alessandra Y, Di Stefano V, Melchionna R, Romani S, Pompilio G, Capogrossi MC, Martelli F. (2008) *MicroRNA-210 modulates endothelial cell response to hypoxia and inhibits the receptor tyrosine kinase ligand Ephrin-A3.* Journal of Biochemical Chemistry; 283(23): 15878-15883.

Fidler, I. J. (2003) *The pathogenesis of cancer metastasis: the 'seed and soil' hypothesis revisited.* Nature Reviews: Cancer; 3(6): 453-458.

Fraga, A., R. Ribeiro, e R. Medeiros. (2009) *Tumour hypoxia. The role of HIF.* Actas Urologicas Espanolas; 33(9): 941-951.

Gatenby, R. A.; Smallbone, K.; Maini, P. K.; Rose, F.; Averill, J.; Nagle, R. B.; Worrall, L.; Gillies, R. J. (2007) *Cellular adaptations to hypoxia and acidosis during somatic evolution of breast cancer.* British Journal of Cancer; 97: 646-653.

Geiger, G. A., W. Fu, e G. D. Kao. (2008) *Temozolomide-mediated radiosensitization of human glioma cells in a zebrafish embryonic system.* Cancer research; 68(9): 3396-3404.

Graeber TG, Osmanian C, Jacks T, Housman DE, Koch CJ, Lowe SW, Giaccia AJ. (1996) *Hypoxia-mediated selection of cells with diminished apoptotic potential in solid tumours.* Nature; 379: 88-91.

Hanahan, D., e R. A. Weinberg. (2000) *The Hallmarks of Cancer.* Cell; 100: 57-70.

He L, He X, Lim LP, de Stanchina E, Xuan Z, Liang Y, Xue W, Zender L, Magnus J, Ridzon D, Jackson AL, Linsley PS, Chen C, Lowe SW, Cleary MA, Hannon GJ. (2007) *A microRNA component of the p53 tumour suppressor network.* Nature; 447(7148): 1130-1134.

Hendrix, M. J. C., E. A. Seftor, R. E. B. Seftor, J. Kasemeier-Kulesa, P.M. Kulesa, e L-M. Postovit. (2007) *Reprogramming metastatic tumour cells with embryonic microenvironments.* Nature Reviews: Cancer; 7(4): 246-255.

Hisaoka, K. K. (1958) *The effects of 4-acetylaminofluorene on the embryonic development of the zebrafish. I. Morphological studies.* Cancer Research; 18(5): 527-535.

Hua Z, Lv Q, Ye W, Wong CK, Cai G, Gu D, Ji Y, Zhao C, Wang J, Yang BB, Zhang Y. (2006) *MiRNA-directed regulation of VEGF and other angiogenic factors under hypoxia.* PLoS One; 27(1): e116.

Iorio MV, Casalini P, Piovan C, Di Leva G, Merlo A, Triulzi T, Ménard S, Croce CM, Tagliabue E. (2009) *microRNA-205 regulates HER3 in human breast cancer.* Cancer Research; 69, n.º 6: 2195-2200.

Kari G, Rodeck U, Dicker AP. (2007) *Zebrafish: An Emerging Model System for Human Disease and Drug Discovery.* Clinical Pharmacological Therapies; 82(1): 70-80.

Kota J, Chivukula RR, O'Donnell KA, Wentzel EA, Montgomery CL, Hwang HW, Chang TC, Vivekanandan P, Torbenson M, Clark KR, Mendell JR, Mendell JT. (2009) *Therapeutic microRNA delivery suppresses tumorigenesis in a murine liver cancer model.* Cell; 137(6): 1005-1017.

Kulshreshtha R, Ferracin M, Wojcik SE, Garzon R, Alder H, Agosto-Perez FJ, Davuluri R, Liu CG, Croce CM, Negrini M, Calin GA, Ivan M. (2007) *A microRNA signature of hypoxia.* Molecular and Cellular Biology; 27(5): 1859-1867.

Lally BE, Geiger GA, Kridel S, Arcury-Quandt AE, Robbins ME, Kock ND, Wheeler K, Peddi P, Georgakilas A, Kao GD, Koumenis C. (2007) Identification and biological evaluation of a novel and potent small molecule radiation sensitizer via an unbiased screen of a chemical library. Cancer Research; 67(18): 8791-8799.

Lawson, N. D., e B. M. Weinstein. (2002) *In Vivo Imaging of Embryonic Vascular Development Using Transgenic Zebrafish.* Developmental Biology; 248(2): 307-318.

Lee KH, Chen YL, Yeh SD, Hsiao M, Lin JT, Goan YG, Lu PJ. (2009).*MicroRNA-330 acts as tumor suppressor and induces apoptosis of prostate cancer cells through E2F1-mediated suppression of Akt phosphorylation.* Oncogene*;* 28(38): *3360-3370*

Lee RC, Feinbaum RL, Ambros V. (1993) *The C. elegans heterochronic gene lin-4 encodes small RNAs with antisense complementarity to lin-14.* Cell; 75(5): 843-854.

Lee, J. T., e M. Herlyn. (2006) *Embryogenesis meets tumorigenesis.* Nature Medicine; 12(8): 882-884.

Lee, L. M., E. A. Seftor, G. Bonde, R. A. Cornell, e M. J. Hendrix. (2005) *The fate of human malignant melanoma cells transplanted into zebrafish embryos: Assessment of migration and cell division in the absence of tumor formation.* Developmental Dynamics; 233(4): 1560-1570.

Liao, D., C. Corle, T. N. Seagroves, e R.S. Johnson. (2007) *Hypoxia-inducible factor-1alpha is a key regulator of metastasis in a transgenic model of cancer initiation and progression.* Cancer Research; 67: 563-572.

Maxwell, P. H., C. W. Pugh, e P. J. Ratcliffe. (2001) *Activation of the HIF pathway in cancer.* Current Opinion in Genetics Development; 11: 293-299.

Melillo, G. (2006) *Inhibiting hypoxia inducible factor 1 for cancer therapy.* Molecular Cancer Research; 4: 601-605.

Nicoli, S., i D. Ribatt, F. Cotelli, e M. Presta. (2007) *Mammalian tumor xenografts induce neovascularization in zebrafish embryos.* Cancer Research; 67(7): 2927-2931.

Rademakers, S.E., P. N. Span, J.H. Kaanders, F. C. Sweep, A.J. van der Kogel, e J. Bussink. (2008) *Molecular aspects of tumour hypoxia.* Molecular Oncology; 2(1): 41-53.

Ruan, K., G. Song, e G. Ouyang. (2009) *Role of hypoxia in the hallmarks of human cancer.* Journal of Cellular Biochemistry; 107(6): 1053-1062.

Santarpia L, Nicoloso M, Calin GA. (2010) *MicroRNAs: a complex regulatory network drives the acquisition of malignant cell phenotype.* Endocrine-related Cancer; 17(1): F51-F75.

Semenza, G. L., e G. L. Wang. (1992) *A nuclear factor induced by hypoxia via de novo protein.* Molecular Cell Biology; 12: 5447-5454.

Spitsbergen, J. M.; Tsai, H. W.; Reddy, A.; Miller, T.; Arbogast, D.; Hendricks, J. D.; Bailey, G. S. (2000a) *Neoplasia in zebrafish (Danio rerio) treated with 7,12-dimethylbenz [a]anthracene by two exposure routes at different developmental stages.* Toxicological Pathology; 28(5): 705-715.

Spitsbergen, J. M.; Tsai, H. W.; Reddy, A.; Miller, T.; Arbogast, D.; Hendricks, J. D.; Bailey, G. S. (2000b) *Neoplasia in zebrafish (Danio rerio) treated with N-methyl-Nnitro-N-nitrosoguanidine by three exposure routes at different developmental stages.* Toxicological Pathology; 28(5): 716-725.

Stanton, M. F. (1965) *Diethylnitrosamine-induced hepatic degeneration and neoplasia in the aquarium fish, Brachydanio Rerio.* Journal of the Nationall Cancer Institute; 34: 117-130.

Stoletov, K., V. Montel, R. D. Lester, S. L. Gonias, e R. Klemke. (2007) *High resolution imaging of the dynamic tumor cell vascular interface in transparent zebrafish.* Prodeedings of the National Academy of Science; 104(44): 17406-17411.

Tanase, C. P., M. Neagu, R. Albulescu, e M. E. Hinescu. (2010) *Advances in pancreatic cancer detection.* Advances in Clinical Chemistry 51: 145-180.

Topczewska, J. M., Postovit, L. M., Margaryan, N. V., Sam, A., Hess, A. R., Wheaton, W. W., Nickoloff, B. J., Topczewski, J., Hemdrix, M.J. (2006) *Embryonic and tumorigenic pathways converge via Nodal signaling: Role in melanoma aggressiveness.*" Nature Medicine; 12(8): 925-932.

Vaupel, P., e A. Mayer. (2007) *Hypoxia in cancer: significance and impact on clinical outcome.* Cancer Metastasis Reviews; 26(2): 225-239.

Voorhoeve PM, le Sage C, Schrier M, Gillis AJ, Stoop H, Nagel R, Liu YP, van Duijse J, Drost J, Griekspoor A, Zlotorynski E, Yabuta N, De Vita G, Nojima H, Looijenga LH, Agami R. (2006) *A genetic screen implicates miRNA-372 and miRNA-373 as oncogenes in testicular germ cell tumors.* Cell; 124(6): 1169-1181.

Weiss FU, Marques IJ, Woltering JM, Vlecken DH, Aghdassi A, Partecke LI, Heidecke CD, Lerch MM, Bagowski CP. (2009) *Retinoic acid receptor antagonists inhibit miR-10a expression and block metastatic behavior of pancreatic cancer.* Gastroenterology; 137(6): 2136-2145.

White, R. M.; Sessa, A.; Burke, C.; Bowman, T.; LeBlanc, J.; Ceol, C.; Bourque, C.; Dovey, M.; Goessling, W.; Burns, C. E.; Zon., L. I. (2008) *Tranparent adult zebrafish as a tool for in vivo transplantation analysis.* Cell Stem Cell; 2(2): 183-189.

WHO. *http://www.who.int/mediacentre/factsheets/fs297/en/.* s.d.

WHO. *http://www.who.int/tobacco/research/cancer/en/.* s.d.

Zhang, L., e R. P. Hill. (2004) *Hypoxia enhances metastatic efficiency by upregulating.* CANCER RESEARCH; 64: 4180-4189.

Zhong H, De Marzo AM, Laughner E, Lim M, Hilton DA, Zagzag D, Buechler P, Isaacs WB, Semenza GL, Simons JW. (1999) *Overexpression of hypoxia-inducible factor 1alpha in common human cancers and their metastases.* Cancer Research; 59: 5830-5835

Zon LI; Peterson, RT. (2005) *In vivo drug discovery in the zebrafish.* Nature Reviews: Drug Discovery; 4(1): 35-44.

Zundel W, Schindler C, Haas-Kogan D, Koong A, Kaper F, Chen E, Gottschalk AR, Ryan HE, Johnson RS, Jefferson AB, Stokoe D, Giaccia AJ. (2000) *Loss of PTEN facilitates HIF-1-mediated gene expression.* Genes and Development 14(4): 391-396.

CHAPTER 2

TRANSCRIPTOME ANALYSIS OF THE RESPONSE TO CHRONIC CONSTANT HYPOXIA (CCH) IN ZEBRAFISH HEARTS

Ines J. Marques, Jelani T. D. Leito, Herman P. Spaink, Janwillem Testerink, Richard T. Jaspers, Frans Witte, Sjoerd van den Berg and Christoph P. Bagowski

Article published in ***Journal of Comparative Physiology-Part B*** **178(1):77-92**

All supplemental material can be found online on:
http://www.ncbi.nlm.nih.gov/pmc/articles/PMC2200676/?tool=pubmed

Abstract

Insufficient blood supply during acute infarction and chronic ischemia leads to tissue hypoxia which can significantly alter gene expression patterns in the heart. In contrast to most mammals, some teleost fish are able to adapt to extremely low oxygen levels. We describe here that chronic constant hypoxia (CCH) leads to a smaller ventricular outflow tract, reduced lacunae within the central ventricular cavity and around the trabeculae and an increase in the number of cardiac myocyte nuclei per area in the hearts of two teleost species, zebrafish (*Danio rerio)* and cichlids *(Haplochromis piceatus)*. In order to identify the molecular basis for the adaptations to CCH, we profiled the gene expression changes in the hearts of adult zebrafish. We have analyzed over 15,000 different transcripts and found 376 differentially regulated genes, of which 260 genes showed increased and 116 genes decreased expression levels. Two notch receptors (notch-2 and notch-3) as well as regulatory genes linked to cell proliferation were transcriptionally upregulated in hypoxic hearts. We observed a simultaneous increase in expression of IGF-2 and IGFbp1 and upregulation of several genes important for the protection against reactive oxygen species (ROS). We have identified here many novel genes involved in the response to CCH in the heart, which may have potential clinical implications in the future.

Keywords: Hypoxia, Zebrafish, Heart, Hyperplasia, Gene expression

Introduction

Low oxygen levels (hypoxia) play important roles in clinical conditions such as stroke and heart failure. Insufficient blood supply leads to tissue hypoxia in the heart during acute infarction and chronic ischemia (Semenza, 2001).

Effective protection of the heart against ischemia/ reperfusion injury is one of the most important goals of experimental and clinical research in cardiology. Besides ischemic preconditioning as a powerful temporal protective phenomenon, adaptation to chronic hypoxia also increases cardiac tolerance to all major deleterious consequences of acute oxygen deprivation such as myocardial infarction, contractile dysfunction and ventricular arrhythmias (Kolar, *et al*., 2003).

Although many factors have been proposed to play potential roles, the detailed mechanism of this long-term protection remains poorly understood. Some of the molecular mechanisms of cardiac protection by adaptation to chronic hypoxia and chronic high-altitude hypoxia have recently been reviewed (Kolar, *et al*., 2003; Ostadal, *et al*., 2007). KATP channels, PKC*5* as well as the different MAPK pathways were shown to be involved in the mechanism of increased tolerance of chronically hypoxic hearts and further the controversial role of ROS in hypoxia tolerance are discussed (Kolar, *et al*., 2003). Furthermore, a recent study has profiled the gene expression changes induced by chronic constant hypoxia (CCH) and chronic intermittent hypoxia (CIH) in newborn mice (Fan, *et al*., 2005).

In contrast to most mammals (with the exception of some marine mammals), some teleosts, have developed the ability to withstand extreme chronic hypoxia (Stecyk, *et al*., 2004). It is assumed that these vertebrate species possess unique adaptations in order to survive short and long term oxygen deprivation.

However, the molecular basis of these adaptations in fish has so far not been extensively investigated.

Several studies have profiled gene expression changes in teleosts exposed to hypoxia. Gracey *et al.* showed in adults of the euryoxic gobiid fish *Gillichthys mirabilis* (the long-jawed mud sucker), that 5 days of hypoxia induced a complex transcriptional response, including a shutdown of energy requiring pathways including protein synthesis and locomotion, and an induction of genes needed for anaerobic ATP production in different tissues (Gracey, *et al*., 2001). Recently, we described phenotypic and behavioral adaptations to long-term hypoxia and described the gene expression changes induced by chronic constant hypoxia in the gills of adult zebrafish (van der Laarse, *et al*., 2005).

Ton *et al.* identified global gene expression changes in zebrafish embryos. Zebrafish embryos at 48 h post fertilization were exposed to water with 5% oxygen saturation for 24 h. The authors identified 138 genes responsive to short-term hypoxia and could also show that transcriptional changes indicated metabolic depression, a switch from aerobic to anaerobic metabolism and energy conservation (Ton, *et al*., 2003).

In this study, we have identified CCH-induced gene expression changes in the zebrafish heart by looking at over half of the zebrafish genome. We have compared several of these novel changes described in other species and tissues. We have here identified the heart-specific molecular adaptations to CCH. Future functional experiments are warranted to determine whether some of the findings can be used to better adapt mammalian hearts to CCH.

Material and methods

Animal handling

Adult wild-type zebrafish (*Danio rerio*) around 3 month of age, were obtained from a local pet store. Cichlids (*Haplochromis piceatus*) have been collected in the Mwanza Gulf of Lake Victoria in 1984 and were bred in our laboratory for about 20 generations. All animals were handled in compliance with animal care regulations. Our animal protocols were approved by the review board of Leiden University in accordance with the requirements of the Dutch government. Zebrafish were kept at 25°C in aquaria with day/night light cycles (12h dark vs. 12h light). Cichlids were kept at 25°C with the same day/night light cycles.

Hypoxia treatment

For gradual hypoxia treatment, oxygen levels were gradually decreased in 4 days from 100% air saturated water to 40% (day 1), 30% (day 2), 20% (day 3) and the final 10% air saturation (day 4). After day 4, the Fish were kept for an additional 21 days at 10% air saturation (at 100% air saturation and 28°C the O_2 concentration is 8mg/l and pO_2 is 15 Torr). In parallel, a control group was kept at 100% air saturated water. Both groups were kept in identical aquaria of 100l. The oxygen level on the hypoxia group was kept constant by a controller (Applikon Biotechnology, The Netherlands) connected to an O_2-electrode and solenoid valve in line with an air diffuser. The oxygen level in the tank was kept constant by adding oxygen via the diffuser and thereby compensating the oxygen consumption of the Fish. In case of immediate hypoxia exposure, tanks were pre-equilibrated to the respective pO_2 concentration and fish were then directly set in the equilibrated aquaria.

Perfusion of cichlid hearts

In order to minimize blood clotting, a perfusion protocol was developed in which the whole blood volume of clinically dead animals was initially replaced with isotonic buffer and then with a fixative solution.

Heart dissection

The fish were killed with an overdose of anesthetic (MS-222; Tricaine Methanesulfonate from Argent Chemical Laboratories, USA). Hearts were dissected from the fish immediately after the anesthetic worked. For RNA preparation the hearts were immediately shock-frozen in liquid nitrogen. For histology and microscopy, the hearts were left intact and fixed immediately in Karnovsky (1965) (Karnovsky, 1965) fixative (4% paraformaldehyde (PFA) and 2.5% glutaraldehyde in 0.1M phosphate buffer, pH 7.2) for 4 h at 4°C. After three washes in 0.1M phosphate buffer, pH7.2, they were transferred to 70% ethanol.

Histology of adult fish hearts, statistical analysis and scanning electron microscopy

Hearts from zebrafish and cichlids raised either under normoxic or hypoxic conditions, were dissected from the Fish and Fixed for 24 h in 4% PFA in PBS. After fixation, hearts were washed with 1x PBS, cut in halves (sagittal through the midline) and then dehydrated through ethanol series starting at 70% ethanol, followed by 80, 90, 96 and 100% ethanol, each step was done once for 1h except the last one which was done twice. After dehydration the hearts were embedded in increasing gradients of historesin (Technovit 7100, Heraus Kulzer, Germany) (25, 50, 75 and 100% Historesin in ethanol, for 2h at room temperature; 100% Historesin, 24h at 4°C). Afterwards the plastic with the hearts was polymerized at

40°C (overnight). Five nm sagittal sections were made using the ultramicrotome (Reichter-Jung) and a glass knife. Approximately 500 sections on each side of the midline were visually analyzed per heart (1,000 sections in total per heart). Sections were left to dry and later stained with haematoxylin–eosin staining. Pictures were taken with Axioplan 2 imaging, (Carl Zeiss, Jena). Azan staining of histological sections was done as follows. Paraffin sections of the hearts were prepared as described before (van der Meer, *et al*., 2006). Sections were incubated with Azocarmine solution, for 30min at 60°C. Afterwards they were washed in water and differentiated in 0.2% anilin alcohol. They were then rinsed in 1% acetic acid in 95% alcohol, followed by 45min incubation period, in 5% phosphotungstic acid. After that, sections were rinsed in distilled water and incubated for 45min with aniline blue. Finally, they were rinsed with distilled water, differentiated and dehydrated in 95% alcohol followed by absolute, cleared in xylene and mounted in Entallan. The protocols used here for SEM had been described before (van der Meer, *et al*., 2005). The statistical analysis of cardiac myocyte nuclei per section was done using Statistica by performing an independent *t* test. A *P* value of less than 0.05 was considered significant.

Immunohistochemistry and statistical analysis

Zebrafish raised either under normoxic or hypoxic conditions were killed with an overdose of anesthetic MS-222 and frozen in liquid nitrogen. Subsequently, transversal cross-sections (10nm thick) of the body, were cut using a cryostat at -20°C and mounted on glass slides coated with Vectabond (Vector Laboratories, Burlingame, USA). Sections were fixed in 4% formaldehyde in Tris-buffered saline (TBS; 50mM Tris and 150mM NaCl, pH 7.5) for 10 min and subsequently washed in TBS with 0.05% Tween-20 (TBST) (Sigma-Aldrich, Zwijndrecht, The

Netherlands). Subsequently, sections were incubated for 10 min with 10% normal swine serum (Vector laboratories) in TBST after which sections were incubated for 24h at 4°C with anti-phospho Akt polyclonal antibody (Santa-Cruz Biotechnology, USA) diluted 1:50 in TBST. After incubation with primary antibody, the slides were washed in TBST and subsequently placed in 0.25% (v/v) acetic anhydride in 0.1 M triethanolamine buffer (pH 8) for 10min followed by rinsing in TBST. After this, sections were incubated for 60min at 20°C with secondary anti-rabbit immunoglobulin G (IgG) antibody covalently coupled to alkaline phosphatase (Vector Laboratories) diluted 1:100 and washed in TBST. After this, sections were incubated for 5 min with alkaline phosphatase (AP) buffer (0.1M NaCl, 0.1M Tris, 50mM MgCl2 and 0.1% Tween-20, pH 9.5) followed by incubation with BM Purple AP substrate (Roche Applied Sciences, Almere, The Netherlands) for 30, 45 or 60min which was followed by rinsing in TBST. All sections were mounted in glycerin/gelatin and stored at 4°C in the dark until staining intensity was measured. The absorbance values of the BM Purple in the sections were determined using a Leica DMRB microscope (Wetzlar, Germany) fitted with calibrated gray filters using different interference filters. Absorbencies for BM Purple were determined at 550 nm. Images were recorded with a 20x objective and a Sony XC-77CE camera (Towada, Japan) connected to a LG-3 frame grabber (Scion; Frederick, MD) in an Apple Power Macintosh computer. Recorded images were analyzed with the public domain program NIH-Image V1.61 (US National Institutes of Health, available at http://rsb.info.nih.gov/nih-image/). Gray values were converted to absorbance values per pixel using the gray filters and a third-degree polynomial Wt in the calibrate option of NIH-image program. Morphometry was calibrated using a slide micrometer and the set scale option in NIH-image, taking the pixel-aspect ratio into account. An

independent *t* test was used to test for differences in phospho-Akt levels in cardiac myocytes of normoxic and hypoxic fish. A *P* value of less than 0.05 was considered significant. Values are means ± S.E.M.

RNA preparation and biological sampling

After dissection hearts were homogenized in a Dounce homogenizer using 1ml Trizol solution (GibcoBrl, Life technologies). The whole heart was used and for each biological sample hearts were pooled from five different animals. After Trizol extraction, total RNA was further purified using RNA easy columns (Qiagen). RNA samples were analyzed for quality control by Lab-on-a-chip analysis (Agilent) and on agarose gels. For the array experiment five arrays were done for normoxic and 5 arrays for the hypoxic condition. Biological samples (BS) came from two independent experiments and one technical replicate (TR) was included (2BS + 2BS + TR for normoxia and 2BS + 2BS + TR for hypoxia). As mentioned above for each BS, hearts from five different animals were pooled.

Microarray analysis

The Affymetrix GeneChip® Zebrafish Genome Arrays containing 15,509 *Danio rerio* gene transcripts were used. Probe sets on the arrays were designed with 16 oligonucleotide pairs to detect each transcript and procedures were in full support of MIAME standards. Labeling and microarray hybridization were performed by ServiceXS (Leiden, The Netherlands), including prior a standard round of RNA amplification according to standard Affymetrix protocols. The criteria used for differential expression were greater or equal than 2-fold induced or reduced and $P<0.02$. Data analysis was done using Rosetta Resolver. All expression data was submitted to the NCBI Gene Expression Omnibus

(http://www.ncbi.nlm.nih.gov/geo). The series entry number is GSE4989 and the following 10 accession numbers were assigned: GSM112796 and GSM112798-GSM112806. A complete list of differential regulated genes is shown in Supplemental Table 1.

Gene ontology analysis

The Gene ontology analysis was performed using eGOn and the database of the Norwegian Microarray Consortium (http://www.genetools.microarray.ntnu.no/egon/) and the most recent updated Unigene numbers for zebrafish (May 2007). 13414 Unigene numbers were annotated to the Affymetrix gene chip used. eGOn Enrichment analysis was used for the entire Affymetrix set versus the identified 376 gene set based on the new Unigene numbers. A master target test was performed (using Fishers exact test) and the cut off for positives was set to $P<0.05$. The available three categories, molecular function, biological process and cellular component were all tested and are shown in this dataset (Supplemental Data 1). The fold enrichment was based on the percentage found within the differentially expressed genes divided by the percentage on the total chip. A list of all Unigene numbers found in the different categories is given in Supplemental Data 2.

Real-time quantitative RT-PCR

For verification of gene expression data, we used quantitative real-time RT-PCR. Biological RNA samples were obtained from a third independent experiment and as mentioned above for the microarrays, for each BS hearts from five different animals were pooled. The Roche Master SYBR Green kit was used for the RT-PCR reactions. The annealing and synthesis temperature was 55°C alternating with

96°C for 45 cycles. Dissociation protocols were used to measure melting curves and control for unspecific signals from the primers. A measure of 100 ng of total RNA was used per reaction. A standard curve for *fl*-actin using 1, 5, 10, 100 and 500 ng of total RNA was used for normalization. Samples were measured in the Roche LightCycler. The primer3 software (http://frodo.wi.mit.edu/cgi-bin/primer3/primer3_www.cgi) was used to design primers for short amplicons between 50 and 100 bases. The primers used are shown in Supplemental Table 2.

Results

We describe here the survival rates of adult zebrafish upon immediate and gradual exposure to different pO_2 concentrations. Immediate exposure to pO_2 of 15Torr (O_2 concentration of 0.8mg/l or 10% air saturated water) was lethal for the adult zebrafish and none survived for longer than 72h (Figure 1). If lowered gradually (see experimental procedures for regimen in section "Hypoxia treatment") zebrafish were able to grow and gain weight at O_2 levels of 10% air saturation. The zebrafish were able to survive for longer than 6 months and no mortality was observed, demonstrating that they can well adapt to these conditions (data not shown). For the experiments with zebrafish and cichlids, the pO_2 concentration was gradually lowered to 10% air saturation (0.8mg/l) (see "Material and methods") and fish were kept under 10% air saturation for 3 weeks. Control groups were always kept in parallel under normoxic conditions.

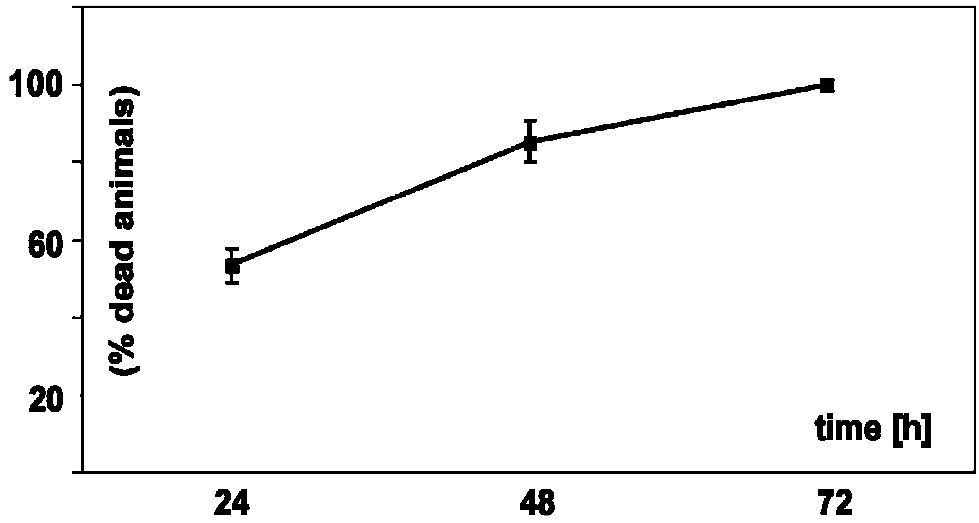

Figure 1 Survival of zebrafish embryos after immediate exposure to hypoxia. Zebrafish were immediately exposed to hypoxia (15Torr; 0.8mg/ml; 10% air saturated water). Results are derived from three independent experiments with n=30 in each experiment (adding to a total of 90 fish tested). After 24, 48 and 72h, dead and alive fish were counted. Shown here is the percentage of dead fish at the respective time points and the standard deviation. At 24h 53.3 %(±4.4) of fish were dead, at 48 hours 85.3% (±5.1) and at 72h 100% (±0). Control groups (n = 30), which were in parallel exposed to normoxic conditions showed no mortality (not shown). None of the zebrafish survived the immediate exposure to an O_2 concentration of 0.8mg/l (10% air saturation) over the 3-day period. In contrast, fish gradually exposed to hypoxia showed no induced mortality for even the 25 day time periods used in our experiments

Phenotypic changes in the heart of adult teleosts under chronic constant hypoxia (CCH)

In comparison to the normoxic control groups, we observed a significantly smaller ventricular outflow tract and reduced lacunae within the central ventricular cavity and reduced lacunae around the trabeculae in midline sections of hearts of both zebrafish (*Danio rerio*) (Figure 2a) and cichlids (*Haplochromis piceatus*) (Figure 2b) exposed to CCH. In addition to the midline sections, none of the sections investigated from hypoxia treated fishes showed a ventricular outflow tract in comparable size to the normoxic controls (data not shown). In addition to the midline sections, none of the lateral sections (to both sides of the midline) investigated from hypoxia treated fishes showed a ventricular outflow tract as well as lacunae in a comparable size to the normoxic controls (data not shown). The larger cichlid hearts were also perfused and midline sectioned and showed similar results with a smaller ventricular outflow tract and reduced lacunae (Figure 2b-H). This might represent ventricular hypertrophy or hyperplasia in both walls and trabeculae, which could lead to the observed cavity obliteration in these sections. We quantified the number of cardiac myocyte nuclei per area in the midline sections of both zebrafish and cichlids under normoxic, as well as hypoxic conditions. A significant difference in both species was observed and showed that hypoxia led to a 1.4- and 1.6-fold increase in the number of cardiac myocyte nuclei per area in zebrafish and cichlid hearts, respectively (Table 1).

Table 1 Statistical analysis of histological sections (5 µm) from zebrafish (*Danio rerio*) and cichlid (*Haplochromis piceatus*) hearts

Number of cardiomyocytes nuclei per section				
	Zebrafish (nuclei per 900µm^2)		Cichlid (nuclei per 10 000µm^2)	
	Normoxia	Hypoxia	Normoxia	Hypoxia
Mean	9.81	13.67	14.7	24
SD	0.30	0.39	0.50	0.68
p-Value	$9.9x10^{-17}$		$7.6x10^{-12}$	

Midline sections of zebrafish and cichlids raised under normoxic and hypoxic conditions were chosen and subdivided in smaller areas. In the case of D. rerio, each subarea of the section was 900 µm2 whereas in the case of the H. piceatus it was 10,000 im2. Then, subareas were randomly picked and the amount of cardiac myocyte nuclei was counted. The vast majority of cardiac myocytes were mononucleated cells. Hundred subareas per section were counted per specimen. Three sections per heart were visually analyzed (with a magnification of 20 xs). In total 6 different zebrafish hearts (from three independent experiments) were investigated for hypoxic conditions and 6 for normoxic condition. In total 1,800 subareas were quantified per heart and condition used. The same was done for the cichlids (for which bigger subareas were counted). A two-tailed t test was applied and a significant difference ($P < 0.001$) in the amount of nuclei present in the hearts of normoxia versus hypoxia groups was observed for both species

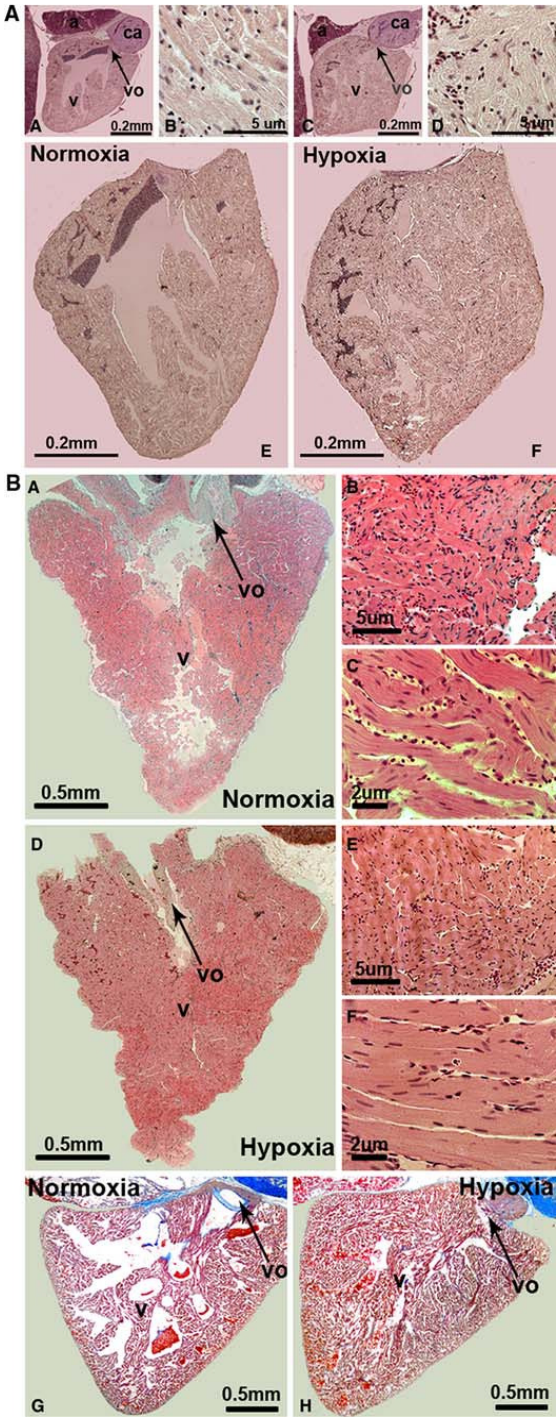
A
a
ca
v
vo
A
0.2mm
B
5 um
C
0.2mm
D
5um
Normoxia
Hypoxia
0.2mm
E
0.2mm
F
B
A
vo
v
0.5mm
Normoxia
B
5um
C
2um
D
vo
v
0.5mm
Hypoxia
E
5um
F
2um
Normoxia
vo
v
G
0.5mm
Hypoxia
v
vo
H
0.5mm

Figure 2. Histological changes of zebrafish and cichlid hearts after exposure to chronic constant hypoxia. **A** shows zebrafish hearts that were dissected, sectioned and stained with a haematoxylin–eosin staining with A, B and E representing normoxic and C, D and F hypoxic conditions. Cell nuclei are seen in dark and cell cytoplasm in light. Pictures A, C, E and F have the same magnification (10x). Images B and D represent a 20x magnification of cardiac muscle. Abbreviations used are: *a* atrium; *v* ventricle; *vo* ventricular outflow tract and *ca* conus arteriosus. **B** (A–F) corresponds to sections of cichlid hearts, which were treated the same way as the ones above from zebrafish and G and H show cichlid hearts which have been perfused prior to dissection and were stained with either haematoxylin–eosin (A–F) or Azan blue (G, H). In A, B, C and G pictures of normoxic conditions are shown and D, E, F and H represent the corresponding hypoxic conditions.

Cardiac myocyte nuclei in sections were clearly distinguishable from nuclei of other cells like erythrocytes and fibroblasts and only centralized nuclei in cardiac myocytes (which are more elongated than nuclei from erythrocytes) were counted. Furthermore, scanning electron microscopy (SEM) was used to confirm these findings in the smaller zebrafish hearts (Figure 3).
Future research is warranted in order to assess further how the cardiac myocytes adapt to CCH in the fish heart.

<u>Gene expression changes in the heart of adult zebrafish under chronic constant hypoxia (CCH)</u>

In this study, we used microarrays for the transcriptional profiling of up and down regulated genes in response to hypoxia in the zebrafish heart. We identified 376 genes that were differentially expressed under hypoxic conditions,

out of which 116 genes showed a decrease in gene expression (30.9%) in comparison to 260 genes which showed increased expression levels (69.1%).

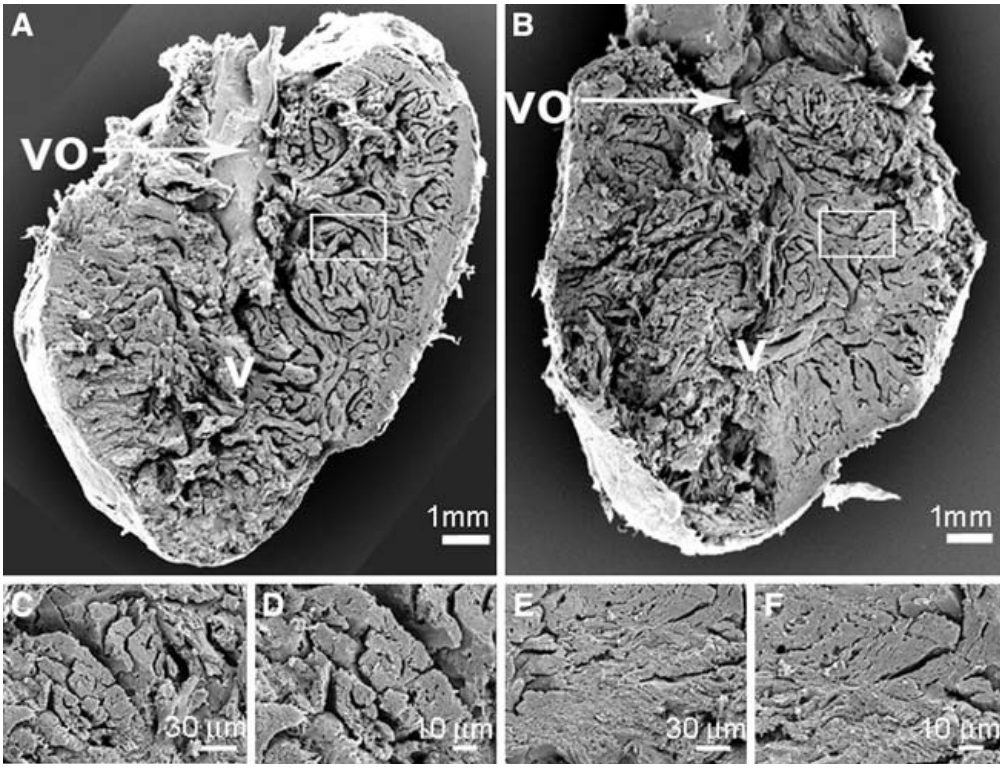

Figure 3. Morphological changes of zebrafish and cichlid hearts after exposure to chronic constant hypoxia. Scanning electron microscopy pictures of hearts from normoxia control zebrafish (a, c and d) and hypoxia-treated zebrafish (b, e and f). The bigger images show half of a heart ventricle, sectioned longitudinally. The smaller images represent a higher magnification of cardiac muscle. The scale is given at the bottom of each picture. Abbreviations used are *v* ventricle and *vo* ventricular outflow tract

All 376 deferentially expressed genes, including the ones with oligonucleotide sequences which could not be annotated so far (referred therein either as transcribed locus or zebrafish clone) are shown in the complete file (Supplemental Table 1). Functional groups are color coded and if possible, gene functions are briefly summarized and OMIM (Online Mendelian Inheritance in Man) (http://www.ncbi.nlm.nih.gov/sites/entrez?db=omim) links given.

Functional groups of differentially expressed genes in the heart

We have clustered the differential expressed genes according to known functions (Table 2). Genes can have more than one particular function assigned, so some genes can appear in more than one group. In addition, a gene ontology analysis was performed using eGOn to determine gene enrichment and overrepresentation in the three categories of molecular function, biological processes and cellular components (Supplemental Data 1 and 2).

Protein biosynthesis (Translation): In the group linked to protein biosynthesis, only three genes showed decreased expression under hypoxic conditions. All three were found to be part of the mitochondrial translational machinery. In contrast, 9 non mitochondrial genes linked to protein biosynthesis showed all increased expression (Table 2).

Metabolism: The group with metabolic genes contains 11 repressed and 28 genes with enhanced expression (Table 2). The repression majorly involves metabolic genes linked to *fl*-oxidation and lipid metabolism. Among the metabolic genes with enhanced expression, are pyruvate kinase and aldolase which both are key enzymes for glycolysis, indicating a shift from aerobic to anaerobic metabolism induced by hypoxia.

Table 2 Functional groups of differentially expressed genes

UNIGENE	GENEBANK	FOLD	GENE NAME
UPREGULATED GENES			
ANGIOGENESIS			
Dr.11575	NM_173244	2.3	T-cell acute lymphocytic leukemia 1; TAL1
Dr.845	BG729013	2.8	Fibrinogen alpha/alpha-E chain
Dr.4907	BC045868	4.2	Fibrinogen, gamma polypeptide
APOPTOSIS			
Dr.15862	AF493987	2.1	BCL2adenovirus E1b 19 interacting protein3
DrAVx.1.39	AF302789	2.3	Death receptor
Dr.20106	AI722277	2.8	Apoptosis inhibitor 5
Dr.4039	BQ480688	21.8	BAX inhibitor 1
CELL ADHESION			
Dr.6007	NM_131820	2.9	Cadherin 1
Dr.25140	BQ262802	3.3	Tumor-associated calcium signal transducer
Dr.4409	BC049036	4.4	CD9 antigen
Dr.25140	BQ262802	7.7	Tumor-associated calcium signal transducer glycoprotein
DEVELOPMENT			
Dr.11575	NM_1732	2.3	T-cell acute lymphocyte leukemia 1 (tal 1)
Dr.23348	BE201653	2.6	Bone morphogenetic protein 3b; (bmp 3)
Dr25405	BC013923	2.8	SOX2 SRY-box 2
Dr.6382	AW165053	2.9	Hedgehog-interacting protein

Dr.10879	U97669	3.0	NOTCH3 Notch homolog 3 (*Drosophila*)
Dr.15055	BC050172	3.6	Chemokine receptor 4a
Dr.6787	BI533426	5.5	Noelin
Dr.16720	BI980847	6.3	notch 2
DISEASE RELATED			
Dr.6349	AW116668	2.4	Eparin cofactor II
Dr.21064	BC046075	4.5	4hydroxyphenylpyruvate dioxygenase HPD
Dr.12584	NM_131211	5.4	Gata binding protein 3 (GATA3)
Dr.3530	AI497545	79.3	Prion protein (prp) gene
GROWTH REGULATION			
Dr.8145	NM_13143	2.2	Insulin like growth factor 2 (IGF-2)
Dr.7609	BI475857	2.4	Prolactin receptor
Dr.8285	NM_13136	2.4	Mad homolog 2
Dr.8947	CD594735	2.5	Spint 2
Dr.822	BM184127	2.5	Spint 2
Dr.3563	CD014488	2.8	Tetraspan membrane protein IL-TMP
Dr.8587	NM_17328	2.9	Insulin-like growth factor binding protein 1
Dr.2596	BM342901	3.2	Cyclin I
Dr.8587	AL910822	3.4	Insulin-like growth factor binding protein 1
Dr.26458	BC053206	5.6	m-ras
HEART RELATED			
Dr.15088	BM181749	4.3	Lectin galactoside-binding soluble 1; (galectin10-like 3)

Dr.4867	AI496840	5.5	Haptoglobin
Dr.3585	AY049731	6.6	Angiotensinogen
Dr.2452	BQ284848	4.3	Complement component C9
Dr.18453	BC044525	4.8	Uridine phosphorylase
Dr.3025	BG738204	2.7	Alpha-2 macro-globulin; A2MG
INFLAMMATION			
Dr.12491	BI672168	2.1	Complement C4–2
Dr.4047	NM_131627	2.3	Small inducible cytokine A (scyba)
Dr.5053	NM_131723	2.3	Kruppel-like factor 4
Dr25207	X06465	2.5	Complement component 8, gamma polypeptide
Dr.6845	K02765	2.9	C3 complement component 3
Dr.5741	BU710482	3.2	Complement component b fb
Dr.7722	BI878414	3.5	Complement C3-H1
Dr.22244	AW019781	3.6	Complement C1s
Dr.22133	AW076768	3.7	c1rs-A and clrs-B
Dr.5528	AI497212	4.2	Complement component C9
Dr.2452	BQ284848	4.3	Complement component C9
Dr.1730	AI721528	4.8	cfI-B complement control protein factor I-B
Dr.2452	BM778002	5.8	Complement component C9
Dr.20291	BM036389	6.5	Complement C3-S
Dr.190	NM_131338	7.9	Complement component factor B
Dr.1192	AB071601	2.	Lipocalin-type prostaglandin D synthase-like protein
METABOLISM			
Dr.9492	BI882244	2.0	SulWde dehydrogenase like

Dr.15574	BM571467	2.1	Hypoxanthine _hosphor-ribosyltransferase 1
Dr.3332	AI943053	2.2	Angiopoietin 5
Dr.16130	CD014898	2.3	Alcohol dehydrogenase 8 b
Dr.3959	BI43001	2.5	5‘-nucleotidase
Dr.22205	AW019477	2.6	Oxidoreductase
Dr.1699	AI667249	2.7	Pyruvate kinase
Dr.5504	BI879550	3.2	Cystathionine-beta-synthase
Dr.1202	AJ245491	3.9	Apolipoprotein A-I
Dr.4111	BC053267	4.2	Fructose-1,6-bisphosphatase 1
Dr.18834	AW019321	4.2	Urate oxidase
Dr.19224	BC050167	4.3	Aldolase b
Dr.4938	NM_131645	4.4	Fatty acid desaturase 2
Dr.12654	BC046901	14.8	ELOVL family member 6,
Dr.5488	AI545593	17.3	Apolipoprotein A-IV
MUSCLE RELATED			
Dr.3585	AY049731	6.6	Angiotensinogen
Dr.2452	BQ284848	4.3	Complement component C9
PROTEOLYSIS			
Dr.20934	AF541952	2.6	Trypsin precursor
Dr.3025	BG738204	2.7	Alpha-2-macroglobulin
Dr.22139	AW018965	3.0	Alpha-1-antitrypsin
Dr.25331	AI658072	4.1	Alpha-2-macroglobulin-2
Dr.12602	NM_139180	4.3	Lysozyme
Dr.1605	BM185388	4.4	Protease inhibitor 1
Dr.17459	CD586837	4.8	Inter-alpha-trypsin inhibitor heavy chain H3
Dr.3073	AI585030	5.0	Serine protease inhibitor alpha 1

Dr.26371	AI667676	5.4	Prostasin
Dr.3025	BM530427	5.6	Alpha-2-macroglobulin-1
Dr.3025	BM316867	6.5	Alpha-2-macroglobulin-2
Dr.2960	X67055	3.5	ITIH3 pre-alpha (globulin) inhibitor, H3 polypeptide
Dr.25379	BI326783	6.7	Alpha-2-macroglobulin
Dr.4797	AI959534	7.8	26–29 kD-Proteinase protein
ROS PROTECTION			
Dr.20068	NM_131075	2.1	Metallothionein (mt)
Dr.5399	AI957765	2.3	Biliverdin I Beta Reductase
Dr.14058	CD015351	3.5	Glutathione *S*-transferase theta 1
Dr.25160	BC049475	5.9	Metallothionein 2
Dr.3613	BC048037	6.0	Cerulopasmin
Dr.4905.1	BC045464	6.5	Uncoupling protein 4
SIGNAL TRANSDUCTION			
Dr.9852	AW826425	2.1	CAM kinase 1
Dr.8591	BM186508	2.9	Rho guanine nucleotide exchange factor 10
Dr.6236	AW115973	3.1	Rho guanine nucleotide exchange factor 5
Dr.1267	BC051157	3.4	Phospholipase C delta
Dr.22129	BC016668	3.9	RRAGC Rag C (Ras-related GTP binding C)
Dr.7255	AW116479	4.4	Protein phosphatase 1,
Dr.4453	BC044421	5.8	Phosphoprotein phosphatase
TRANSLATION			
Dr.13234	BM036471	2.0	Ribonuclease P

Dr.382	CB363830	2.1	Nucleolin
Dr.6949	AW078116	2.1	RNA 3‘-terminal phosphate cyclase-like protein (HSPC338)
Dr.13563	BI890729	2.3	Methionyl aminopeptidase 2
Dr.26328	AL723696	2.3	Eukaryotic translation initiation factor 4A,
Dr.17693	BQ078285	3.7	40 S ribosomal protein S6
Dr.20270	BI674050	5.9	Ribosomal protein L12
Dr.25224	CD015330	20.4	Ribosomal protein L12
Dr.12439	BM533848	17.5	Heterogeneous nuclear ribonucleoprotein K
Dr.12439	BM533848	24.2	Heterogeneous nuclear ribonucleoprotein K
Dr.14821	BM071714	33.8	Heterogeneous nuclear ribonucleoprotein K
Dr.12502	BQ284686	40.7	Heterogeneous nuclear ribonucleoprotein K
Dr.12439.	BM534432	40.9	Heterogeneous nuclear ribonucleoprotein K
Dr.12439	BQ616930	45.4	Heterogeneous nuclear ribonucleoprotein K
TRANSPORT			
Dr.1084	BQ109772	3.0	Clathrin coat assembly protein AP19
Dr.5562	X04506	3.0	APOB apolipoprotein B (including Ag(x) antigen)
Dr.13231	BM778646	4.2	Solute carrier family 22
Dr.30444	AY329629	4.3	Embryonic globin beta e2
Dr.24250	AF489105	2.0	Uroporphyrinogen III synthase

Dr.10343	NM_131687	4.7	Na^+K^+ transporting, alpha 1a.2 polypeptide
Dr.7634	AW115757	11.3	Hemopexin
DOWNREGULATED GENES			
ANGIOGENESIS			
Dr.26411	BQ783571	-8.9	Fast muscle troponin I
Dr.15501	BM316040	-2.1	Similar to CYR6 HUMAN CYR61 protein precursor, Insulin-like growth factor-binding protein 10
CELL ADHESION			
Dr.251	BQ285646	-2.3	Cadherin 11
DISEASE RELATED			
Dr.22774	AW280206	-5.7	ras-like GTP-binding protein
Dr.1816	AL720262	-4.4	RAB27A Ataxin 2-binding protein
Dr.9893	BM036473	-2.3	Fibrillarin
Dr.16726	BI429372	-2.0	netrin G1
GROWTH REGULATION			
Dr.12986	CA787334	-5.3	v-fos
Dr.12986	BI881979	-5.0	v-fos
Dr.12986	BM957279	−4.5	v-fos
Dr.1221	AW510198	−4.3	Pmx-1b (PHOX-1)
Dr.12986	BI881979	−4.2	v-fos
Dr.12410	NM_131826	−2.4	Sprouty homolog 4
Dr.6431	BC049326	-2.3	Suppressors of cytokine signaling 3
Dr.6511	NM_130922	-2.2	B-cell translocation gene 2
Dr.5365	AI601685	-2.2	Dual specificity phosphatase 5

Dr.12062	BC047814	−2.1	Epidermal growth factor receptor kinase substrate EPS8
Dr.17286	BM777144	−2.0	Hormone-regulated proliferation associated 20KDa protein
Dr.9448	BM156058	-2.0	TGF-beta-inducible early growth response protein 2
HEART RELATED			
Dr.20010	BQ826502	-7.0	ATPase, Ca++ transporting, cardiac muscle (ATP2A1)
Dr.1448	AL717344	-3.5	Fast skeletal myosin light chain 1a
Dr.20990	AY081167 AY033829	-2.4–2.1	Titin
METABOLISM			
Dr.24950	BC053305	-4.1	Creatine kinase CKM3
Dr.9528	BC045993	-3.5	Pyruvate dehydrogenase kinase
Dr.146	AI477401	-2.9	Carnitine α-palmitoyltransferase II
Dr.21501	AI667180	-2.4	Short-chain acyl-CoA dehydrogenase
Dr.19643	AL918850	-2.4	FabG beta-ketoacylreductase
Dr.15059	BM530407	-2.2	Elongation of very long chain fatty acids (Cig30)
Dr.21040	BC045479	-2.1	Glucose-6-phosphatase, transport protein 1
Dr.988	AW154697	-2.1	Dodecenoyl-coenzyme A delta isomerase
Dr.11971	BG727588	-2.0	Carnitine *O*-acetyl-transferase

Dr.4777	AW420997	-2.0	Succinate-CoA ligase
Dr.11252	BC047826	-2.0	Creatine kinase, mitochondrial 1
MUSCLE RELATED			
Dr.21800	AI883923	-5.0	Myosin binding protein C
Dr.5066	AF524840	-3.4	Alpha-actinin 3
Dr.24260	NM_131619	-3.0	Myosin, light polypeptide 3
Dr.2914	BC045520	-2.5	Myosin light polypeptide 2; mylz2
Dr.20990	AY033829 AY081167	-2.4–2.1	Titin
Dr.1435	AI353817	-2.0	Caveolin 3
Dr.18657	BQ479700	-2.1	Carbonic anhydrase II
Dr.26411	BQ783571	-8.9	Troponin I
PROTEOLYSIS			
Dr.3581	BM101561	-8.3	Chymotrypsinogen B1
Dr.3581	BM101561	-7.5	Chymotrypsinogen B1
SIGNAL TRANSDUCTION			
Dr.22841	AI641080	-2.4	Serum deprivation response protein (SDPR)
TRANSLATION			
Dr.7939	AW281840	-2.7	Mitochondrial elongation factor G1
Dr.1286	BM036808	-2.2	Mitochondrial ribosomal protein L48
Dr.18218	AL909921	-2.1	Mitochondrial 28 S ribosomal protein S12

TRANSPORT			
Dr.676	BC050956	-4.4	ADT2, ADP,ATP carrier protein
Dr.25199	CD014403	-2.1	Calcium-binding mitochondrial carrier protein Aralar2 (Citrin)
Dr.2784	AI942949	-2.0	Solute carrier family 25
Dr.11127	BG306498	-3.7	Synaptotagmin I
Dr.11127 A	W826278	-3.2	Synaptotagmin I
Dr.13273	BI885460	-2.3	GTP-binding protein rab15
Dr.22748	AW280026	-2.7	trpn1
Dr.11302	BG306530	-2.1	ATPase (Ca++ transporting plasma membrane 2)

Protection against reactive oxygen species (ROS): The group of genes important for protection against ROS contains 6 genes which are all enhanced under hypoxia.

Apoptosis: We found four genes linked to programmed cell death to be enhanced by hypoxia. Two of these, the death receptor 5 (DR5) and the BNIP3 homologue, are considered to be pro-apoptotic, whereas apoptosis inhibitor 5 and Bax inhibitor have been shown to have anti-apoptotic properties (Tewari, *et al*., 1997; Xu, *et al*., 1998).

Growth regulation: In the group of genes linked to growth regulation, we found 9 genes to be repressed and 8 genes with enhanced expression. Within the group of 8 repressed genes, we found 5 anti-proliferative genes: spry4 and dual specificity phosphatase 5 both inhibit mitogen-activated kinases (MAPK), SOCS3 binds and inhibits Janus kinases (JAK) and thereby prevents STAT3 activation. BTG2 which is important in the G1/S transition and TIEG2 is a transcriptional repressor with ant proliferative functions. Although some genes involved in cell

proliferation, such as the transcription factor c-fos were repressed by hypoxia (see also "Discussion"), the regulation of the vast majority (13 of 17) of identified genes in this group suggests stimulation of proliferation (Table 2).

Inflammation: 14 genes involved in the inflammatory response were identified to be differentially regulated and all showed increased expression upon hypoxia treatment.

Heart-related function: Several genes linked to cardiac hypertrophy, cardiomyopathy (disease of the heart muscle) and cardiac infarction were identified in this study (see Table 2 and "Discussion").

Muscle-related function: Several sarcomeric genes linked to hypertrophy showed decreased expression under hypoxic conditions (Table 2 and "Discussion").

Development: The genes in this group were all found to be upregulated by hypoxia among them the gene for notch-2 and notch-3. Notch receptors are transmembrane receptors with essential roles in development including heart development.

Transport (cellular and vascular): A heterologous group containing the gene for embryonic hemoglobin beta e2, important for oxygen transport and hemopexin which is important for heme and iron transport and was found to be upregulated.

Angiogenesis: It is well known that hypoxia via the hypoxia inducible factor 1*α* (HIF1*α*) pathway leads to angiogenesis. In the zebrafish heart under CCH, we observed increased expression of HIF1*α* as well as fibrinogen-*α* and -*γ*. Fibrinogen-*o* has been shown to stimulate HIF1*α* and VEGF expression and thereby induces angiogenesis (Shiose, *et al*., 2004)

Expression changes of known hypoxia responsive genes

Examples for regulation of known hypoxia responsive genes are HIF1α, insulin growth factor-2 (IGF-2), insulin growth factor binding protein 1 (IGFbp1) and caveolin 3. The transcription factor Hif1α is pivotal in the cellular response to hypoxic stress (Semenza, 1999). We further observed increased expression of *egl nine homolog*, a gene which was shown to be induced by hypoxia through the Hif1α pathway (Pescador, *et al*., 2005). IGF-2 gene and protein expression had been shown to be upregulated by hypoxia (Beilharz, *et al*., 1995). It was shown that IGFbp1 also is a hypoxia-inducible gene in zebrafish embryos and it mediates hypoxia-induced embryonic growth-inhibition and developmental retardation (Kajimura, *et al*., 2005a). Both IGF-2 and IGFbp1 were found upregulated in our study. We observed decreased expression of caveolin 3 in the hearts of zebrafish exposed to CCH, earlier findings showed that chronic myocardial hypoxia led to decreased caveolin-3 protein expression in rabbit hearts (Shi, *et al*., 2000). These findings indicate that the hypoxic conditions used lead to hypoxic stress in the fish heart.

Evaluation of microarray results by quantitative real-time RT-PCR

To further verify our results, we used quantitative real-time PCR for 10 of the transcripts. We confirmed the gene expression changes found in the microarray studies for these 5 up- and 5 down-regulated transcripts by this independent method (Figure 4). The down-regulated zebrafish genes tested were: c-fos, phox1, creatine kinase (ckm3), nebulin, titin, and the upregulated genes tested were: metallothionein, pyruvate kinase, apoptosis inhibitor 5, igfbp1 and notch-2. The fold induction values were not always directly comparable to the array data but in all cases induction or reduction was

confirmed. Quantitative differences between array data and qPCR results have been reported before (Meijer, *et al*., 2005; Ton, *et al*., 2003; van der Meer, *et al*., 2005)

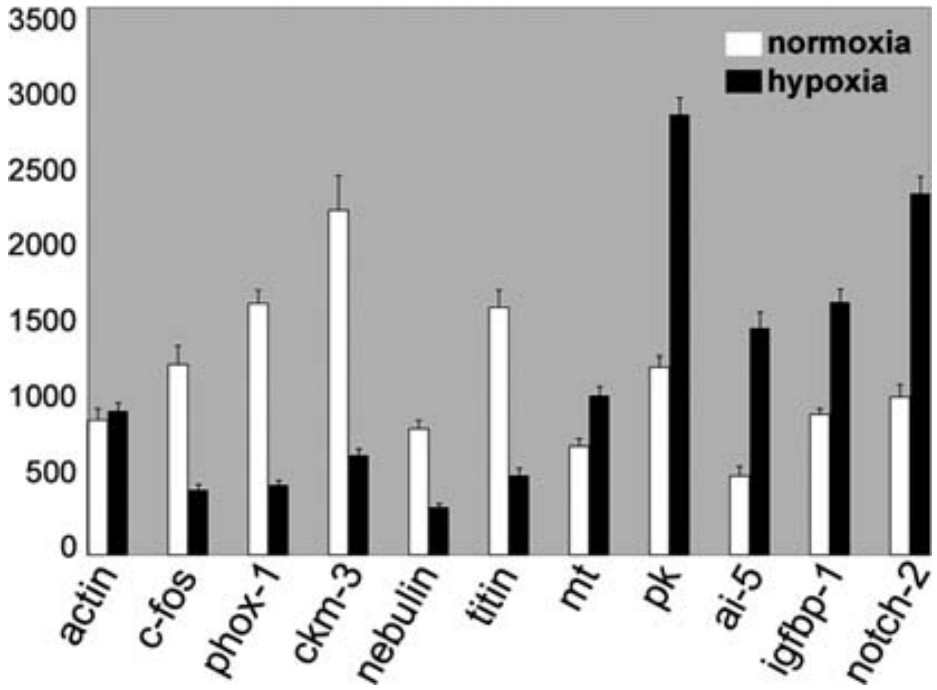

Figure 4. Verification of gene expression changes by quantitative real- time PCR. 10. Selected genes, which were found to be differentially ex- pressed on the microarrays, were further analyzed by quantitative real- time RT-PCR. Relative expression is given based on normalization to fl-actin. A standard curve for fl-actin was included in each experiment and data represents three independent experiments each done in triplicates. The primers used are given in Supplemental Table 2

*A*ssessment of microarray results for the IGF/PI3K/Akt pathway by comparing phospho-Akt levels in cardiac myocytes of normoxic versus hypoxic zebrafish hearts

The IGF/PI3K/Akt pathway is activated by IGFs, which are antagonized by the IGFbp1. To test the effects of the upregulation of both IGF-2 and IGFbp1, we assayed phospho-Akt levels in cardiac myocytes and showed that phospho-Akt levels were not different between normoxic and hypoxic cells. Figure 5 shows cytoplasmic immunohistochemical staining of phospho-Akt. The antibody recognizes phosphorylated and detects the phospho-Akt1/2/3 forms. The incubation times for the primary and secondary antibody as well as the BM Purple were optimized to obtain a good signal to noise ratio. Absorbances were linearly related to the time of incubation with the primary and secondary antibodies as well as that of BM Purple. Figure 5d shows for normoxic fish the absorbance values of the phospho-Akt staining in cardiac myocytes as well as skeletal muscle fibers from the tail as a function of the incubation time with BM Purple AP substrate. The absorbance values for the heart are considerably higher than for the skeletal muscle fibers. However, for both cardiac and skeletal muscle the absorbances are linearly related with the incubation time with BM Purple AP substrate and increase at the same relative rate. This implicates that the absorbance of BM Purple after 45 min incubation with BM Purple AP substrate did not reach saturation and therefore provides a semi-quantitative estimate of the phospho-Akt content in the cardiac myocytes. Absorbances of staining for phospho-Akt in normoxic and hypoxic cardiac myocytes were not shown to be significantly different (Figure 5E, $P<0.48$), which indicates that hypoxia did not change the activation of the Akt pathway in the cardiac myocytes.

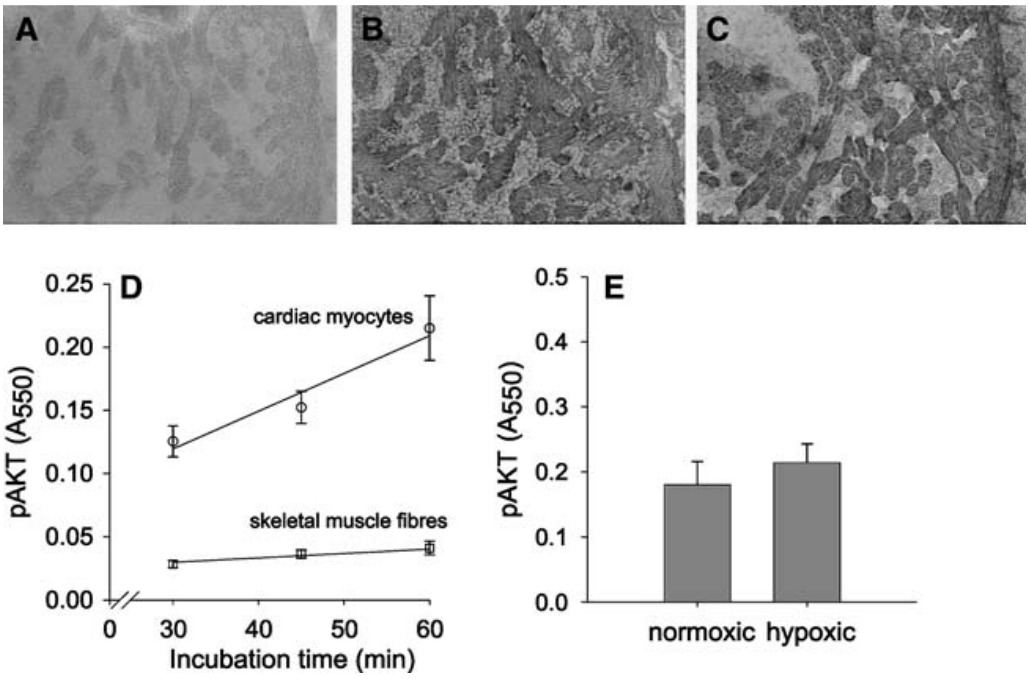

Figure 5 Effects of chronic constant hypoxia of the activation of Akt in zebrafish cardiac myocytes. Immunohistochemical staining of phospho-Akt in cardiac myocytes of zebrafish raised under hypoxic **(a)** or normoxic **(b)** conditions. Specificity is shown by the control sections obtained from normoxic fish which were not incubated with primary antibody against phospho-Akt **(c)**. For both cardiac myocytes and skeletal muscle fibers, the absorbance of the BM Purple is linearly increasing at the same relative rate with the incubation time with BM Purple AP substrate at the same relative rate **(d)**. Mean absorbances of phospho-Akt staining (+S.E.M.) from normoxic and hypoxic cardiac myocytes was not different **(e)**

Discussion

In the aquatic environment, oxygen concentrations can often vary, and being able to adapt to changes in oxygen levels can be advantageous for the survival of aquatic animals. This might be in part the reason why some teleost have developed the ability to withstand extreme hypoxic conditions.

In this study, we have focused on the long-term response to hypoxia in the fish heart. The hypothesis is that the zebrafish heart, in contrast to most mammalian hearts, which are characterized by relative intolerance to injury or the lack of oxygen, are able to adapt to extreme hypoxic conditions.

We showed that chronic hypoxia of zebrafish caused a smaller ventricular outflow tract, reduced lacunae and increased cardiac myocyte densities in the heart. These findings suggest that hypoxia induced an increase of the cardiac myocyte volume or at least did not result in a loss of cardiac myocytes. This is in contrast to mammals where tissue hypoxia in chronic heart failure leads to apoptosis and considerable losses of cardiac myocytes (see for review Sabbah, *et al*. (2000a)). In mammals, compensation for this loss of cardiac myocytes occurs mainly by hypertrophy of the remaining cardiac myocytes (Ostadal, *et al*., 2007), although regeneration of myocardium by proliferation of cardiac myocytes may occur also but to a limited extend (Beltrami, *et al*., 2001). Our assay for phospho-Akt did not show any enhancement of Akt activity in response to the CCH, suggesting a lack of hypertrophic signaling via the phosphotadilinositol 3 kinase pathway. However, the density of cardiac myocyte nuclei increased by 50% during CCH, which indicates substantial proliferation of cardiac myocytes and/or nuclear hyperplasia. Recently, it has been shown that the zebrafish heart has the ability to regenerate from mechanical cardiac injury by proliferation of cardiac myocytes (Poss, *et al*., 2002). If the zebrafish heart

responds to chronic hypoxia in a similar way as to mechanical dissection, this will be beneficial in preventing apoptosis of cardiac myocytes as the diffusion distance for oxygen are not increased as during hypertrophy, which will help to prevent the development of anoxic cores in the cardiac myocytes (Des Tombe, *et al*., 2002; van der Laarse, *et al*., 2005). In the case that the increase in cardiac myocyte nuclear density during chronic hypoxia was due to nuclear hyperplasia and nuclear ploidy, the observed smaller ventricular outflow tract and reduced lacunae may have been the result of hypertrophy of the existing cardiac myocytes. The histological assay in this study does not clearly distinguish between hyperplasia and hypertrophy of cardiac myocytes. Future investigation of the mechanisms underlying the general morphological adaptations of teleost fish heart in response to CCH requires a nuclear stain in combination with a clear membrane stain, which allows determination of cell sizes in addition to counts of cardiac myocyte nuclei.

We were interested in the underlying gene expression changes of these adaptations. We found gene regulations in a transcriptional network of the serum response element (SRE), which are opposed to the ones described in mammals. In the zebrafish heart hypoxia repressed c-fos and phox1 expression. Both genes are important in the same transcriptional network; phox1 can transduce serum responsive transcriptional activity to the c-fos (SRE) by interacting with serum response factor (SRF) (Simon, *et al*., 1997). In mammals many studies showed increased expression of c-fos by hypoxia, e.g. in rats hypoxia induces c-fos expression in the LV and RV (Deindl, *et al*., 2003) and the same held true in tissue culture cells (Webster, *et al*., 1993). Interestingly, repression of c-fos by hypoxia has also been shown for the short-term response to anoxia in anoxia tolerant turtles (Greenway, *et al*., 2000). It is possible that

repression of c-fos and phox-1 are important adaptations in hypoxia tolerant animals.

Several novel gene expression changes induced by CCH have been identified in this study (Table 2 and Supplemental Table 1). An example is the two Notch receptors, notch-2 and notch-3, whose expression were induced by CCH. Notch receptors have been shown to be important for heart patterning and differentiation (Armstrong, *et al*., 2004), cell fate determination and self-renewal of stem cells (Androutsellis-Theotokis, *et al*., 2006; Bianchi, *et al*., 2006) but so far have not been linked to the hypoxic response.

Several genes with links to human heart pathology were found to be upregulated in this study. Among these were two markers for myocardial infarction, complement component C9 and haptoglobin. C9 is used as a marker for myocardial infarction (Doran, *et al*., 1996) and a polymorphism for haptoglobin predicts 30-day mortality and heart failure in patients with diabetes and acute myocardial infarction (Levy, *et al*., 2002). We also observed increased expression of fetuin-*α*, a circulating calcium-regulatory glycoprotein that inhibits vascular calcification. Low fetuin-*α* levels have been associated with heart failure in mice (Merx, *et al*., 2005). Upregulation of fetuin-*α* in the zebrafish heart could help to better tolerate CCH. Selenoprotein P (SEPP1) is a heparin-binding protein that appears to be associated with endothelial cells and has been implicated as an oxidant defense in the extracellular space. Human populations that are selenium deficient are susceptible to the development of Keshan disease, a potentially fatal form of cardiomyopathy (Nezelof, *et al*., 2002). SEPP1 expression was found to be increased in our study indicating a potential protective mechanism against oxidative stress in the heart. This was further supported by the increased expression observed for several genes important for

the protection against reactive oxygen species (ROS) (Table 2). Among them were metallothionein and glutathione *S*-transferase, which are both known ROS scavengers. Metallothionein has further been described to be protective against hypoxia-induced apoptosis when over expressed (Wang, *et al*., 2001). Our findings suggest ROS protection as an important adaptation to CCH in the fish heart.

Furthermore, our data show for the first time that CCH simultaneously induced upregulation of IGF-2 and the insulin-like growth factor binding protein 1 (IGFbp1). In isolated cardiomyoblasts, angiotensin II stimulates IGF-2 expression which is involved in the induction of apoptotic signaling in rat hearts (Lee, *et al*., 2006). We have observed here both angiotensin and IGF-2 upregulation (Table 2). The upregulation of IGFbp1 seems to be a general response to hypoxia in zebrafish embryos, where it mediates hypoxia-induced embryonic growth retardation and developmental delay (Kajimura, *et al*., 2005b). IGFbp1 is a secreted protein, which binds to IGFs in the extracellular environment and prevents receptor activation (Florini, *et al*., 1996; Stewart, *et al*., 1996). Here, IGFbp1 by binding IGF-2 may have prevented both cardio protective as well as apoptotic effects of enhanced IGF-2 expression. To test the effects of the upregulation of both IGF-2 and IGFbp1, we assayed phospho-Akt levels in cardiac myocytes and showed that phospho-Akt levels were not different between normoxic and hypoxic cells. This suggests that either hypoxia-induced changes in mRNA expression did not occur at the protein level or the effects of increased IGF-2 expression on the IGF-1 receptor (which can be activated by IGF-2) were blunted by the upregulation of the IGFbp1. The fact that we did not observe increased phospho-Akt levels suggests a lack of hypertrophic signaling as enhanced phospho-Akt is required for cardiac hypertrophy (DeBosch, *et al*.,

2006). This may be beneficial for the heart as hypertrophy of cardiac myocytes implicates an increase in the diffusion distance for oxygen which may cause the development of anoxic cores (Des Tombe, *et al*., 2002), release of cytochrome *c* (van Beek-Harmsen, *et al*., 2005) and production of ROS (Lee, *et al*., 2006; Powers, *et al*., 2007) and eventually causing apoptosis of cardiac myocytes. The importance of the IGF-2/IGFbp1 signaling in the protection of the zebrafish heart and its underlying mechanisms remain to be determined.

The gene expression changes we observed for the specific response to CCH in the fish heart were very different from the responses we observed in an earlier study in the gills (van der Meer, *et al*., 2005). Under the same criteria as used in this study, we found that the majority of differentially regulated genes in the gills showed a decrease in gene expression (68.1% or 250 genes in total) in comparison to genes, which showed increased expression levels (31.9% or 117 genes in total). This is opposed to the heart where 69.1% of differentially regulated genes (260 genes in total) showed increased and 30.9% (116 in total) decreased expression levels. Many genes linked to protein synthesis showed a similar trend, and were down regulated in the gills (van der Meer, *et al*., 2005) and upregulated in the heart (Table 2). The major differences observed in gene regulation between heart and gills point to very tissue specific responses to CCH. A list of genes identified in both studies, as identified by a direct comparison based on Accession numbers and old Unigenes numbers are shown in Supplemental Data 3.

Teleosts have developed specific phenotypic adaptations to low oxygen, due to the natural occurrence of hypoxia in the water environment. Here, we identified the changes in gene expression as well as associated morphological changes of the fish heart to hypoxia. We observed repression of c-fos, which differs

compared to the described increase in expression in mammals (Deindl, *et al*., 2003). Other changes found like upregulation of the two Notch receptors have not been described before to the best of our knowledge. Similarly, the simultaneous increase in expression of IGF-2 and IGFbp1 has not been shown. The changes identified here can contribute to the ability of teleosts to adapt to severe hypoxia (for example, the upregulation of fetuin-*o* and sepp1 levels). Future functional studies are warranted to validate the role of the identified genes in cardiac protection to hypoxia

Acknowledgments We would like to thank Guido van den Thillart for essential help with the hypoxia set up, Gerda Lamers for intensive help with EM microscopy, Maximilian Corredor for his help with data analysis and software, Carlo Rutjes and Patrick Niemantsverdriet for animal care. Dr. Willem van der Laarse and Dr. Siona Slob are acknowledged for their assistance in the optimization of immunohistochemistry. This work was in part supported by a European Commission 6th Framework Program grant (contract LSHG-CT-2003-503496, ZF-Models) and a grant from the Portuguese foundation for Science and Technology (SFRH/BD/27262/2006). All experiments comply with the current laws of the Netherlands.

References

Androutsellis-Theotokis A, Leker RR, Soldner F, Hoeppner DJ, Ravin R, Poser SW, Rueger MA, Bae S-K, Kittappa R, McKay RDG (2006) Notch signaling regulates stem cell numbers in vitro and in vivo. Nature 442(7014):823-826

Armstrong EJ, Bischoff J (2004) Heart valve development: endothelial cell signaling and differentiation. Circulation Research 95:459–470

Beilharz EJ, Bassett NS, Sirimanne ES, Williams CE, Gluckman PD (1995) Insulin-like growth factor II is induced during wound repair following hypoxic-ischemic injury in the developing rat brain. Molecular Brain Research 29:81–91

Beltrami AP, Urbanek K, Kajstura J, Yan SM, Finato N, Bussani R, Nadal-Ginard B, Silvestri F, Leri A, Beltrami CA, Anversa P(2001) Evidence that human cardiac myocytes divide after myocardial infarction. New England Journal of Medicine 344:1750–1757

Bianchi S, Dotti MT, Federico A (2006). Physiology and pathology of notch signaling system. Journal of Cell Physiology 207:300–308

DeBosch B, Treskov I, Lupu TS, Weinheimer C, Kovacs A, Courtois M, Muslin AJ (2006) Akt1 is required for physiological cardiac growth. Circulation 113:2097–2104

Deindl E, Kolar F, Neubauer E, Vogel S, Schaper W, Ostadal B (2003) Effect of intermittent high altitude hypoxia on gene expression in rat heart and lung. Physiological Research 52:47–57

Des Tombe AL, Van Beek-Harmsen BJ, Lee-De Groot MB, Van Der Laarse WJ (2002) Calibrated histochemistry applied to oxygen supply and demand in hypertrophied rat myocardium. Microscopy Research Tech 58:412–420

Doran JP, Howie AJ, Townend JN, Bonser RS (1996) Detection of myocardial infarction by immunohistological staining for C9 on formalin fixed, paraffin wax embedded sections. Journal of Clinical Pathology 49:34–37

Fan C, Iacobas DA, Zhou D, Chen Q, Lai JK, Gavrialov O, Haddad GG (2005) Gene expression and phenotypic characterization of mouse heart after chronic constant or intermittent hypoxia. Physiological Genomics 22:292–307

Florini JR, Ewton DZ, Coolican SA (1996) Growth hormone and the insulin-like growth factor system in myogenesis. Endocrinology Reviews 17:481–517

Gracey AY, Troll JV, Somero GN (2001) Hypoxia-induced gene expression profiling in the euryoxic fish *Gillichthys mirabilis*. Proceedings of the National Academy of Sciences 98:1993–1998

Greenway SC, Storey KB (2000) Mitogen-activated protein kinases and anoxia tolerance in turtles. Journal of Experimental Zoology 287:477–484

Kajimura S, Aida K, Duan C (2005a) From the Cover: Insulin-like growth factor-binding protein-1 (IGFBP-1) mediates hypoxia-induced embryonic growth and developmental retardation Proceedings of the National Academy of Sciences 102:1240–1245

Kajimura S, Aida K, Duan C (2005b) Insulin-like growth factor-binding protein-1 (IGFBP-1) mediates hypoxia-induced embryonic growth and developmental retardation. Proceedings of the National Academy of Sciences 102:1240–1245

Kolar F, Ostadal B (2003) Molecular mechanisms of cardiac protection by adaptation to chronic hypoxia. Physiology Research 53:S3–S13

Lee SD, Chu CH, Huang EJ, Lu MC, Liu JY, Liu CJ, Hsu HH, Lin JA, Kuo WW, Huang CY (2006) Roles of insulin-like growth factor II in cardiomyoblast

apoptosis and in hypertensive rat heart with abdominal aorta ligation. American Journal of Physiology Endocrinology and Metabolism 291:E306–E314

Levy AP, Hochberg I, Jablonski K, Resnick HE, Lee ET, Best L, Howard BV (2002) Haptoglobin phenotype is an independent risk factor for cardiovascular disease in individuals with diabetes: the strong heart study. Journal of the American College of Cardiology 40:1984–1990

Meijer AH, Verbeek FJ, Salas-Vidal E, Corredor-Adamez M, Bussman J, van der Sar AM, Otto GW, Geisler R, Spaink HP (2005) Transcriptome profiling of adult zebrafish at the late stage of chronic tuberculosis due to Mycobacterium marinum infection. Molecular Immunology 42:1185–1203

Merx MW, Schafer C, Westenfeld R, Brandenburg V, Hidajat S, Weber C, Ketteler M, Jahnen-Dechent W (2005) Myocardial stiffness, cardiac remodeling, and diastolic dysfunction in calcification-prone fetuin-a-deficient mice. Journal of the American Society of Nephrology 16:3357–3364

Nezelof C, Bouvier R, Dijoud F (2002) Multifocal myocardial necrosis: a distinctive cardiac lesion in cystic fibrosis, lipomatous pancreatic atrophy, and keshan disease. Fetal Pediatrics Pathology 21:343–352

Ostadal B, Kolar F (2007) Cardiac adaptation to chronic high-altitude hypoxia: Beneficial and adverse effects. Respiratory Physiology & Neurobiology 150 (2-3):224-236

Pescador N, Cuevas Y, Naranjo S, Alcaide M, Villar D, Landazuri MO, Del Peso L (2005) Identification of a functional hypoxia- responsive element that regulates the expression of the egl nine homologue 3 (egln3/phd3) gene. Biochemistry Journal 390:189–197

Poss KD, Wilson LG, Keating MT (2002) Heart regeneration in zebrafish. Science 298:2188–2190

Powers SK, Kavazis AN, McClung JM (2007) Oxidative stress and disuse muscle atrophy. Journal of Applied Physiology 102(6):2389–2397

Sabbah HN, Sharov VG, Goldstein S (2000a) Cell death, tissue hypoxia and the progression of heart failure. Heart Fail Reviews 5:131–138

Semenza GL (1999) Regulation of mammalian O2 homeostasis by hypoxia-inducible factor 1. Annual Reviews of Cell and Developmental Biology 15:551–578

Semenza GL (2001) Hypoxia-inducible factor 1: oxygen homeostasis and disease pathophysiology. Trends in Molecular Medicine 7:345–350

Shi Y, Pritchard Jr KA, Holman P, Raffee P, GriYth OW, Kalyanar- aman B, Baker JE (2000) Chronic myocardial hypoxia increases nitric oxide synthase and decreases caveolin-3. Free Radical Biology & Medicine 29:695–703

Shiose S, Hata Y, Noda Y, Sassa Y, Takeda A, Yoshikawa H, Fujisawa K, Kubota T, Ishibashi T (2004) Fibrinogen stimulates in vitro angiogenesis by choroidal endothelial cells via autocrine VEGF. Graefes Archive of Clinical and Experimental Ophthalmology 242:777–783

Simon KJ, Grueneberg DA, Gilman M (1997) Protein and DNA contact surfaces that mediate the selective action of the Phox1 homeodomain at the c-fos serum response element. Molecular Cell Biology 17:6653–6662

Stecyk JAW, Stenslokken K-O, Farrell AP, Nilsson GE (2004) Maintained cardiac pumping in anoxic crucian carp. Science 306:77

Stewart CE, Rotwein P (1996) Growth, differentiation, and survival: multiple physiological functions for insulin-like growth factors. Physiology Reviews 76:1005–1026

Tewari M YM, Ross B, Dean C, Giordano A, Rubin R (1997) AAC-11, a novel cDNA that inhibits apoptosis after growth factor withdrawal. Cancer Research 57:4063–4069

Ton C, Stamatiou D, Liew C-C (2003) Gene expression profile of zebrafish exposed to hypoxia during development. Physiology Genomics 13:97–106

van Beek-Harmsen BJ, van der Laarse WJ (2005) Immunohistochemical determination of cytosolic cytochrome C concentration in cardiomyocytes. Journal of Histochemistry & Cytochemistry 53:803–807

van der Laarse WJ, des Tombe AL, van Beek-Harmsen BJ, Lee-de Groot MB, Jaspers RT (2005) Krogh's diffusion coefficient for oxygen in isolated Xenopus skeletal muscle fibers and rat myocardial trabeculae at maximum rates of oxygen consumption. J Appl Physiol 99:2173–2180

van der Meer DL, van den Thillart GE, Witte F, de Bakker MA, Besser J, Richardson MK, Spaink HP, Leito JT, Bagowski CP (2005) Gene expression profiling of the long-term adaptive response to hypoxia in the gills of adult zebrafish. American Journal of Physiology. Regulatory, Integratuve and Comparative Physiology 289:R1512–R1519

van der Meer DL, Marques IJ, Leito JT, Besser J, Bakkers J, Schoonheere E, Bagowski CP (2006) Zebrafish cypher is important for somite formation and heart development. Developmental Biology 299:356–372

Wang G-W, Zhou Z, Klein JB, Kang YJ (2001) Inhibition of hypoxia/ reoxygenation-induced apoptosis in metallothionein-overexpressing cardiomyocytes. American Journal of Physiology. Heart and Circulatory Physiology 280:H2292–H2299

Webster KA, Discher DJ, Bishopric NH (1993) Induction and nuclear accumulation of fos and jun proto-oncogenes in hypoxic cardiac myocytes. Journal of Biological Chemistry 268:16852–16858

Xu Q, Reed JC (1998) Bax inhibitor-1, a mammalian apoptosis suppressor identified by functional screening in yeast. Molecular Cell 1:337–346

CHAPTER 3

METASTATIC BEHAVIOR OF PRIMARY HUMAN TUMORS IN A ZEBRAFISH XENOTRANSPLANTATION MODEL

Ines J Marques, Frank Ulrich Weiss, Danielle H Vlecken, Claudia Nitsche, Jeroen Bakkers, Anne K Lagendijk, Lars Ivo Partecke, Claus- Dieter Heidecke, Markus M Lerch and Christoph P Bagowski

Article published in ***BMC Cancer* 2009, 9:128**

All supplemental material can be found online on:

http://www.biomedcentral.com/1471-2407/9/128/additional/

Abstract

Aberrant regulation of cell migration drives progression of many diseases, including cancer cell invasion and metastasis formation. Analysis of tumor invasion and metastasis in living organisms to date is cumbersome and involves difficult and time consuming investigative techniques. For primary human tumors we establish here a simple, fast, sensitive and cost-effective *in vivo* model to analyze tumor invasion and metastatic behavior.

We fluorescently labeled small explants from gastrointestinal human tumors and investigated their metastatic behavior after transplantation into zebrafish embryos and larvae. The transparency of the zebrafish embryos allows to follow invasion, migration and micrometastasis formation in real-time. High resolution imaging was achieved through laser scanning confocal microscopy of live zebrafish.

In the transparent zebrafish embryos invasion, circulation of tumor cells in blood vessels, migration and micrometastasis formation can be followed in real-time. Xenografts of primary human tumors showed invasiveness and micrometastasis formation within 24 hours after transplantation, which was absent when non-tumor tissue was implanted. Furthermore, primary human tumor cells, when organotopically implanted in the zebrafish liver, demonstrated invasiveness and metastatic behavior, whereas primary control cells remained in the liver. Pancreatic tumor cells showed no metastatic behavior when injected into cloche mutant embryos, which lack a functional vasculature.

Our results show that the zebrafish is a useful *in vivo* animal model for rapid analysis of invasion and metastatic behavior of primary human tumor specimen.

Introduction

Approximately 90% of all cancer deaths arise from the metastatic spread of primary tumors (Jemal, et al., 2007). Metastasis formation is a complex, multi-step process in which primary tumor cells invade neighboring tissues, enter the systemic circulation (intravasate), translocate through the vasculature, arrest in distant capillaries, extravasate into the perivascular tissue, and finally proliferate from micrometastasis into macroscopic secondary tumors (Fidler, 2003). Invasiveness and early formation of metastases are the main reasons why for example pancreatic cancer continues to have a dismal prognosis, with a 5 year survival rate of <5% and a mean life expectancy of <6 month (Jemal, et al., 2007). Zebrafish and their transparent embryos have been employed in several useful models for therapeutic drug research and preclinical studies (Zon, et al., 2005). High throughput screening (HTS) in zebrafish embryos has been established and is nowadays commonly used for different applications (Zon, et al., 2005; Kari, et al., 2007; den Hertog, 2005). A number of unique features make this animal model very attractive: zebrafish are inexpensive to maintain, breed in large numbers, develop rapidly *ex vivo*, and can be maintained in small volumes of water (Parng, et al., 2002). Recently, the zebrafish and its transparent embryos have also come into view as a new model system to investigate tumor development, cancer cell invasion and metastasis formation (Goessling W, 2007; Hendrix, et al., 2007; Grunwald DJ, 2002; Langenau, et al., 2003; Stoletov, et al., 2007). Mary Hendrix and her group have pioneered the field of cancer cell transplantation in zebrafish embryos and could show that transplanted human malignant melanoma cells are not rejected, but survive and even exhibit motility (Lee, et al., 2005; Topczewska, et al., 2006). Haldi *et al.* observed the formation

of tumor-like cell masses when xenotransplanting human melanoma cells in slightly older zebrafish embryos (Haldi, et al., 2006). Several independent studies have now shown that human melanoma cells and other cancer cell lines are able to induce neovascularization when xenografted in the zebrafish (Stoletov, et al., 2007; Haldi, et al., 2006; Nicoli, et al., 2007; Nicoli, et al., 2007).

The role of the small GTPase RhoC in tumor formation, angiogenesis and cell invasion was investigated in real-time in 1-month-old immunosuppressed zebrafish xenografted with the human breast cancer cell line MDA-435 (Stoletov, et al., 2007). This study achieved high-resolution imaging of the dynamic cell-vascular interface in transparent juvenile zebrafish. All these innovative studies established the use of the zebrafish xenotransplantation model for the analysis of cancer cell lines. In this study we now show that zebrafish embryos can even be used to directly transplant human tumor tissue and primary human tumor cells. Zebrafish embryos thus provide a simple, fast and cost-effective method to test the metastatic behavior of primary tumors in an *in vivo* vertebrate animal model that also permits high throughput drug screening.

Methods

Animal care and handling

Zebrafish (*Danio rerio*) (Tuebingen line, *alb* strain (Albinos) and Tg(fli1:eGFP) were handled in compliance with local animal care regulations and standard protocols of the Netherlands and Germany. Fish were kept at 28°C in aquaria with day/night light cycles (10h dark versus 14h light periods). The developing embryos were kept in an incubator at constant temperatures. The cloche (clo) mutant line has been previously described (Herpers, et al., 2008). Heterozygous

fish (clo-/+) are kept and bred under normal conditions. 25% of offspring will consist of homozygous clo-/-mutants who lack functional vasculature and circulation 75% will be siblings with no phenotype. Lack of circulation, an enlarged pericardium and curvature of the tail (at a later time point) are hallmarks of the cloche phenotype.

Cell culture

EpRas cells were cultured at 37°C in DMEM high glucose containing L-glutamine, 4% FCS and 1:100 Pen/Strep (GIBCO, Invitrogen). PaTu8988T and PaTu8898S cells were cultured in DMEM high glucose, with 10% FCS and 1:100 Pen/Strep. The EpRas cells were treated with recombinant human TGF-β1 (RD systems) at a final concentration of 2ng/ml. To induce epithelial to mesenchymal transition (EMT), cells were seeded at 70% confluence in 6-well plates and media containing TGF-β1 (2ng/ml final concentration) was added and replaced every other day for 10 days. After this period, cells were ready for injection.

Cell staining, injections and incubations

Cells were stained with either CM-DiI (red fluorescence) or DiO (green fluorescence) (Vybrant, Invitrogen). Cells were seeded in 6-well plates, grown to confluence trypsinized (without EDTA for EpRas cells or with EDTA for all other cells used). Subsequently, cells were washed with 67% DPBS (GIBCO, Invitrogen), transferred to 1.5ml Eppendorf tubes and centrifuged 5min, at 1500rpm. Cells were re-suspended in DPBS containing either CM- DiI (4ng/μl final concentration) or DiO (200μM final concentration). Cells stained with CM-DiI were incubated 4 min at 37°C and then 15 min at 4°C. Cells stained with DiO were incubated 20min

at 37°C. After this period cells were centrifuged 5 min at 1500 rpm, the supernatant discarded and cells re-suspended in 100% FCS, centrifuged again and washed 2 times with 67% DPBS. Cells were suspended in 67% DPBS for injection into the embryos. 2 dpf zebrafish embryos were dechorionated and anesthetized with tricaine (Sigma). Using a manual injector (Eppendorf; Injectman NI2), the cell suspension was loaded into an injection needle (15µm internal and 18 µm external diameter). Cells were now injected in 2dpf albino or Tg(fli1:eGFP) zebrafish embryos. After injection, embryos were incubated for 1 h at 31°C and checked for cell presence at 2hpt. Fish with fluorescent cells outside the implantation area at 2hpt were excluded from further analysis. All other fish were incubated at 35°C for the following days.

Tissue preparation for transplantation into zebrafish embryos

Human material from surgical resection specimens was obtained at the Universitätsklinikum Greifswald according to local ethical guidelines and after obtaining informed patient consent. Tumor tissue and control tissue were cut into very small pieces using a scalpel blade. A piece of tissue was then transferred to a 2ml Eppendorf tube, washed with 67% DPBS and stained with 1:500 CM-Dil. The tissue was incubated for 6min at 37°C and 20 min at 4°C. Washing procedures were the same as mentioned above for the cells. Before transplantation small pieces of stained tissue were further disaggregated using Dumont forceps (No.5) into a relative size of 1/5 to 1/2 the size of the yolk. Tissue pieces with the correct size were transferred to agarose plates in which the embryos were laying, ready for transplantation. For tumor and control transplantations, a glass transplantation needle was used to transfer the tissue

into the yolk. With the glass transplantation needle a piece of tissue was picked up, put on top of the yolk and then pushed inside. The yolk usually sealed itself and in the majority of embryos, the tumor remained in the yolk. After transplantation, embryos were incubated for 1h at 31°C, and then embryos were checked for presence of tissue and incubated at 35°C for the following days.

Cell dissociation from tissue

Tissue samples were cut in very small pieces using a scalpel blade. Cut tissue pieces were then transferred to 6ml glass containers with 3ml isolation media (180ml DMEM high glucose, 20ml 100 mM HEPES, 46 ml 5% BSA) and Collagenase (Invitrogen) (50µl of a 6mg/ml stock solution for each 12ml of isolation media). Tissue was incubated in a water bath for 15min at 37°C. The supernatant was decanted and tissue pieces were cut further into smaller pieces using a scalpel blade. Tissue pieces were again incubated 15min at 37°C in 3ml isolation media with collagenase. Afterwards tissue pieces were transferred to 15ml falcon tubes and cells were dissolved by pipetting up and down through serial cut blue pipette tips (5 different diameters). The cell suspension was now filtered through 2 sheets of gaze, into 2ml Eppendorf tubes and centrifuged 5min at 1500rpm. The supernatant was discarded and cells re-suspended in isolation media. The described procedure was then repeated once. For injections, cells were stained with either CM-DiI or DiO and injected into 2dpf zebrafish embryos, as described above.

Western-Blotting

Pancreatic cancer cell lines PaTu-S and PaTu-T were lysed in iced Triton-X-100 lyses buffer (0.1%) containing protease inhibitors (1ml/mg tissue, 10µg/ml aprotinin, 10µg/ml leupeptin, 0,01M sodiumpyrophosphate, 0,1M sodiumfluoride, 1mM dihydrogenperoxide, 1mM L-phenylmethylsulfonylfluoride [PMSF] and 0,02% soybean-trypsin inhibitor). Protein concentration was determined by a modified Bradford-assay (Bio Rad Laboratories, München, Germany) and equal amounts of protein were used in subsequent experiments. Cell lysates were separated by SDS-PAGE on a 7.5% polyacrylamide gel in a discontinuous buffer system and gels were blotted on nitrocellulose membranes (Hybond C, GE Healthcare Europe GmbH). After overnight blocking in NET-gelatin (10mM Tris/HCl pH 8.0, 0.15mM NaCl, 0.05% Tween 20, 0.2% gelatin) immunoblot analysis was performed followed by enhanced chemoluminescence detection (GE Healthcare Europe GmbH) using horseradish peroxidase coupled sheep anti-mouse IgG or goat anti-rabbit IgG GE Healthcare Europe GmbH). Monoclonal E-cadherin antibody (Clone 36), directed against the carboxy-terminus, was purchased from Transduction Laboratories (San Diego, CA, USA) as well as antibodies against α-, β-, and γ-Catenin. A polyclonal G3PDH antibody was purchased from Biozol (Eching, Germany).

Immunofluorescence microscopy

PaTu-S and PaTu-T cells grown on glass coverslips for 24–48 h were washed 3 times with PBS, fixed for 15 min in 4% paraformaldehyde and permeabilised in 0.1% Triton-X-100 for 5 min. Blocking of unspecific binding was achieved by a 1 h incubation in 10% Aurion BSA-c (Aurion, Waageningen, The Netherlands).

Following a primary antibody incubation overnight (dilutions 1:100) and subsequent PBS washing steps detection was per-formed using dichlortriacinyl aminofluoresceine (DTAF) or Cy3-coupled sheep IgG (dilutions 1:200). Nuclei were stained by 30 sec. incubation with DAPI (1:10000 in PBS). After a final washing step in PBS cell were mounted in Vectashield (Vector Labs, Burlingame, CA, USA). Microscopic Images were taken using an AxioCam digital microscope camera on a Zeiss Axiophot microscope.

In vitro migration assay ("scra*tch"-assay*)

The scratch-assay was performed as previously described by Liang *et al.* (2007). Cells were grown to confluence in 6-well dishes and mitomycin C was added at 10 µM for 2 h. Then the cell monolayer was scraped in a straight line with a 200 µl pipette tip. Pictures of the scratch were taken under an invert Olympus microscope at 0h, 12h and 24h.

Histology of zebrafish embryos

Transvers sections at 4 µM thickness were prepared as described before (te Velthuis, et al., 2007). Sections were directly imaged with fluorescence microscopy or differential interference (DIC) microscopy. After fluorescent pictures were taken, Haematoxylin/Eosin (HE) staining was performed as described earlier (Marques, et al., 2008).

Whole mount immunofluorescence of zebrafish embryos

Zebrafish embryos at 2 dpt were fixed overnight in 4%PFA in PBS at 4°C. After fixing, embryos were washed with BSAc 0.1%-TritonX100 1% in PBS (blocking

buffer; 3x10 minutes). Subsequently, the embryos were incubated for 2h in blocking buffer at RT. Incubation with the primary antibody (Mouse anti-Proliferating Cell Nuclear Antigen, PCNA, from Zymed Laboratories, 1:100) was done overnight at 4°C. After washing (3 × 10 minutes) with blocking buffer, embryos were incubated with the secondary antibody (Fluorescein (DTAF)-conjugated AffiniPure Goat anti-Mouse IgG, Jackson Immuno Research Laboratories, Inc., 1:100) for 1h and washed afterwards with blocking buffer (3×10 minutes). Embryos were mounted in 3% methylcellulose to orient them properly for imaging. Imaging was done with confocal scanning laser microscopy (Biorad 1024ES; Software: Biorad Laser sharp 2000).

Imaging, selection and positioning of transplanted zebrafish embryos

Confocal pictures were taken either with the Biorad Confocal microscope 1024ES (Zeiss microscope) combined with Krypton/Argon laser, or the dual laser scanning confocal microscope Leica DM IRBE (Leica) or with the Nikon TE300 confocal microscope and a coherent Innova 70C laser (Chromaphor, Duisburg, Germany). Pictures were further taken by DIC microscopy using the Axioplan 2 microscope with an AxioCam MR5 camera (Carl Zeiss). Further, fluorescent stereomicroscope pictures were taken with the Leica DFC 420C camera attached to a Leica MZ16FA microscope. Two hours post implantation the embryos were anesthetized with tricaine and positioned laterally, with the site of the implantation to the top, on 3% methylcelulose, on a slide with depression. Each time two rows of twenty embryos were screened. Two hours post implantation every embryo that showed cells outside the area of implantation were discarded and not considered for the experiment.

Results

Tumor cell xenografts in zebrafish embryos

Mouse mammary epithelial cells (EpH4), transformed with oncogenic Ras (EpRas), have been used to establish a mouse tumorigenesis model over a decade ago (Oft, et al., 1996). In these EpRas cells, TGF-β signaling causes epithelial to mesenchymal transition (EMT) which transforms cells to a highly invasive phenotype and enables distant metastasis formation when transplanted into nude mice (Oft, et al., 1998). Initially, we evaluated metastasis formation using this well characterized system in the zebrafish cell xenograft model. We transplanted fluorescently labeled EpRas cells into the yolk sac of 2 day old zebrafish embryos to study metastatic behavior *in vivo*. EpRas cells that had been stimulated with TGF-β for 10 days prior to injection, showed metastatic behavior in the zebrafish, comparable to results previously reported in mice (Oft, et al., 1998; Oft, et al., 1996; Waerner, et al., 2006). Following EMT the cells invaded embryonic tissue, entered the circulation and homed in at distant tissues and organs. EpRas TGFβ treated cells were found in blood islands, brain, caudal fin, caudal vein, gill arches, heart, intestine, liver, mandible, optic cup (eye), otic cup, pericardium, somites, swim bladder. However, they had a tendency to invade and home in to muscle tissue, head structures, caudal fin and blood islands (Figure. 1 and Additional File 1). To a lesser extent, we observed invasion of these cells into the liver or other organs of the gastrointestinal tract. In contrast, non-stimulated EpRas control cells remained at the place of injection in the yolk and neither did not invade the developing zebrafish nor did they enter blood circulation (Figure. 1 and Additional file 2). In three independent experiments the average percentage of migrating cells observed for the EpRas TGF-β-stimulated

cells was 46.6% (SD±2.0; p-value < 0.001) compared to 0.5% (SD± 0.7; p-value<0.001) for the parental EpRas cells (see Additional file 1). Furthermore, the TGF-β stimulated EpRas cells formed tumor cell masses in the developing zebrafish (Figure. 1), which resemble the formation of metastases in nude mice (Waerner, et al., 2006). In the zebrafish, cells begin to invade the embryo already several hours after injection (on average 4 hours post injection) (see Additional File 3) and tumor cell masses are visible as early as 3 days post implantation (dpi).For optimal visualization, we used the transgenic zebrafish line, Tg(fli1:eGFP) (Stoletov, et al., 2007; Waerner, et al., 2006), which expresses GFP under the *fli1* promoter (an early endothelial marker) and therefore exhibits a green fluorescent vasculature (Stoletov, et al., 2007; Lawson, et al., 2002). In a time lapse movie (see Additional file 4; rate: 1 frame/ minute) we show an example of fluorescently labeled EpRas TGF-β cells (3 dpi) which have invaded the zebrafish body, have translocated into the vasculature and have colonized at distant sites in the zebrafish larvae (5 dpf). Some cells are visible in the blood stream whereas others have extravasated from the vasculature. Evaluation of metastasis formation in the zebrafish model is therefore significantly faster than in currently used mouse models, where it may take several weeks until metastases become detectable (Waerner, et al., 2006). The sensitivity of the zebrafish tumor xenograft model further allows observation of individual cells and their daughter cells *in vivo*.

We also compared the two established human pancreatic tumor cell lines, PaTu8988-S and PaTu8988-T (Elsässer HP, 1992) (referred to herein as PaTu-S and PaTu-T) in their invasive and metastatic potential in a single zebrafish. Both sister cell lines originate from liver metastases of the same human pancreatic

adenocarcinoma (Elsässer HP, 1992). E-Cadherin expression in PaTu-S cells (Figure 2A and 2B (a)) correlates with the maintenance of functional cell-cell contacts (Figure 2B) and a reduced tendency of cells to migrate (Figure2C) (Menke, et al., 2001; Mayerle, et al., 2005). Whereas PaTu-S cells show localization of E-cadherin/β-catenin complexes at the plasma membrane (Figure 2B (e)), PaTu-T cells lack E-Cadherin expression (Figure 2A and 2B (b)) and β-catenin is mainly localized in the cytoplasm (Figure 2B (d). This observation is paralleled by enhanced migratory capabilities of PaTu-T cells compared to PaTu-S cells, which we confirmed in an *in vitro* migration assay ('scratch assay' (Cha, et al., 1996) (Figure 2C and Additional file5).

We then labeled PaTu-S cells with green fluorescence and PaTu-T cells with red fluorescence. When implanted successively in the yolk sac of the same zebrafish embryo, green PaTu-S cells remained in the yolk, whereas red PaTu-T cells displayed invasion and metastatic behavior (Figure 2D and Additional file 1). Similar results were observed when cells were mixed prior to injections (data not shown).

PaTuT cells were found in the brain, caudal vein, gill arches, gut, heart, intestine, liver, operculum, pericardium, somites, and swim bladder. They showed a tendency to invade and home in to organs of the gastrointestinal tract. Micrometastasis was often observed in organs such as the liver, the gut and the intestine. Invasion and homing of these cells into muscle tissue was observed to a lesser extent. This behavior was qualitative different from what we observed for TGF-β treated EpRas cells. We further tested the metastatic behavior of PaTu-T cells in homozygous *cloche* mutants (cloche$^{-/-}$), which lack a functional vasculature and circulation (Herpers, et al., 2008) Additional File 6). In contrast

to control zebrafish, no metastatic behavior was observed in the cloche$^{-/-}$-fish, indicating that the observed invasion/migration of PaTu-T cells indeed involves metastasis formation through the vascular sys- tem. Zebrafish were followed until three days post injections (Figure 2E; see Additional files 1 and 7).

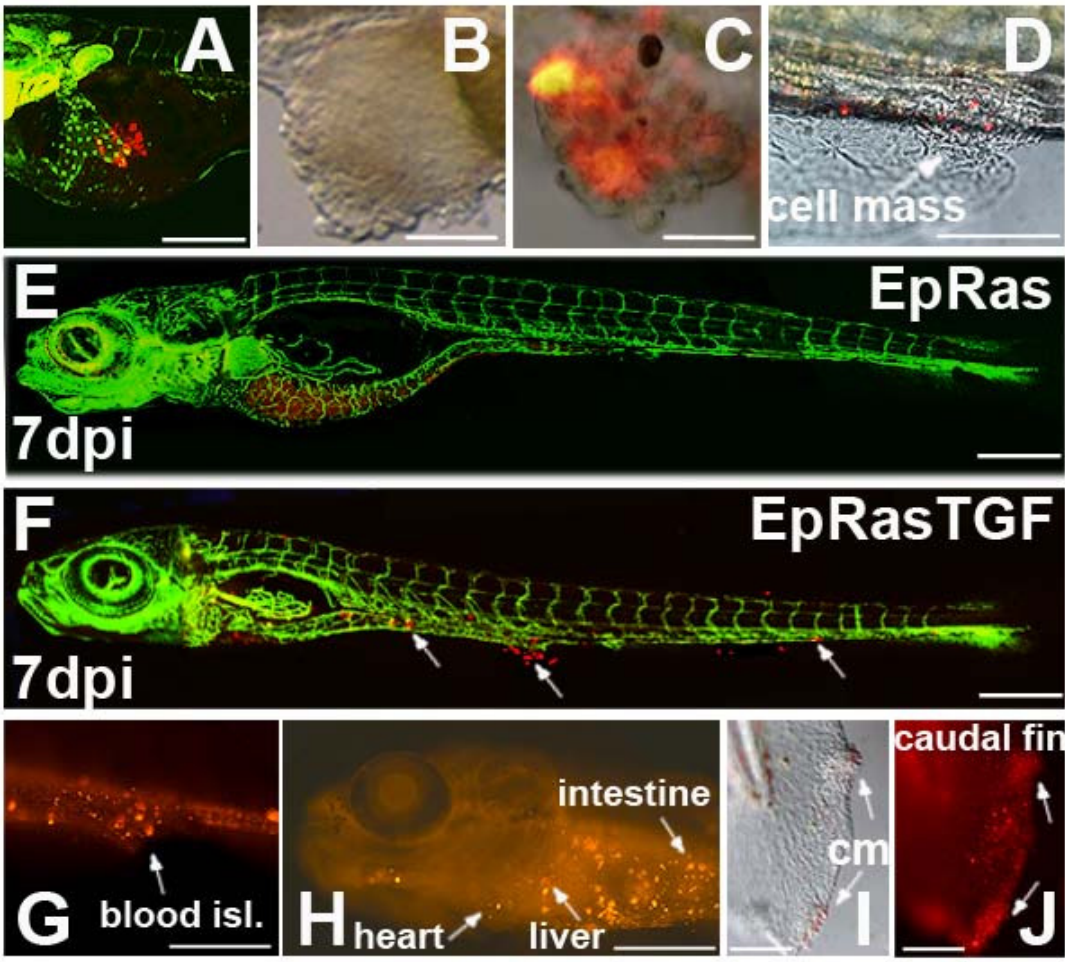

Figure 1 Migration and cell mass formation of Ha-Ras transformed mouse mammary epithelial cells injected into the yolk sac of zebrafish embryos. EpRas (parental) and EpRas cells stimulated with TGF-β (EpRasTGF) were labeled and ectopically injected into the yolk sac of 2 dpf zebrafish embryos. In A, E and F transgenic zebrafish embryos expressing GFP under an endothelial promoter (Tg(fli1:eGFP) were used. An example of newly injected EpRas cells at 1 hour post injection is given in (A). In (B) an ectopic tumor cell mass formed in the yolk sac by EpRasTGF cells is shown. Examples of cell masses formed by EpRasTGF cells at distance from the place of injection are shown for the tail region (C) and blood islands with surrounding ventral fin (D). Pictures in B-D were taken at 3 dpi. While EpRas cells remained in the yolk and never invaded the embryo (E), EpRasTGF cells invaded, migrated and formed distant micrometastasis, which are indicated with arrows (F). Red fluorescence of cells is still visible after 7 dpi (E, F).Images G to J show tumor cell masses (cm) and migrated cells in blood islands (blood isl.), the liver, heart, intestine and the caudal fin of 6 dpi larvae. Scales shown are for A: 200 µm; D-H: 600 µm, for B, C, I and J: 100 µm. 3D reconstructions of EpRAS and EpRasTGF cells in zebrafish larvae are shown in two supplemental movies (see Additional files 2 and 3).

Human tumors transplanted into zebrafish display metastatic behavior

We then pursued our primary goal to employ the zebrafish also as a simple, fast and effective test system for metastasis formation of primary human tumors. After informed patient consent small fragments of tumor explants from pancreas, colon and stomach carcinoma, as well as tumor free areas from the same resection specimen were fluorescently labeled with CM-DIL and directly xenotransplanted into the yolk sac of zebrafish embryos. Tumor and non-tumor control cells were followed live by laser scanning confocal microscopy.

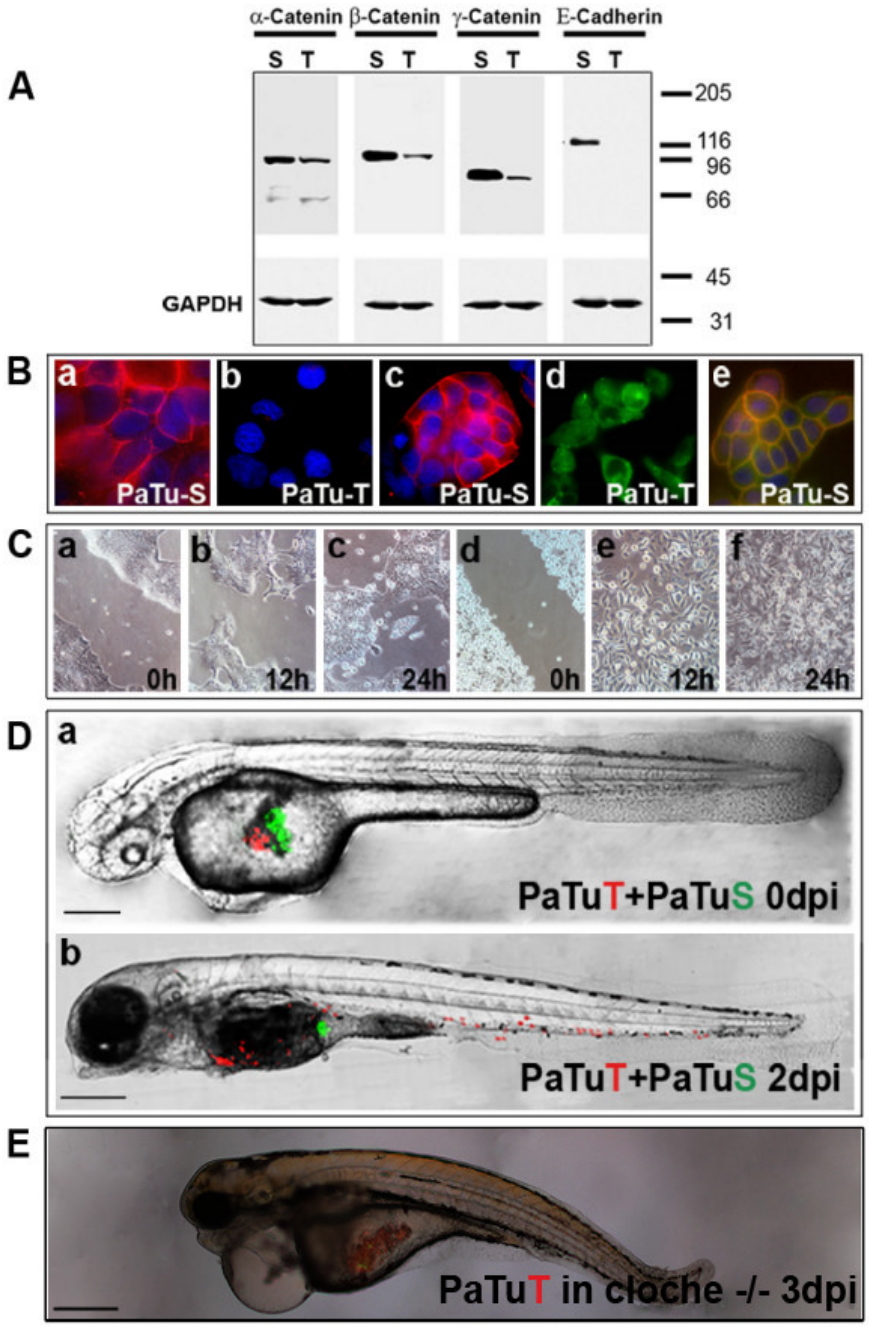
A
α-Catenin
β-Catenin
γ-Catenin
E-Cadherin
S T S T S T S T
205
116
96
66
45
31
GAPDH
B
a
PaTu-S
b
PaTu-T
c
PaTu-S
d
PaTu-T
e
PaTu-S
C
a
0h
b
12h
c
24h
d
0h
e
12h
f
24h
D
a
PaTuT+PaTuS 0dpi
b
PaTuT+PaTuS 2dpi
E
PaTuT in cloche -/- 3dpi

Figure 2 Implantation of two pancreatic cancer cell lines into the same zebrafish embryo. **(A**) Western blot analysis shows that PaTu-S but not PaTu-T cells express E-cadherin and both express α-, β- and γ-catenin. GAPDH expression is shown as a control. (**B**) Cellular localization of E-cadherin and β-catenin was analyzed by immunofluorescence. E-cadherin expression is shown for PaTu-S cells (a) and absence of E-cadherin expression for PaTu-T cells (b). Dapi staining was used to visualize cell nuclei in blue. β-catenin localization is shown for PaTu-S (c) and for PaTu-T (d). Co-localization of E-cadherin (green) and β-catenin (red) in PaTu-S cells is indicated by yellow staining of the plasma membrane (e). (**C**) An in vitro migration assay ('scratch assay') shows differences in migration of the two cell lines (PaTu-S: a-c and PaTu-T: d-f). Similar results were obtained in four independent experiments. Gap closure (gap width) over time is shown in Additional file 5. (**D**) Non-invasive PaTu-S cells (green) and invasive PaTu-T cells (red) were implanted consecutively in the same embryo (a and b) (Scales: 250 μm (a) and 300μm (b)). (**E**) Homozygous cloche mutants [17] were injected with PaTu-T cells and followed over time. Shown is an example of a cloche^{-}/$^{-}$ zebrafish at 3 dpi (scale bar: 300 μm). In contrast to control zebrafish none of the tested cloche^{-}/$^{-}$mutants showed any sign of metastatic behavior (see Additional file 1 and Additional file 7). The cloche phenotype and its lack of a functional vasculature and circulation is observable by DIC microscopy (see Additional file 6).

Tumor cells started to invade the embryo on average 12 hours post injection and micrometastasis formation was visible as early as 24 h post injection. In parallel, we also investigated and compared the invasive and metastatic behavior of tumor cells that had been dissociated from primary human tumors by collagenase digestion prior to transplantation.

In total, pancreatic tumors of four different patients were analyzed. Three had carcinomas of the pancreas head and one had an adenocarcinoma of the

ampulla vateri with infiltration of the pancreas (cancer grades and pTMN stages for all tumors are shown in table 1). On average 59.8% (SD±5.2) of transplanted pancreatic tumor fragments showed invasion and migration in the developing zebrafish (table 1 and Figure 3).

Evaluation criteria for invasion and migration were that at least 5 cells had to be identified outside of the yolk and detectable within the developing zebrafish (table 1). Development of micrometastasis was assessed by the presence of daughter cells at 3dpt. The results are listed in table 1 and in Figure 4 examples of micrometastasis in different tissues detected in sections of 5dpf zebrafish are shown at high resolution (Figure 4B, C, D, G, H, K and 4L). An example showing proliferating pancreatic tumor cells and the initial formation of a micrometastasis is given in Figure 5(E). Cell division is further indicated by PCNA immunostaining of invasive tumor cells in the zebrafish embryo (see Additional file 8). After 5dpf embryos fall under strict local animal experiment regulations, therefore most embryos were not followed for longer periods. It is likely that the number of micrometastasis would still increase over time.

Invasive cells were found for pancreatic tumors in blood islands, caudal fin, caudal vein, gut, heart, hindbrain, intestine, liver, mesonephric duct, mesonephric tubule, mandible, operculum, pericardium, somites, swim bladder, for the colon tumor in caudal vein, gut, heart, intestine, liver, pericardium; and for the stomach tumors in the caudal vein, gill arches, heart, intestine, liver, *mandible, otic cup, pericardium.*

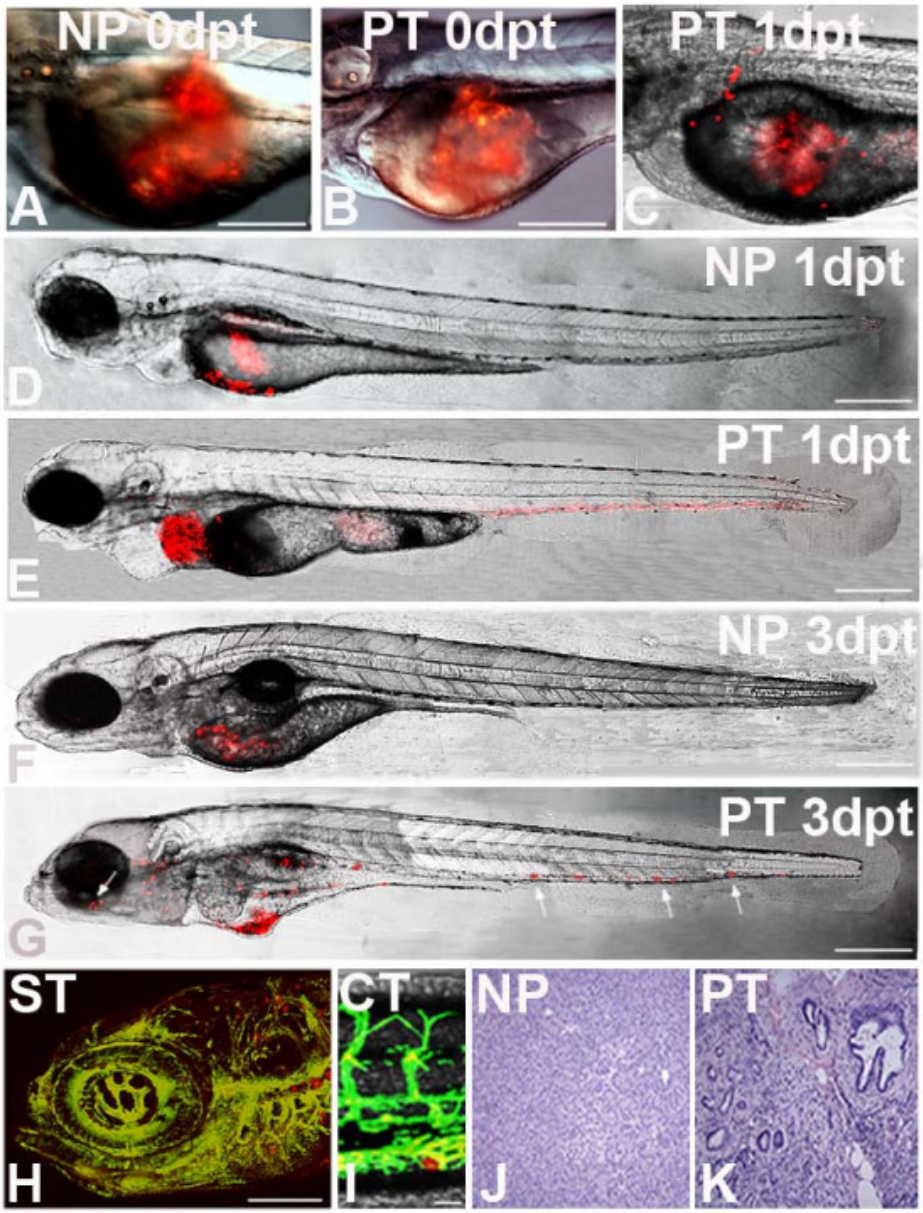
NP 0dpt
A
PT 0dpt
B
PT 1dpt
C
NP 1dpt
D
PT 1dpt
E
NP 3dpt
F
PT 3dpt
G
ST
H
CT
I
NP
J
PT
K

Figure 3 Tumor transplantation in zebrafish. Primary human tumours of the pancreas, the stomach and the colon were transplanted into 2 dpf embryos. Non-tumour tissue was used as control. At the respective time points indicated laser confocal microscopy images were taken. Images A and B show newly transplanted embryos with normal pancreas (NP) and pancreatic tumour (PT) respectively. Image C shows an example of an embryo transplanted with an adeno-carcinoma of the pancreas at 1 day post transplantation (dpt) in which tumour cells have already invaded the embryo. Images D to G are confocal microscopy images of transplanted embryos at 1 dpt and 3 dpt. Normal, non-transformed pancreas transplants remain in the yolk and cells never migrate or spread in the embryo (D and F). In contrast, tumour transplants show metastatic behaviour (E and G). Some of the cell masses are marked with arrows, including one formed near the retina of the eye (G). On the bottom an example is shown for brain metastases of a transplanted gastric cancer (stomach tumour) in a Tg(fli1:eGFP) zebrafish 3 days after implantation(H). Cell masses are visible in the rhombencephalon (hindbrain) surrounding the otic capsule and near the gill arches (H). A colon tumour transplant shows a migrated tumour cell in the caudal vein region at 3 dpt (I). Both pictures (H and I) were taken by confocal microscopy. HE staining of representative histological sections of normal human pancreas tissue (J) and pancreatic cancer (K) are shown. Scales shown are in A-E: 300 µm; F, G: 400 µm; in H: 100 µm and in I: 20 µm.

Similar to preferences observed for PaTu-T cells, tumor cells of implanted gastrointestinal tumor tissue fragments had a tendency to invade and home in to organs of the gastrointestinal tract. Micrometastasis was often observed in the liver, the gut and the intestine. Homing of these cells in muscle tissue and the formation of micrometastasis was rarely observed. Although we observed qualitative differences for the preferential homing of the two cell lines tested

(PaTu-T and TGF-β treated EpRAS cells), a future study, with a larger cohort of tumor specimen and tumor types is necessary to determine tumor specific preferences.

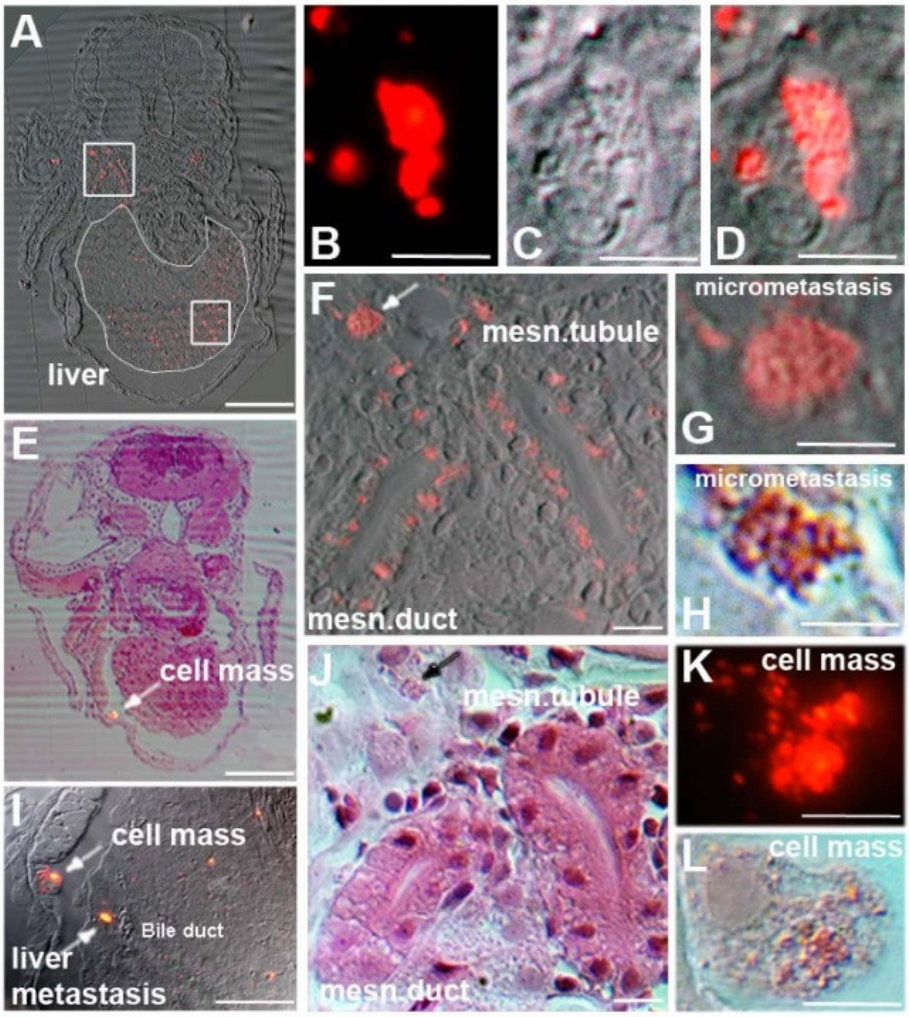

Figure 4 Histology of zebrafish embryos transplanted with a human pancreatic tumor. Transversal sections of zebrafish embryos trans-planted with a primary human pancreatic tumor show the presence of micro-metastases in different tissues at 3 dpt in 5 day old zebrafish. (A) The transversal section is approximately 40 µm caudal to the anterior end of the liver. The liver is circled with a thin white line and contains many tumor cells and some micrometastases. The square in the liver contains several micrometastases, of which one is depicted in higher magnification in B (fluorescence), C (DIC) and D (overlay). The upper square shows tumor cells and micrometastases around the mesonephric tubule (msn. tubule) and the mesonephric duct (msn. duct). The enlargement of the square is shown in F and J (HE staining). In both, F (white arrow) and J (black arrow) micrometastasis is indicated (high magnifications in G and H). In (E) HE staining of a transversal section approximately 24 µm rostral to the anterior start of the liver is shown and overlaid with the fluorescent image. A larger cell mass is indicated by an arrow. The same cell mass is indicated in I in which also a liver metastasis is seen. The cell mass is shown in high magnification in K (fluorescent picture) and in L (HE staining). Scales shown are A and E 1 mm, B-D, F-H and J-L 10 µm and in I: 500 µm.

Figure 3 shows examples of fish embryos directly after transplantation (A, B) and at 1 and 3dpt (C-G). Cell invasion and micrometastasis formation of pancreatic tumor cells is clearly detectable 24 h after transplantation (E). Similar results were also obtained for transplanted tissue fragments of a colon adenocarcinoma (43.9% invasion and migration) and two moderately differentiated adenocarcinomas of the stomach (average 53.5%, SD±1.2) (p-values in all tumor experiments were <0.001). As a control for the tumors we used colon and gastric mucosal fragments or peritumoral, non-transformed tissue of the respective tissue explants from the same patients. In the pancreas the non-transformed

tissue controls mostly showed histological manifestations of chronic pancreatitis and only one was considered as having a normal pancreatic histology.

Histological sections of control pancreas and of pancreatic cancer tissue of human patients are shown in Figure 3(J, K). In all control transplantations of chronic pancreatitis specimen and of fragments of normal pancreas, colon and stomach tissue cellular invasion and migration was never observed (see Additional file 1 and Figure 3D, F). In addition, we also tested the metastatic behavior of a benign tumor. Tissue fragments of adenomateous colonic polyps (0,4cm and 1cm) were investigated, which had not yet invaded through the lamina muscularis mucosae. No metastasis was observed for either of them in the zebrafish embryo (Additional file 1). Comparable results were seen when cells were dissociated from tumor or control tissue samples prior to their injection into the zebrafish. All four primary pancreatic tumor cells showed cellular invasion and migration with an average of 48.8% (SD±9.0) (see Additional file 1). In the case of dissociated primary colon and stomach tumor cells 44.4% and 35.3% of cell injections, respectively, resulted in cellular invasion and migration (see Additional file 1).

Xenotransplantation experiments of tumor fragments as well as the injection of isolated primary tumor cells allowed discriminating between non-invasive chronic pancreatitis and infiltrating pancreatic adenocarcinoma. In real-time, we show an example of pancreatic tumor cells in the zebrafish 1 day after a pancreatic cancer fragment was transplanted (see Additional file 9). This movie shows circulating tumor cells and tumor cells which have extravasated into the perivascular tissue of a 3 day old zebrafish. A moving primary human tumor cell passing through the caudal vein and into an intersegmental vessel is also visible.

In a supplemental movie we show how a pancreatic tumor cell is slowly traversing through the caudal vein of a 3 dpt Tg(fli1:eGFP) zebrafish (see Additional file 10). In Figure 4 histological sections of zebrafish embryos transplanted with a pancreatic human tumor are shown at 3 dpt. Examples of micrometastasis in the liver (B, C and D) and near the mesonephric duct (G and H) are shown at higher magnifications. A cell mass is further shown in K and L.

Organotopic transplantation of primary human tumor cells in the fish liver and the effects of protease inhibitors on the invasiveness of implanted tumor cells and tumor fragments

Some xenograft models that have been established in the mouse involve the orthotopic transplantation of specific human tumors and tumor cells (Sharpless, et al., 2006; Frese, et al., 2007). Surgical orthotopic implantations (SOI) of tumor cells or of resected primary tumor fragments into immune deficient mice have proven useful for studying their growth and metastatic potential (Hoffman, 2005).

Here we transplanted freshly dissociated primary pancreatic tumor cells and normal pancreatic control cells into the liver of zebrafish larvae. For these experiments, we used the Tg(fli1:eGFP) transgenic zebrafish line (with the advantage of a fluorescent vasculature), which allows an exact localization and injection into the highly vascularized liver. Primary cells of control pancreatic tissue, when transplanted into the liver, remained at the site of the injection and did not invade the developing zebrafish nor did they enter the blood circulation (Figure. 5). In contrast, primary tumor cells invaded the neighboring tissue, entered the circulation and migrated and homed in on distant tissues and organs (Figure. 5).

Furthermore we investigated in our zebrafish xenotransplantation model the effects of protease inhibitors on the invasiveness of implanted tumor cells and tumor fragments. Two different protease inhibitors were able to inhibit the invasiveness of tumor cells and of a primary pancreatic tumor (see Additional file 1).

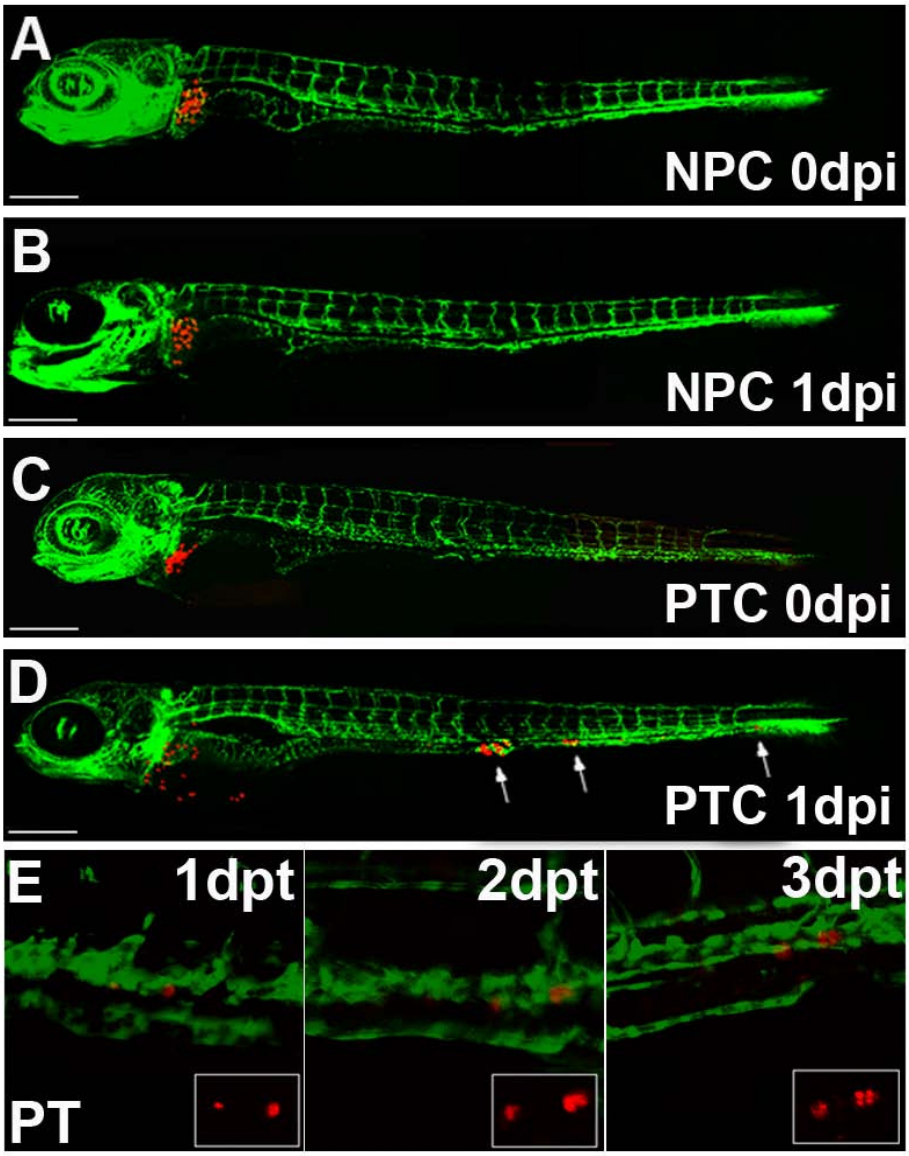

Figure 5 Implantation of primary human tumor cells into the zebrafish liver. (A-D) Organotopic implantation of primary tumor cells into the liver of larvae of Fli-1 zebrafish. Representative examples of zebrafish at 5 days of development injected with primary normal pancreatic cells (NPC) and with primary dissociated pancreatic tumor cells (A and C, respectively) are shown. The same fish are depicted at 1 day post injection (1 dpi). While normal pancreatic cells remained at the site of implantation in the liver (B), pancreatic tumor cells invaded the embryo and formed distant metastases, indicated with arrows (D). Scales indicated are: A-D 300 μm. Individuals were followed for up to 7 dpi and untransformed control cells never invaded the host embryos and remained in the liver for the entire observation period (data not shown). Image E shows an example of proliferating tumor cells of a transplanted pancreatic tumor fragment on consecutive days. The single cell on the right seen at 1 day post transplantation is divided into two daughter cells on 2 dpt and four cells are visible at 3 dpt. Dual color laser scanning confocal images of the Fli-1 zebrafish are shown and in the smaller insert the red fluorescence of the CM-DiI labeled tumor cells can be seen.

Discussion

Analysis of tumor metastasis in an in vivo model depends on intrinsic tumor cell properties, host factors and the experimental techniques used. The engraftment of human neoplasms in the mouse normally requires the use of nude (athymic) or severe combined immune deficient (SCID) mice that are T-and B-cell deficient. In these animal models further attention has to be paid to the site of implantation, as host factors may differ between tissues and organs. Nude mice also have an upregulated innate immunity and elevated numbers of natural killer cells and tumoricidal macrophages, which may limit tumor growth or even prevent metastasis. Efficacy of pharmacological and toxicological studies in

murine xenograft models normally use tumor growth, body weight loss and mortality as parameters of toxicity. These studies are cumbersome, time consuming and drug activity against xenografts does not always correlate with its clinical activity (Johnson, et al., 2001).

In our study we established the zebrafish as a robust *in vivo* model for investigating invasiveness and metastatic behavior of human primary tumors. It is known that early zebrafish embryos do not reject xenotransplanted human cells (Topczewska, et al., 2006; Haldi, et al., 2006; Nicoli, et al., 2007), whereas 1 month old zebrafish already need to be immune suppressed (Stoletov, et al., 2007).

The early embryos and larvae used here did not reject the primary tumor xenografts, most likely due to the fact that their immune system is not fully developed. It has been observed that while lymphopoiesis and lymphoid organogenesis are initiated at the middle to late embryo period, they remained in their rudimentary and immature form throughout the early larval stages. The major maturation events leading to immune competence occur between 2 and 4 weeks post fertilization (wpf), coinciding with the larval to juvenile transitory phase (Lam, et al., 2004).

The observed metastasis in an animal model primarily should reflect the intrinsic metastatic ability of the tumor cells, but may depend to some extent also on the experimental system. Other experimental animal systems have demonstrated that only a small subset of metastatic cells (approximately 2%) survive and grow at secondary sites (Weiss, 1990). The significantly higher percentage of micrometastases observed using fish embryos may in part reflect the absence of the humeral immune response and/or other selective pressures on tumors cells

which would lead to tumor cell death following extravasation into secondary organs.

The transparency of the fish embryo enables an investigation of fluorescently labeled tumor cells in real time and at high resolution. The unique availability of transgenic zebrafish without a functional vasculature (Herpers, et al., 2008) further allowed us to show that the metastatic spread of tumor cells in zebrafish embryos involves the vascular system. Even the very early steps of invasion, circulation of tumor cells in blood vessels, colonization at secondary organ sites and metastasis formation can be observed this way-something which to date cannot be investigated in established mouse tumor models. Advantages of the model system such as good accessibility, easy handling, low costs and short incubation times make it a promising system for future functional studies in primary tumors.

The experiments described here provide the basis for the future development of a screening methodology of drugs, which inhibit invasion and metastasis of human tumors. Recently, adult zebrafish with an almost entirely transparent body have been described, as a novel tool for *in vivo* transplantation analysis (White, et al., 2008). These will be of interest for additional comparative analysis of metastasis formation of primary tumors in the immune competent animal.

Conclusion

We demonstrate here the applicability of the zebrafish embryo as an *in vivo* model for the analysis of metastatic behavior of human tumor cells, including resection specimen from human tissue. High resolution imaging of live zebrafish has and will further assist in better understanding the underlying mechanisms of

cancer cell invasion and metastasis formation. Advantages of the model system such as good accessibility, easy handling, low costs and rapidness are unparalleled by other vertebrate organisms and make it a promising system for future functional studies in primary tumors. The advantages of the "short term" zebrafish embryo model could nicely complement established "longer term" tumor models, e.g. mouse models, and may be a valuable and efficient tool to evaluate novel therapeutic strategies for cancer.

Acknowledgements

We would like to thank G. Posern for supplying the mouse cells, Davy de Witt for his part of animal welfare and Joost Woltering and Jaya Besser for critical remarks on the manuscript. We would further like to acknowledge and thank the Tübingen 2000 Screen Consortium and Exelixis, as the original source of the cloche mutant embryos. This work was supported by grants from the Portuguese foundation for Science and Technology (SFRH/ BD/27262/2006), the Deutsche Krebshilfe (10-2031-Le) and the Alfried-Krupp-Foundation.

References

Jemal A, Siegel R, Ward E, Murray T, Xu J, Thun MJ (2007) *Cancer Statistics, 2007. CA*: A Cancer Journal for Clinician, 57(1):43-66.

Fidler IJ (2003) *The pathogenesis of cancer metastasis: the 'seed and soil' hypothesis revisited.* Nature Reviews: Cancer, 3(6):453-458.

Zon LI, Peterson RT (2005) *In vivo drug discovery in the zebrafish.* Nature Reviews: Drug Discovery. 4(1):35-44.

Kari G, Rodeck U, Dicker AP (2007) *Zebrafish: An Emerging Model System for Human Disease and Drug Discovery.* Clinical Pharmacology Therapy, 82(1):70-80.

den Hertog J (2005) *Chemical Genetics: Drug Screens in Zebrafish.* Bioscience Report, 25(5):289-297.

Parng C, Seng WL, Semino C, McGrath P (2002) *Zebrafish: A Preclinical Model for Drug Screening.* ASSAY and Drug Development Technologies, 1(1):41-48.

Goessling W, North TE, Zon LI: *New Waves of Discovery: Modeling Cancer in Zebrafish.* Journal of Clinical Oncology, 25(17):2473-2479.

Hendrix MJC, Seftor EA, Seftor REB, Kasemeier-Kulesa J, Kulesa PM, Postovit L-M: (2007) *Reprogramming metastatic tumor cells with embryonic microenvironments.* Nature Reviews Cancer, 7(4):246-255.

Grunwald DJ, Eisen JS (2002) *Headwaters of the zebrafish [mdash] emergence of a new model vertebrate.* Nature Reviews: Genetics, 3(9):717-724.

Langenau DM, Traver D, Ferrando AA, Kutok JL, Aster JC, Kanki JP, Lin S, Prochownik E, Trede NS, Zon LI, Look AT (2003) *Myc-Induced T Cell Leukemia in Transgenic Zebrafish.* Science, 299(5608):887-890.

Stoletov K, Montel V, Lester RD, Gonias SL, Klemke R (2007) *High-resolution imaging of the dynamic tumor cell vascular interface in transparent zebrafish.* Proceedings of the Natural Academy of Sciences, 104(44):17406-17411.

Lee Lisa MJ, Seftor EA, Bonde G, Cornell RA, Hendrix MJC (2005) *The fate of human malignant melanoma cells transplanted into zebrafish embryos: Assessment of migration and cell division in the absence of tumor formation.* Developmental Dynamics, 233(4):1560-1570.

Topczewska JM, Postovit L-M, Margaryan NV, Sam A, Hess AR, Wheaton WW, Nickoloff BJ, Topczewski J, Hendrix MJC (2006) *Embryonic and tumorigenic pathways converge via Nodal signaling: role in melanoma aggressiveness.* Nature Medicine, 12(8):925-932.

Haldi M, Ton C, Seng W, McGrath P: Human melanoma cells transplanted into zebrafish proliferate, migrate, produce melanin, form masses and stimulate angiogenesis in zebrafish. Angiogenesis 2006, 9(3):139-151.

Nicoli S, Ribatti D, Cotelli F, Presta M (2007) *Mammalian Tumor Xenograft Induce Neovascularization in Zebrafish Embryos.* Cancer Research, 67(7):2927-2931.

Nicoli S, Presta M (2007) *The zebrafish/tumor xenograft angiogenesis assay.* Nature Protocols, 2(11):2918-2923.

Herpers R, Kamp E van de, Duckers HJ, Schulte-Merker S (2008) *Redundant Roles for Sox7 and Sox18 in Arteriovenous Specification in Zebrafish.* Circulation Research, 102(1):12-15.

Liang C-C, Park AY, Guan J-L (2007) *In vitro scratch assay: a convenient and inexpensive method for analysis of cell migration in vitro.* Nature Protocols, 2(2):329-333.

te Velthuis AJW, Ott EB, Marques IJ, Bagowski CP (2007) *Gene expression patterns of the ALP family during zebrafish development.* Gene Expression Patterns, 7(3):297-305.

Marques I, Leito J, Spaink H, Testerink J, Jaspers R, Witte F, Berg S van den, Bagowski C (2008) *Transcriptome analysis of the response to chronic constant hypoxia in zebrafish hearts.* Journal of Comparative Physiology B: Biochemical, Systemic, and Environmental Physiology, 178(1):77-92.

Oft M, Peli J, Rudaz C, Schwarz H, Beug H, Reichmann E (1996) *TGF-beta1 and Ha-Ras collaborate in modulating the phenotypic plasticity and invasiveness of epithelial tumor cells.* Genes & Development, 10(19):2462-2477.

Oft M, Heider K-H, Beug H (1998) *TGF[beta] signaling is necessary for carcinoma cell invasiveness and metastasis.* Current Biology, 8(23):1243-1252.

Waerner T, Alacakaptan M, Tamir I, Oberauer R, Gal A, Brabletz T, Schreiber M, Jechlinger M, Beug H (2006) *ILEI: A cytokine essential for EMT, tumor formation, and late events in metastasis in epithelial cells.* Cancer Cell, 10(3):227-239.

Lawson ND, Weinstein BM (2002) *In Vivo Imaging of Embryonic Vascular Development Using Transgenic Zebrafish.* Developmental Biology, 248(2):307-318.

Elsässer H, PL U, Agricola B, Kern HF (1992) *Establishment and characterization of two cell lines with different grade of differentiation derived from one primary human pancreatic adenocarcinoma.* Virchows Archive B: Cell Pathology Including Molecular Pathology, 61(5):295-306.

Menke A, Philippi C, Vogelmann R, Seidel B, Lutz MP, Adler G, Wedlich D (2001) *Down-Regulation of E-Cadherin Gene Expression by Collagen Type I and Type III in Pancreatic Cancer Cell Lines.* Cancer Research, 61(8):3508-3517.

Mayerle J, Schnekenburger J, Kruger B, Kellermann J, Ruthenburger M, Weiss FU, Nalli A, Domschke W, Lerch MM (2005) *Extracellular Cleavage of E-Cadherin by Leukocyte Elastase During Acute Experimental Pancreatitis in Rats.* Gastroenterology, 129(4):1251-1267.

Cha D, OB P, O'Toole EA, Woodley DT, Hudson LG (1996) *Enhanced modulation of keratinocyte motility by transforming growth factor-alpha (TGF-alpha) relative to epidermal growth factor (EGF).* Journal of Investigative Dermatology 106(4):590-597.

Sharpless NE, DePinho RA (2006)*The mighty mouse: genetically engineered mouse models in cancer drug development.* Nature Reviews: Drug Discovery, 5(9):741-754.

Frese KK, Tuveson DA (2008) *Maximizing mouse cancer models*. Nature Reviews Cancer, 7(9):654-658.

Hoffman R (2005) *Orthotopic metastatic (MetaMouse) models for discovery and development of novel chemotherapy.* Methods in Molecular Medicine, 111:297-322.

Johnson JI, S D, Zaharevitz D, Rubinstein LV, Venditti JM, Schepartz S, Kalyandrug S, Christian M, Arbuck S, Hollingshead M, Sausville EA (2001) *Relationships between drug activity in NCI preclinical in vitro and in vivo models and early clinical trials.* British Journal of Cancer, 84:1424-1431.

Lam SH, Chua HL, Gong Z, Lam TJ, Sin YM (2004) *Development and maturation of the immune system in zebrafish, Danio rerio: a gene expression profiling, in*

situ hybridization and immunological study. Developmental & Comparative Immunology, 28(1):9-28.

Weiss L (1990) *Metastatic inefficiency.* Advances in Cancer Research, 54:159-211.

White RM, Sessa A, Burke C, Bowman T, LeBlanc J, Ceol C, Bourque C, Dovey M, Goessling W, Burns CE, Zon LI (2008) *Transparent Adult Zebrafish as a Tool for In Vivo Transplantation Analysis.* Cell Stem Cell, 2(2):183-189.

CHAPTER 4

RETINOIC ACID RECEPTOR (RAR) ANTAGONISTS INHIBIT MIR-10A EXPRESSION AND BLOCK METASTATIC BEHAVIOR OF PANCREATIC CANCER

Ines J. Marques*, Frank Ulrich Weiss*, Joost M. Woltering, Danielle H. Vlecken, Ali Aghdassi, Lars Ivo Partecke, Claus-Dieter Heidecke, Markus M. Lerch and Christoph P. Bagowski

* These authors have equally contributed for this manuscript

Article published in ***Gastroenterology.*** **2009. 137(6):2136-45**

All supplemental material can be found online on:
http://www.gastrojournal.org/article/S0016-5085(09)01557-1/addOns

Abstract

The infiltrating ductal adenocarcinoma of the pancreas is among the most lethal of all solid malignancies, largely due to a high frequency of early metastasis. We identify microRNA-10a (miR-10a) as an important mediator of metastasis formation in pancreatic tumor cells and investigate the upstream and downstream regulatory mechanisms of miR-10a. Northern blot analysis revealed elevated expression levels of miR-10a in metastatic pancreatic adenocarcinoma. The role of miR-10a was analyzed by Morpholino and siRNA transfection of pancreatic carcinoma cell lines and resected specimen of human pancreatic carcinoma. Metastatic behavior of primary pancreatic tumors and cancer cell lines was tested in xenotransplantation experiments in zebrafish embryos. We show that miR-10a expression promotes metastatic behavior of pancreatic tumor cells and that repression of miR-10a is sufficient to inhibit invasion and metastasis formation. We further demonstrate that miR-10a is a retinoid acid target and that retinoic acid receptor (RAR) antagonists effectively repress miR-10a expression and completely block metastasis. This anti-metastatic activity can be prevented by specific knock down of HOX genes, HOXB1 and HOXB3. Interestingly, suppression of HOXB1 and HOXB3 in pancreatic cancer cells is sufficient to promote metastasis formation. These findings suggest that miR-10a is a key mediator of metastatic behavior in pancreatic cancer which regulates metastasis via suppression of HOXB1 and HOXB3. Inhibition of miR-10a expression (with RAR antagonists) or function (with specific inhibitors) is a promising starting point for anti-metastatic therapies.

Introduction

Pancreatic cancer is a highly invasive malignancy which is characterized by early metastasis formation. Although metastases spawned by malignant tumors are responsible for over 90% of all cancer death (Jemal, et al., 2007), our understanding of the mechanisms involved in metastasis formation is still rather limited.

There is increasing evidence that microRNAs can function as oncogenes or as tumor suppressors and that differential expression of specific microRNAs is critically involved in the progression of many cancers (Johnson, et al., 2005; Esquela-Kerscher, et al., 2006; He, et al., 2005; Tavazoie, et al., 2008). Large scale transcriptome analysis data are available for microRNA signatures of different human tumors (Calin, et al., 2006; Lu, et al., 2005) including pancreatic cancer (Roldo, et al., 2006; Bloomston, et al., 2007). These studies used microarray technology to reveal specific microRNA expression profiles in specimen from pancreatic adenocarcinoma, which could be differentiated from normal pancreatic tissue and chronic pancreatitis.

In a recent publication, it was shown that miR-10b is highly expressed in human breast tumors and that expression correlates with metastatic potential (Ma, et al., 2007). In pancreatic cancer miR-10b expression is not elevated, but instead an upregulated expression of the related miR-10a has been described (Roldo, et al., 2006; Bloomston, et al., 2007) Both microRNAs belong to the same microRNA family, but miR-10b is located in the HOXD cluster on chromosome 2, whereas miR-10a is present in the HOXB cluster on chromosome 17 (Tanzer, et al., 2005). Since related microRNAs are expected to share similar target genes, we

hypothesized that elevated miR-10a levels in pancreatic tumors could be involved in their metastatic behavior.

It is known that many of the 39 mammalian Homeobox genes are regulated by retinoids through retinoic acid response elements (RARE) and miR-10a is located in the 3'genomic region of the well-known RA target HOXB4, in the vicinity of a RARE (reviewed in Mainguy, et al., 2003). Retinoids, that is, retinoic acid (RA) and its derivatives, regulate a wide variety of different biological processes during development. Experimentally applied retinoid agonists and antagonists promote differentiation, inhibit proliferation and accordingly show promise for the prevention and treatment of cancer (Hong, et al., 1997). Retinoid derivatives have been reported to inhibit invasion of breast and hepatocellular carcinoma cells *in vitro* (Wu, et al., 2006; Simeone, et al., 2006). Interestingly, RAR antagonists also seem to have anti-invasive potential, possibly by their inhibitory activity to matrix metalloproteinases (MMPs) (Schoenermark, et al., 1999).

In this study, we investigated the importance of miR-10a in pancreatic cancer metastasis and the possible link with retinoic acid. We demonstrate that miR-10a is involved in the causal mechanism of tissue invasion and metastasis formation in pancreatic cancer. We find that miR-10a is under transcriptional control of RA in pancreatic cancer cells and that two target genes, HOXB1 and HOXB3 are involved in promoting metastatic behavior. Our findings show that both, miR-10a inhibitors and RAR antagonists are effective compounds for targeting metastatic tumor behavior through regulating miR-10a function and expression.

Materials and methods

Animal care and handling

Zebrafish (*Danio rerio*) (Tuebingen line, Alb strain (Albinos) and Tg (fli1:eGFP) were handled in compliance with local animal care regulations and standard protocols of the Netherlands and Germany. Fish were kept at 28°C in aquaria with day/night light cycles (10h dark versus 14h light periods). The developing embryos were kept in an incubator at constant temperatures of 28°C.

Retinoic acid and RA Inhibitors

The selective RARα antagonist Ro-41-5253 was purchased from Biomol International, dissolved in DMSO and cells were treated overnight prior to injections at a final concentration of 200nM (50% inhibition at 60nM) (Keidel, et al., 1994; Bertram, et al., 2005) Retinoic acid (ATRA – all trans retinoic acid, Sigma) was added to cells ON at a final concentration of 1µM.

Cell Culture

Cell lines PaTu8988T, PaTu8898S, AsPC1, Capan1, Capan2, MiaPaCa2, PANC1 and PaTu8902 cells were cultured in DMEM high glucose, with 10% FCS and 1:100 Pen/Strep.

Cell Staining, Injections, Incubations and Antibodies

Cells were stained with CM-Dil (red fluorescence) at a 1:1000 dilution according to the manufacturers' protocol (Vybrant, Invitrogen). Cells were suspended in 67% DPBS for injection into embryos. 2dpf zebrafish embryos were dechorionated and tranquilized with tricaine (Sigma). An injection needle (2.8µm

diameter) with a manual injector (Eppendorf; Celltram Vario) was used to inject cells into the yolk sac of 2dpf zebrafish embryos. Between 100 and 200 cells were injected per embryo. On average 80 embryos were injected in the experiments for each treatment. Presence of cells was checked after 2h incubation at 31°C and embryos were subsequently kept at 35°C. We defined three categories based on the number of migrated cells (<5; between 5-20; and >20). We defined here migration for the two latter categories and percentages given refer to this. All data are shown in Table 2 and Supplemental Table 1. A micrometastasis is defined as a cluster of at least 4 cells in close proximity indicating origin from cell division.

PaTu-S cells were transfected ON with indicated concentrations of miR-10a siRNA in the presence of ICA-Fectin TM442 (Eurogentec, Belgium). Whole cell lysates were prepared 36h post-transfection and 40µg of total lysates were separated on 7.5% PAA-gels and blotted with anti E-cadherin, α-catenin, β-catenin (all mAbs, Transduction Labs) and actin antibodies (mAb Sigma-Aldrich, Germany).

Tissue preparation for transplantation into zebrafish embryos

Human resection specimens were obtained at the Universitätsklinikum Greifswald according to local ethical guidelines and after obtaining informed patient consent. Tumor tissue was cut into small pieces using a scalpel blade. Tissue fragments were then washed with 67% DPBS and stained with 1:500 CM-DiI. Stained tissue fragments of approximately $^1/_5$ to $^1/_2$ the size of the yolk sac were transferred with a glass transplantation needle into the yolk. After 2h at

31°C the embryos were checked that the yolk had sealed itself and the embryos were incubated at 35°C for the remainder of the experiment.

Northern Blot, RT-PCR and quantitative RT-PCR (RT-qPCR)

Northern Blot analysis was performed essentially according to Kloosterman *et al*. (2006) using a miR-10 LNA probe (CACAAATTCGGATCTACAGGGTA) (Exiqon, Denmark). We had previously described protocols for RT-PCR (Ott, et al., 2007) and RT-qPCR (Marques, et al., 2008). Primers for the RT-PCR were: HOXB1: sc-38686 and HOXB3: sc-38690-PR and RARα: sc-29465-PR all from Santa Cruz Biotechnology. For quantitative RT-PCR we used 100 ng of total RNA and the Roche Master SYBR Green kit. Single-band amplification was verified by melting curve dissociation protocols. A standard curve for β-actin using 1, 5, 10, 100, and 500 ng of total RNA was used for normalization. RT-qPCR primers for HOXB1 were: forward 5'-ctccgaggacaaggaaacac-3' and reverse 5'-ccttcatccagtcgaaggtc-3' and for HOXB3: forward 5'-actccaccctcaccaaacag-3' and reverse 5'-ttgcctcgactctttcatcc-3'.

Morpholino knockdown, siRNA expression and Sensor Construct

Morpholino antisense oligonucleotides were obtained from Gene Tools, LLC (OR, USA) and used as previously described (Woltering, 2008). The miR-10a antisense Morpholino sequence is: CACAAATTCGGATCTACAGGGTA. Standard control Morpholino was CCTCTTACCTCAGTTACAATTTATA. Both miR-10a and control morpholinos were fluorescein labeled. The siRNAs for human HOXB1, human HOXB3 and human RARα were purchased from Santa Cruz Biotechnology (HOXB1: sc-38686, HOXB3: sc-38690 and RARα: sc-29465). Endoporter (Gene

Tools, LLC) was used to deliver Morpholinos and siRNAs into cells and efficiencies for Morpholinos were checked by fluorescence microscopy to be >95%. For the miR-10a siRNA, the sense strand corresponds to UACCCUGUAGAUCCGAAUUUGUGUG, The sequence of control siRNA (miR-196a) was UAGGUAGUUUCAUGUUGUUGG and a corresponding antisense sequence). 30 µl of each siRNA oligonucleotide (50µM) were annealed by gradually cooling from 98°C to 20°C in a volume of 75µl annealing buffer (50mM Tris, pH 7.8, 100 mM NaCl RNAse free). The effect of miR-10a Morpholinos on miR-10a function was tested with a sensor construct: pCS2+ EGFP 4x miR-10 AS containing 4 copies of a miR-10a antisense sequence.

Statistical Analysis

Significance between groups was assessed by Student's t-test.

Imaging

Confocal pictures were taken with the Biorad Confocal microscope 1024ES (Zeiss microscope) combined with Krypton/Argon laser, a dual laser scanning confocal microscope Leica DM IRBE (Leica) or with the Nikon TE300 confocal microscope and a coherent Innova 70C laser (Chromaphor, Duisburg, Germany). Pictures were further taken in a differential interference contrast (DIC) microscope (Axioplan 2) with an AxioCam MR5 camera (Carl Zeiss). For fluorescent stereomicroscope images we used a Leica MZ16FA microscope and a Leica DFC 420C camera.

Results

miR-10a expression is elevated in pancreatic tumor cell lines and specimen of chronic pancreatitis and pancreatic tumors.

To evaluate the role of miR-10a in pancreatic tumor cells, we performed northern blot analysis in a series of pancreatic tumor cell lines including PaTu8988-S and PaTu8988-T (Elsässer HP, 1992). (PaTu-S and PaTu-T), and observed expression of this specific microRNA in all but two (PaTu-S and AsPC1) cell lines (Figure 1 A). Expression differences in PaTu-S and PaTu-T cells are interesting as both sister cell lines originate from liver metastases of the same human pancreatic adenocarcinoma (Elsässer HP, 1992) and we and others have previously shown that E-Cadherin expression in PaTu-S cells correlates with the maintenance of functional cell-cell contacts and a reduced tendency of cells to migrate (Menke, et al., 2001; Mayerle, et al., 2005; Marques, et al., 2009) In PaTu-T cells, loss of E-Cadherin is associated with little cell aggregation and enhanced migratory capabilities, which we confirmed in a zebrafish xenotransplantation model (Marques, et al., 2009). These different migratory capacities seem to correlate with an elevated miR-10a expression in PaTu-T cells and a very low expression in PaTu-S cells (Figure 1 A).

We also assessed the expression of miR-10a in resection specimen of 4 pancreatic adenocarcinoma, 4 chronic pancreatitis patients and 2 normal pancreatic tissues and found a ~2.8 fold upregulation of miR-10a expression in all 4 pancreatic tumors in comparison to control pancreatic tissue. In contrast to the previous microarray study (Bloomston, et al., 2007) we also observed increased miR-10a expression in chronic pancreatitis. (Figure 1 B).

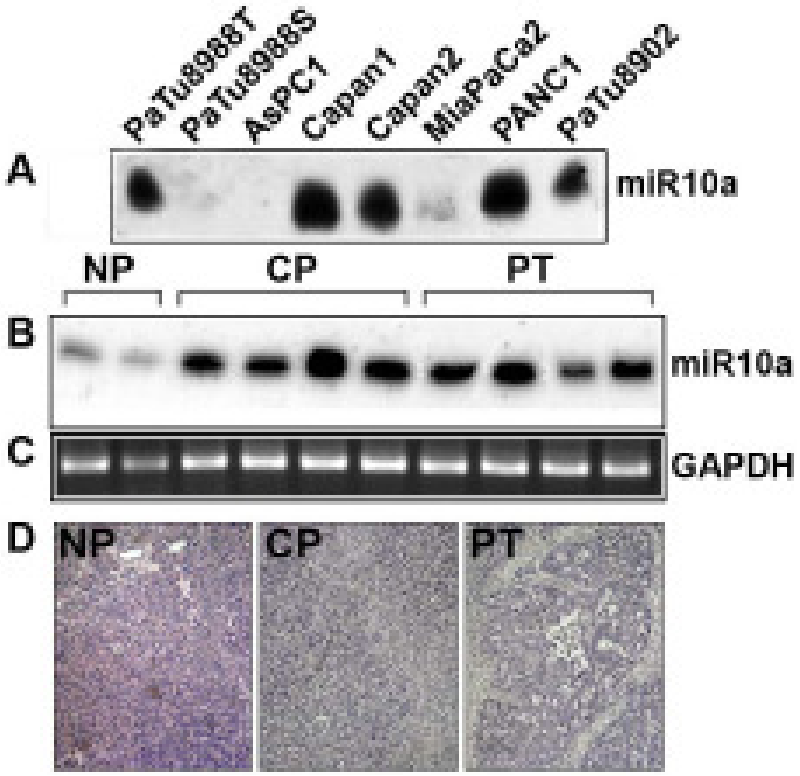

Figure 1 MicroRNA-10a expression in pancreatic tumor cell lines and human specimen of pancreatic tumors or chronic pancreatitis By Northern blot analysis we evaluated miR-10a expression in human pancreatic cancer cell lines (A) and in resection specimen (B) of normal human pancreas (NP), chronic pancreatitis (CP) and pancreatic tumors (PT). Densitometric analysis (Biorad GS800) showed average intensities of 4.2 (+/-0.5) for NP, 11.9 (+/-1.1) for PT and 12.7 (+/-0.6) for CP, suggesting a ~3-fold elevated miR-10a expression in chronic pancreatitis and pancreatic tumor compared to normal pancreatic tissue. Control GAPDH expression, analyzed by RT-PCR of the same RNA samples used in the northern blot, is shown in (C). HE staining of representative histological sections of the utilized human tissue specimen are shown in (D) (NP: normal pancreas, CP: chronic pancreatitis, PT: pancreatic tumor).

miR-10a is required and sufficient for tissue invasion and metastasis formation in pancreatic tumor cells

The zebrafish and its transparent embryos have recently been established as a model system to investigate tumor development (Langenau, et al., 2003; Stoletov, et al., 2007; Park, et al., 2008; Nicoli, et al., 2007). Xenotransplantation in fish is utilized to study invasiveness and metastatic behavior of established cancer cells (Marques, et al., 2009; Stoletov, et al., 2007; Nicoli, et al., 2007; Topczewska, et al., 2006; Nicoli, et al., 2007; Lee, et al., 2005; Haldi, et al., 2006) and of fragments of resected gastrointestinal tumor tissue (Marques, et al., 2009)

To study the role of miR-10a in metastatic behavior, we labeled the pancreatic tumor cell lines with a carbocyanine dye (CM-DiI) and ectopically transplanted them in the yolk sac of 2 dpf zebrafish embryos. As expected, PaTu-S cells remained in the yolk, whereas PaTu-T cells invaded the embryo and showed metastatic behavior (Table 1 and Supplemental Table 1). The expression of miR-10a in these cell lines therefore correlates with their metastatic potential in the zebrafish xenotransplantation model. We further tested 6 additional pancreatic tumor cell lines and find a correlation of metastatic behavior with the presence of miR-10a but not with its absolute levels of expression (Figure 1A and Supplemental table 1).

To investigate the involvement of miR-10a in the metastatic behavior *in vivo*, we performed a loss of function analysis by silencing miR-10a with specific Morpholino antisense oligonucleotides which we previously have demonstrated to work well in silencing miR-10a in the developing zebrafish embryo (Woltering, 2008). More than 95% of cancer cells incorporated the miR-10a Morpholino

(Figure 2 B) and also resection specimen of human tumor tissues showed significant uptake of morpholino (Figure 2 C and D).

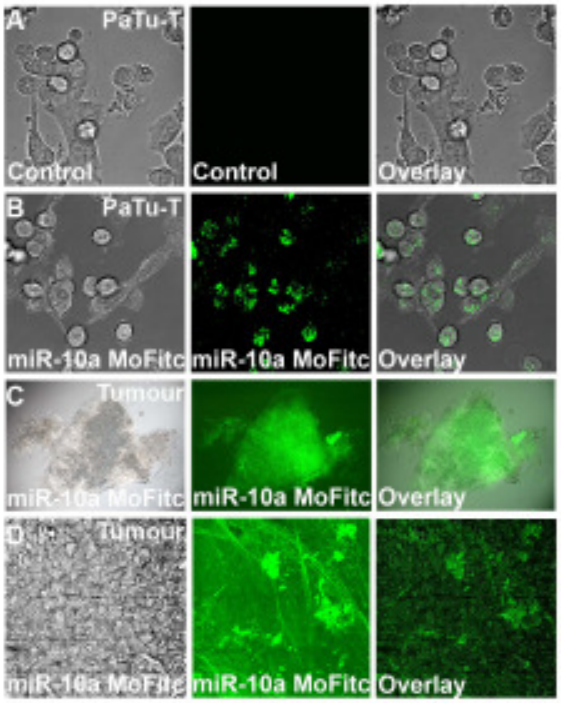

Figure 2 Uptake of miR-10a Morpholino into pancreatic cancer cells and tumor tissue PaTu-T cells (**A-F**) and an ~1 mm long tissue fragment of a human resection specimen of pancreatic tumor (**G-L**) were incubated for 24h in the presence of Endoporter with control Morpholino (**A-C**) or miR-10a-FITC Morpholino (**D-L**). Uptake of FITC-labeled Morpholino was analyzed by confocal microscopy **(B, E, H, K)**. Analysis of bright field (**A, D, G, J**) and overlay images (**C, F, I, L**) demonstrates uptake efficiencies of >95% in PaTu-T cells. Notably significant uptake of Morpholino into cells within the resection specimen was also detected even though exact transfection efficiency could not be determined. No auto fluorescence of tumor tissue was observed (Supplemental Fig. 5).

Expression of an EGFP miR-10a sensor construct, containing 4 miR-10a target sequences in the 3'UTR is repressed by the presence of the endogenous miR-10a in PaTu-T cells (the cell line highly expressing miR-10a) (Figure 3, left panel). Delivery of anti-miR-10a Morpholino to the cells hinders this repression, indicating that miR-10a Morpholinos work well in silencing miR-10a function (Figure 3, right panel).

Targeting endogenous miR-10a with Morpholinos rendered PaTu-T-cells non-invasive and prevented metastatic behavior in zebrafish embryos, whereas a control Morpholino had no such effect (Figure 4 B, Table1 and Supplemental Table 1). Over a three day time course we observed no adverse effects of morpholino treatment on general cell survival (analyzed by propidium iodine (PI) staining - data not shown).

Complementary to this loss of 'metastatic' function, we also performed a gain of function analysis using miR-10a siRNA which can be effectively used to study miR-10a over expression (Woltering, 2008). We transfected PaTu-S cells with miR-10a siRNAs and subsequently transplanted the cells into the yolk sac of 2 dpf embryos. The delivery of miR-10a siRNAs actually conferred invasiveness and metastasis formation to PaTu-S cells (39.2% (SD 7.4)) that were previously non-invasive *in vivo* (Figure 4 C). As a control we used miR-196a siRNAs, which showed no effect on cellular invasion and migration (0.57% (SD 1)) (Figure 4 D, table 1 and supplemental table 1).

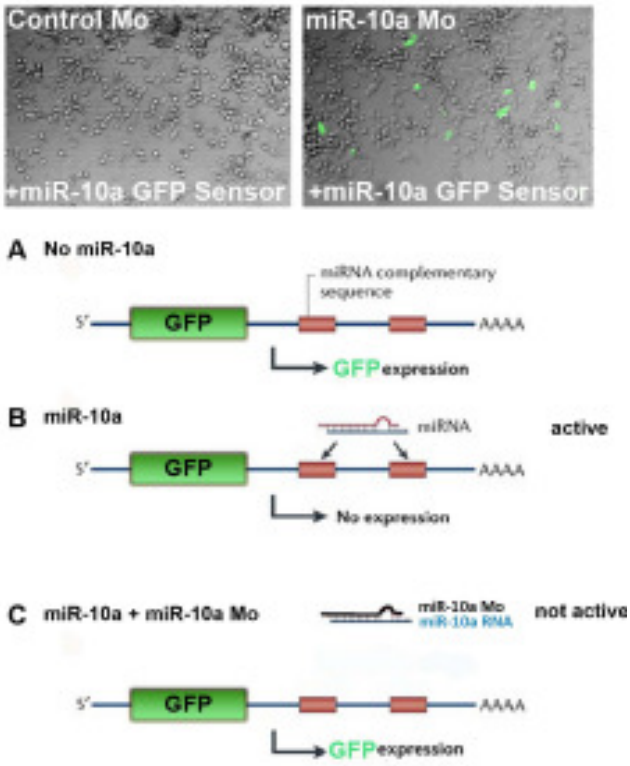

Figure 3: Inhibition of miR-10a function by miR-10a specific Morpholinos in pancreatic cancer cells PaTu-T cells were transfected with a sensor construct containing a green fluorescence protein (GFP) coding sequence followed by multiple miR-10a target sites. As demonstrated in the schematic representation, GFP is expressed from this sensor construct only in the absence of miR-10a (**A**). Due to expression of miR-10a in PaTu-T cells, miR-10a can bind to the 3' target sites and therefore no GFP signal is detected (**B**). This suppressive effect of miR-10a can be released by addition of a specific miR-10a Morpholino which itself targets miR-10a and prevents its binding to the sensor construct (**C**). Following transfection, PaTu-T cells were incubated for 24 h with control or miR-10a Morpholinos and investigated by fluorescence microscopy (upper panel). In contrast to the control cells, fluorescent cells were only detected in miR-10a Morpholino treated PaTu-T cells. A low transfection efficiency of PaTu-T cells is responsible for only limited numbers of fluorescent cells (tested with a GFP-expression construct; data not shown).

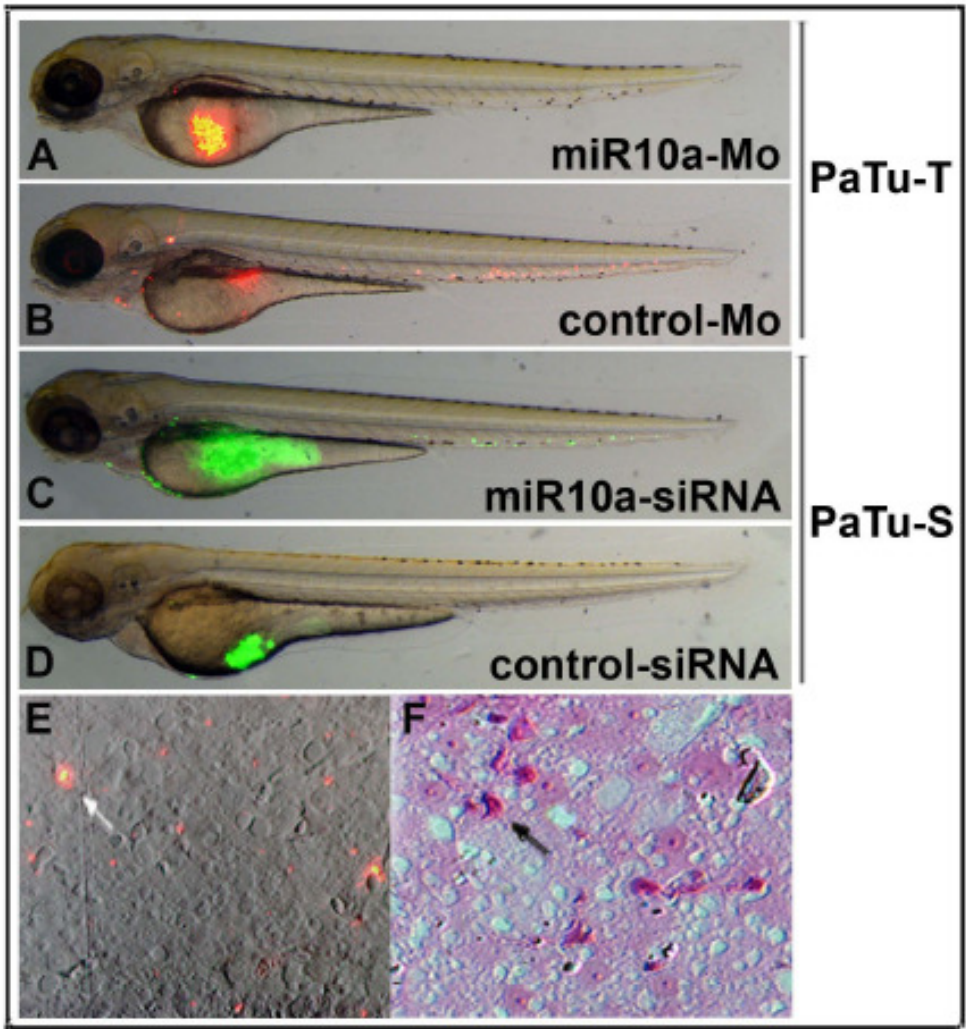
A
miR10a-Mo
B
control-Mo
PaTu-T
C
miR10a-siRNA
D
control-siRNA
PaTu-S
E
F

Figure 4 MicroRNA-10a is required and sufficient for tissue invasion and metastasis formation of pancreatic tumor cells PaTu-T cells were incubated with control and miR-10a Morpholinos, stained with fluorescent CM-DiI and transplanted into the yolk of zebrafish embryos. Blockage of miR-10a by specific Morpholino was found to inhibit migration of PaTu-T cells in xenotransplanted zebrafish (A) whereas PaTu-T cells treated with a control Morpholino still invaded the embryo and formed metastases (B). To determine whether miR-10a is able to induce tissue invasion and migration of non-invasive PaTu-S cells, we incubated the cells with synthetic miR-10a siRNA and, as a control, synthetic miR-196a siRNA (control-siRNA). We observed tissue invasion and migration in miR-10a siRNA (C), but not in control-treated cells (D), which remained in the yolk. Images (A-D) were taken by high resolution fluorescence stereomicroscopy at 3 days post fertilization and 1 day post injection (dpi). The presence of representative tumor cells and micrometastasis at 3 dpi is shown in contrast microscopy pictures overlaid with a fluorescence image (E, F), HE staining (G, I, J) and fluorescence images (H) of transversal sections of zebrafish liver. Arrows point to micrometastasis in the liver.

<u>miR-10a is required for invasion and metastatic behavior of xenotransplanted primary human tumors</u>

We investigated whether miR-10a gene-specific morpholinos could also block metastatic behavior of xenotransplanted primary human tumors. Small fragments of resected tumor tissue were treated with fluorescein labeled miR-10a Morpholinos (miR-10a Mo-FITC) and cellular uptake of miR-10a Mo-FITC was observed (Figure 2 C-D). Treatment of small tumor fragments from three different patients with miR-10a Mo prior to xenotransplantation led to over 90% reduction of invasion and metastatic behavior, when compared to control Mo treated tissue of the same tumor specimen (Table 2 and Supplemental Table 1).

Our results indicate a regulatory function of miR-10a in the metastatic behavior of human pancreatic tumor cells.

miR-10a expression is increased by retinoids and decreased by RAR antagonists in pancreatic tumor cells

To analyze if miR-10a expression is under control of RA signaling in pancreatic cancer, we analyzed miR-10a expression in cells treated either with retinoids or a selective RARα antagonist. Our northern blot data show that miR-10a expression in non-metastatic PaTu-S cells is positively regulated by stimulation with all trans retinoic acid (ATRA) (Figure 5 A and Supplemental Figure 1), whereas a significant decrease in miR-10a expression was observed in the metastatic PaTu-T cells treated with either a selective RARα antagonist (Ro-41-5253; Biomol) or RARα-specific siRNAs (Figure 5 A and Supplemental Figure 1). Using chromatin immune precipitation (CHIP analysis), we identified the DR5 type 10 retinoic acid response element (RARE) as a functional target sequence for RARα binding in PaTu-T cells (but not in PaTu-S cells). This RARE has been previously identified as a mediator of hoxb4 neural expression (Gould, et al., 1998) and thus is likely to regulate miR-10a (Supplemental Figure 2).

RARα inhibition prevents metastatic behavior of pancreatic cancer cells and xenotransplanted tumors

We used the selective RARα antagonist Ro-41-5253; to analyze its anti-migratory activity in an *in vitro* migration assay (“scratch assay”) and in the zebrafish xenotransplantation model, respectively. The RARα antagonist significantly decreased PaTuT-T cell migration in the *in vitro* assay (Figure 5 B) and inhibited

invasion and metastatic behavior in zebrafish embryos (Table 1 and Supplemental Table 1). Similar results were obtained when PaTu-T cells were treated with RARα-specific siRNAs (Supplemental Table 1 and Supplemental Fig. 1). We observed no adverse effects of RARα antagonist treatment on general cell survival (analyzed by propidium iodine (PI) staining or cell cycle distribution (Supplemental Figure 3).

Moreover, we treated small fragments of resected pancreatic tumors specimen with the selective RARα antagonist prior to xenotransplantation into zebrafish embryos. Compared to the DMSO treated control tissue of the same tumor specimen, we observed a strong reduction (> 95%) of invasiveness and metastatic behavior (Table 2 and Supplemental Table 1).

miR-10-a regulates Cadherin/catenin expression

One of the known prerequisites for metastasis is the down regulation of cell-adhesion proteins e.g the proteins that constitute functional cadherin-catenin complexes (Jeanes, et al., 2008). We therefore analyzed if induction of migration in PaTu-S cells by miR-10a specific siRNAs affects expression of E-cadherin, α-catenin and β-catenin. We observed that miR-10a specific siRNAs clearly affected expression of all three proteins, however, to various extents (Figure 5 C). Our results suggest that regulation of metastasis by miR-10a in pancreatic tumor cells involves down regulation of cadherin/catenin proteins which may enable the tumor cell to start migration.

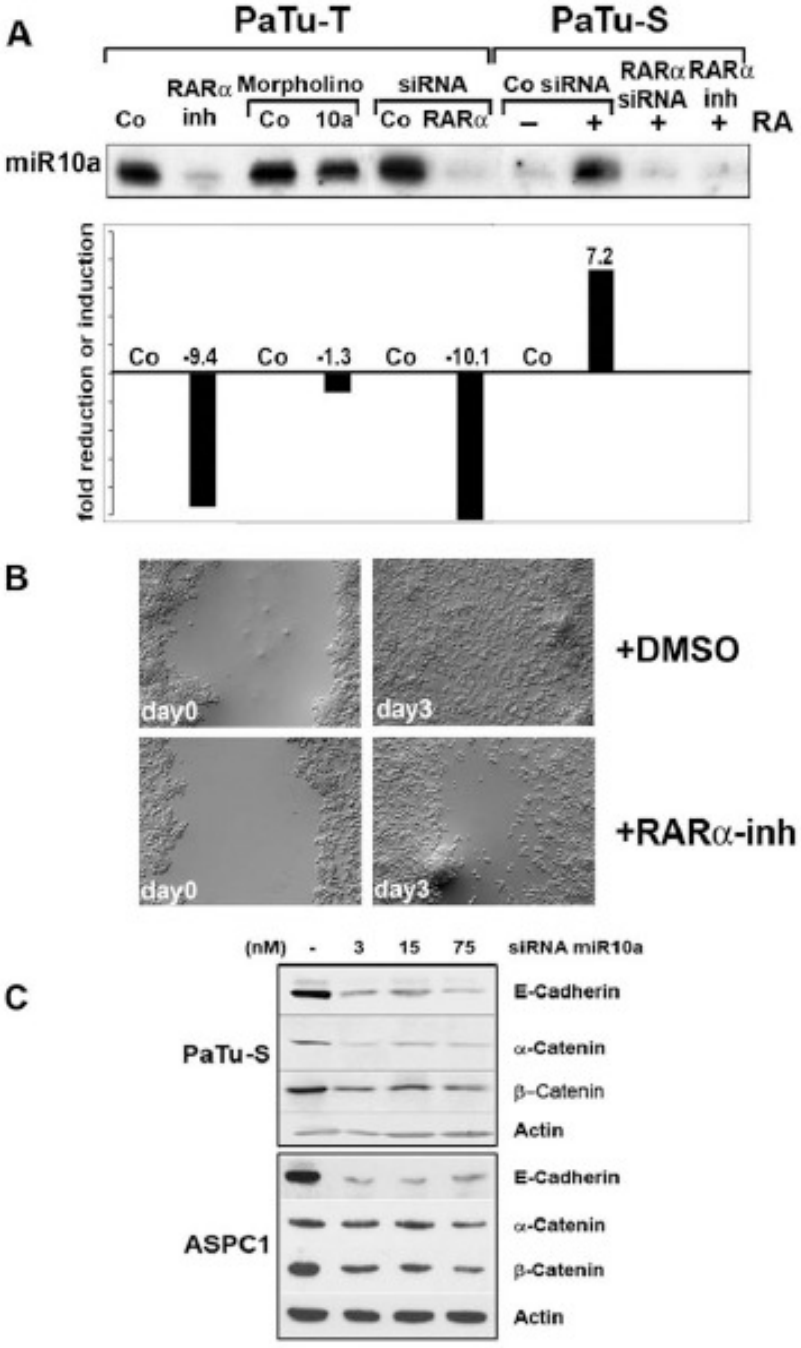
A
PaTu-T
PaTu-S
Co
RARα inh
Morpholino
Co
10a
siRNA
Co
RARα
Co siRNA
–
+
RARα siRNA
+
RARα inh
+
RA
miR10a
fold reduction or induction
Co
-9.4
Co
-1.3
Co
-10.1
Co
7.2
B
day0
day3
+DMSO
day0
day3
+RARα-inh
C
(nM)
-
3
15
75
siRNA miR10a
PaTu-S
E-Cadherin
α-Catenin
β-Catenin
Actin
ASPC1
E-Cadherin
α-Catenin
β-Catenin
Actin

Figure 5: RAR antagonists inhibit miR-10a expression and migration of pancreatic cancer cells PaTu-T cells were incubated, as indicated, with DMSO (Co), 200 nM Ro-415253 (RARα inh), control-Morpholino, miR-10a Morpholino, miR-196 siRNA, or RARα siRNA and PaTu-S cells were co-incubated with 1 μM retinoic acid (RA) and control siRNA, RARα siRNA or Ro-415253 and miR-10a expression was evaluated by Northern blot analysis **(A)**. Densitometric analysis (Biorad GS800) revealed in PaTu-T cells a 9.4 fold reduction of miR-10a expression following Ro-415253 treatment, a 10.1 fold reduction by RARα siRNA treatment and a 1.3 fold reduction following miR-10a Morpholino treatment. In contrast miR-10a expression was upregulated by 7.2 fold in PaTu-S cells following treatment with retinoic acid (1μM final concentration). This upregulation was completely blocked by RARα siRNA or RARα inhibitor. RT-PCR control of GAPDH was used as a loading control (not shown). Dose response curves for RA and the RARα antagonist and the RT-PCR control for RARα siRNA treatment are shown in Supplemental Figure 1. The effect of Ro-415253 on cell migration was analyzed in an in vitro migration assay in PaTu-T cells. Representative images demonstrate significant inhibition of cell migration following Ro-415253 treated in comparison to control (DMSO) cells **(B)**. The regulatory function of miR-10a on expression of proteins of the cadherin catenin complex was demonstrated in PaTu-S cells. Western blot analysis of total lysates of PaTu-S cells (PaTu-T cells as control) showed reduced expression of E-Cadherin, α-Catenin and β-Catenin following treatment with indicated concentrations of miR-10a siRNA (**C**). An actin re-blot confirmed equal loading.

<u>miR-10-a promotes invasiveness and metastatic behavior through suppression of HOXB1 and HOXB3</u>

In the zebrafish we have identified hoxB1 and hoxB3 as conserved downstream targets of the miR-10 family (Woltering, 2008). To investigate whether suppression of HOXB1 and HOXB3 is involved in the observed role of miR-10a in

metastasis formation in human pancreatic cancer we used siRNAs to specifically knock down HOXB1 and HOXB3. Suppression of either HOXB1 or HOXB3 by siRNAs conferred invasiveness and metastasis formation to otherwise non-metastatic PaTu-S cells (Table 1 and Supplemental Table 1). Simultaneous suppression of HOXB1 and HOXB3 resulted in an additive effect (Table 1 and Supplemental Table 1).

To examine whether HOXB1 and HOXB3 expression is required for the anti-metastatic effects of the RARα antagonist, we pre-treated PaTu-T cells with both the RARα inhibitor and HOXB1 and HOXB3 specific siRNAs. Both siRNAs were functional and no transcripts were detectable by RT-PCR (Figure 6 A). The anti-metastatic activity of RARα antagonist was repressed by HOXB1 or HOXB3 suppression in PaTu-T cells (Table 1 and Supplemental Table 1). HOXB1 and HOXB3 suppression had an additive effect and by simultaneous suppression annulled the effects of the RARα antagonist (Table 1 and Supplemental Table 1). PaTu-T cells transfected with HOX siRNA or control siRNA were equally viable as tested by PI staining (data not shown).

By quantitative PCR analysis we could show that RARα antagonist treatment increased HOXB1 and HOXB3 expression in PaTu-T cells and that in contrast RA treatment decreased the expression of both genes in PaTu-S cells (Figure 6 B). These findings correlate with an inverse regulation of miR-10a expression, which is decreased by RARα antagonist and increased by RA stimulation (Figure5 A). Taken together, these results strongly suggest that miR-10a exerts its role in metastasis formation through suppression of HOXB1 and HOXB3.

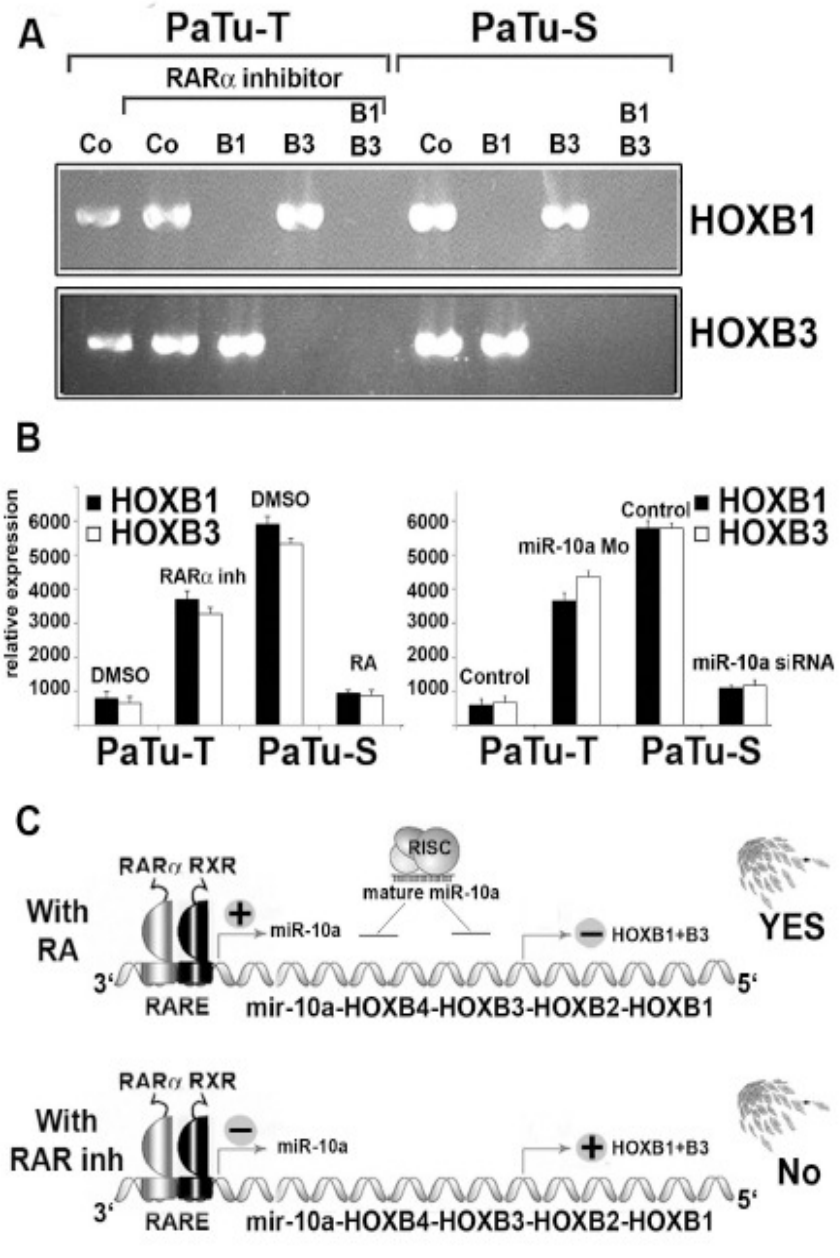
A
PaTu-T
PaTu-S
RARα inhibitor
Co Co B1 B3 B1 B3 Co B1 B3 B1 B3
HOXB1
HOXB3
B
relative expression
HOXB1
HOXB3
DMSO
RARα inh
RA
PaTu-T PaTu-S
Control
miR-10a Mo
miR-10a siRNA
C
RARα RXR
RISC
mature miR-10a
With RA
miR-10a
HOXB1+B3
YES
RARE
mir-10a-HOXB4-HOXB3-HOXB2-HOXB1
With RAR inh
No

Figure 6 Suppression of HOXB1 and HOXB3 confers invasiveness and metastatic behavior PaTu-S and PaTu-T cells were treated as indicated with specific siRNAs against HOXB1 (B1) and HOXB2 (B2) (Co: DMSO control) in presence or absence of Ro-415253 (RARα inh). Migration of these cells was analyzed after transplantation into zebrafish embryos (see Supplemental table 1) and down regulation of HOXB1 and HOXB3 expression in these cells was confirmed by PCR analysis (A). In addition PaTu-S cells were treated with DMSO (control) or with 1 µM ATRA (+RA) and inverse regulation of HOXB1 and HOXB3 expression in response to RARα inh or RA was observed in quantitative RT-PCR (B). Results are normalized to β-actin and similar results were obtained in three independent experiments. The schematic model in (C) summarizes our findings: RA stimulates dimerization of RAR/RXR retinoid receptors which bind to retinoic acid response elements (RAREs) in the regulatory region of miR-10a and triggers increased miR-10a expression. Suppression of HOXB1 and HOXB3 by miR-10a then promotes invasion and metastatic behavior (upper panel). RA stimulation, miR-10a overexpression or suppression of HOXB1 and HOXB3 (by siRNAs) are all sufficient to confer metastatic behavior to these cells. Transcriptional repression of miR-10a by a selective RARα inhibitor (Ro-415253) releases the suppression of HOXB1 and HOXB3 and prevents invasiveness and metastatic behavior (lower panel). The inhibitory function of Ro-415253 can be overruled by a suppression of HOXB1 and HOXB3 with siRNAs.

Discussion

Here, we identified and validated miR-10a as a novel gene with an important function in tissue invasion and metastasis formation. Over expression of miR-10a siRNAs alone suffices to acquire invasiveness and metastatic behavior in otherwise non-metastatic pancreatic cancer cells, whereas silencing miR-10a with gene specific Morpholinos blocks metastatic behavior of metastatic

pancreatic cancer cells and primary human tumors. We demonstrate that specific miR-10a inhibitors can be used to prevent invasion and metastatic behavior even of xenotransplanted resection specimen of human pancreatic tumors in zebrafish embryos. Morpholinos can remain functional for several days (Nasevicius, et al., 2000) and recently "*in vivo* Morpholinos", which are covalently linked to a delivery component, have become available (Gene Tools, LLC).

The early embryos used here (2dpf) do not reject these primary tumor xenografts, due to the fact that their immune system is not fully developed. The major maturation events leading to immune competence occur in the zebrafish between 2 and 4 weeks post fertilization (wpf), coinciding with the larval to juvenile transitory phase (Lam, et al., 2004).

The identification of upstream regulators of miR-10a in pancreatic cancer cells is of importance. We show that miR-10a is regulated by RA signaling in pancreatic cancer cells. Retinoids have been used as chemo preventive and anticancer agents because of their pleiotropic regulator function in cell differentiation, growth, proliferation and apoptosis, however to date limited amount of information on the role of retinoids in metastasis formation is available and nothing is known on the role of RAR antagonists in this process. For pancreatic cancer we clearly demonstrate anti-metastatic properties of RARAα antagonists, which down regulate miR-10a, and therefore may have potential as anti-metastatic drugs. Whether this role of miR-10a and RARs is specific for pancreatic cancer or a common mechanism in other cancer types will need to be determined.

Notably we found upregulated miR-10a expression already in conditions of chronic pancreatitis. It is well recognized that chronic conditions of pancreatitis may represent a risk factor for the development of pancreatic cancer (Lowenfels, et al., 1993). Nevertheless, the route from inflammation to cancer must involve many steps and general observations concerning the risk of pancreatic adenocarcinoma in patients with CP may suggest an accelerated process of mutagenesis and mutation accumulation rather than a unique process. However, the role that miR-10a plays in the progression from chronic pancreatitis to cancer cannot be answered at this time. Upregulation of miR-10a expression could be involved in a more complex regulation mechanism that controls or parallels the malignant transformation of a cell to cancer. miR-10a might regulate additional early steps in tumor progression which are not related to cell migration and additional triggers are necessary for the initiation of the metastatic phenotype that are absent in chronic pancreatitis, but are active in transformed carcinoma cells. It is known that the development of pancreatic cancer from chronic pancreatitis is a slow process and Lowenfels *et al.* (1993) reported a cumulative risk of pancreatic cancer in subjects with CP of 1.8% after 10 years and 4.0%, after 20 years. Future experiments will have to address the specific role of miR-10a in these processes and identification of miR-10a targets in chronic pancreatitis and pancreatic carcinoma might give further insights in these early regulatory mechanisms.

We identified here downstream targets of miR-10a, namely HOXB1 and HOXB3 and the cadherin/catenin complex proteins E-cadherin, α-catenin and β-catenin. Recently, Ma *et al.*, (2007) showed inhibition of metastatic behavior by another microRNA, miR-10b, which is located in the HOXD cluster and targets HOXD10.

This study described suppression of metastatic behavior via a regulatory module consisting of Twist-miR-10b-HOXD10-RHOC [2007]. Upregulated miR-10b expression suppresses translation of HOXD10 and thereby leads to increased expression of the pro-metastatic gene *RHOC* [2007].Our results indicate that both, HOXB1 and HOXB3 also function as metastasis suppressor genes. Whether down regulation of cadherin/catenin proteins is controlled via HOXB1 and HOXB3 or occurs through a parallel signaling pathway of miR-10a will have to be further analyzed. However, our results show that HOX genes can function as metastasis suppressor genes and HOXB1 and HOXB3 and HOXD10 might not be exceptional among the 39 existing mammalian HOX genes.

In summary, we identified miR-10a as a RA responsive mediator of invasiveness and metastatic behavior in pancreatic cancer which promotes its effects through HOXB1 and HOXB3 suppression. Inhibition of miR-10a expression or function represents a promising strategy for anti-metastatic therapy and both RAR antagonists and miR-10a inhibitors could be powerful anti-metastatic compounds.

Acknowledgments

We would like to thank Guido van Roo and Ana Belo for help with FACS and D.N.J. de Witt for taking care of animal welfare. This work was supported by grants from the Portuguese foundation for Science and Technology (SFRH/BD/27262/2006), the Deutsche Krebshilfe (10-2031-Le), (FVMM) University Greifswald and the Alfried-Krupp-Foundation.

References

Jemal A, Siegel R, Ward E, Murray T, Xu J, Thun MJ. (2007) Cancer Statistics. CA: Cancer Journal for Clinicians, 57:43-66.

Johnson SM, Grosshans H, Shingara J, Byrom M, Jarvis R, Cheng A, Labourier E, Reinert KL, Brown D, Slack FJ. (2005) *RAS Is Regulated by the let-7 MicroRNA Family.* Cell 2005;120:635-647.

Esquela-Kerscher A, Slack FJ. (2006) *Oncomirs [mdash] microRNAs with a role in cancer.* Nature Reviews Cancer, 6:259-269.

He L, Thomson JM, Hemann MT, Hernando-Monge E, Mu D, Goodson S, Powers S, Cordon-Cardo C, Lowe SW, Hannon GJ, Hammond SM.(2005) *A microRNA polycistron as a potential human oncogene*. Nature 2005;435:828-833.

Tavazoie SF, Alarcon C, Oskarsson T, Padua D, Wang Q, Bos PD, Gerald WL, Massague J. (2008) Endogenous human microRNAs that suppress breast cancer metastasis. Nature, 451:147-152.

Calin GA, Croce CM. (2006) *MicroRNA signatures in human cancers.* Nature Reviews Cancer;6:857-866.

Lu J, Getz G, Miska EA, Alvarez-Saavedra E, Lamb J, Peck D, Sweet-Cordero A, Ebert BL, Mak RH, Ferrando AA, Downing JR, Jacks T, Horvitz HR, Golub TR. (2005) *MicroRNA expression profiles classify human cancers*. Nature, 435:834-838.

Roldo C, Missiaglia E, Hagan JP, Falconi M, Capelli P, Bersani S, Calin GA, Volinia S, Liu C-G, Scarpa A, Croce CM. (2006) *MicroRNA Expression Abnormalities in Pancreatic Endocrine and Acinar Tumors Are Associated With Distinctive Pathologic Features and Clinical Behavior.* Journal of Clinical Oncology, 24:4677-4684.

Bloomston M, Frankel WL, Petrocca F, Volinia S, Alder H, Hagan JP, Liu C-G, Bhatt D, Taccioli C, Croce CM. (2007) *MicroRNA Expression Patterns to Differentiate Pancreatic Adenocarcinoma From Normal Pancreas and Chronic Pancreatitis.* JAMA, 297:1901-1908.

Ma L, Teruya-Feldstein J, Weinberg RA. (2007) *Tumour invasion and metastasis initiated by microRNA-10b in breast cancer.* Nature, 449:682-688.

Tanzer A AC, Kim CB, Stadler PF. (2005) *Evolution of microRNAs located within Hox gene clusters.* Journal of Experimental Zoology B Molecular and Developmental Evolution, 304:75-85.

Mainguy G, In der Rieden PMJ, Berezikov E, Woltering JM, Plasterk RHA, Durston AJ. (2003) *A position-dependent organisation of retinoid response elements is conserved in the vertebrate Hox clusters.* Trends in Genetics, 19:476-479.

Hong WK, Sporn MB. (1997) *Recent Advances in Chemoprevention of Cancer.* Science, 278:1073-1077.

Wu XZ, Shi P-C, Hu P, Chen Y, Ding S-S. (2006) *N-all-trans-retinoyl-l-proline inhibits metastatic potential of hepatocellular carcinoma cells.* Cell Biology International, 30:672-680.

Simeone A-M, Colella S, Krahe R, Johnson MM, Mora E, Tari AM. (2006) *N-(4-Hydroxyphenyl)retinamide and nitric oxide pro-drugs exhibit apoptotic and anti-invasive effects against bone metastatic breast cancer cells.* Carcinogenesis, 27:568-577.

Schoenermark MP MT, Rutter JL, Reczek PR, Brinckerhoff CE. (1999*) Retinoid-mediated suppression of tumor invasion and matrix metalloproteinase synthesis.* Annuary of the New York Academy of Sciences;878:466-86.

Keidel S, LeMotte P, Apfel C. (1994) *Different agonist- and antagonist-induced conformational changes in retinoic acid receptors analyzed by protease mapping.* Molecular Cell Biology, 14:287-298.

Bertram JS, Vine AL.(2005) *Cancer prevention by retinoids and carotenoids: Independent action on a common target. Biochimica et Biophysica Acta (BBA)* Molecular Basis of Disease, 1740:170-178.

Kloosterman WP, Steiner FA, Berezikov E, de Bruijn E, van de Belt J, Verheul M, Cuppen E, Plasterk RHA. (2006) *Cloning and expression of new microRNAs from zebrafish.* Nucleic Acids Research, 34:2558-2569.

Ott EB, te Velthuis AJW, Bagowski CP. (2007) *Comparative analysis of splice form-specific expression of LIM Kinases during zebrafish development*. Gene Expression Patterns, 7:620-629.

Marques I, Leito J, Spaink H, Testerink J, Jaspers R, Witte F, van den Berg S, Bagowski C. (2008)*Transcriptome analysis of the response to chronic constant hypoxia in zebrafish hearts.* Journal of Comparative Physiology B: Biochemical, Systemic, and Environmental Physiology, 178:77-92.

Woltering JM. (2008) *MiR-10 Represses HoxB1a and HoxB3a in Zebrafish.* PLoS ONE, 3:e1396.

Elsässer HP LU, Agricola B, Kern HF (1992) *Establishment and characterisation of two cell lines with different grade of differentiation derived from one primary human pancreatic adenocarcinoma.* Virchows Archive B Cell Pathology Including Molecular Pathology,61:295-306.

Menke A, Philippi C, Vogelmann R, Seidel B, Lutz MP, Adler G, Wedlich D. (2001) *Down-Regulation of E-Cadherin Gene Expression by Collagen Type I and Type III in Pancreatic Cancer Cell Lines.* Cancer Research, 61:3508-3517.

Mayerle J, Schnekenburger J, Kruger B, Kellermann J, Ruthenburger M, Weiss FU, Nalli A, Domschke W, Lerch MM. (2005) *Extracellular Cleavage of E-Cadherin by Leukocyte Elastase During Acute Experimental Pancreatitis in Rats.* Gastroenterology, 129:1251-1267.

Marques, Weiss FU , Nitsche C, Partecke LI, Heidecke CD, Lerch MM , Bagowski C. (2009) *Metastatic behaviour of primary human tumours in a zebrafish xenotransplantation model*. BMC Cancer, 9:128

Langenau DM, Traver D, Ferrando AA, Kutok JL, Aster JC, Kanki JP, Lin S, Prochownik E, Trede NS, Zon LI, Look AT. (2003) *Myc-Induced T Cell Leukemia in Transgenic Zebrafish*.Science, 299:887-890.

Stoletov K, Montel V, Lester RD, Gonias SL, Klemke R. (2007) *High-resolution imaging of the dynamic tumor cell vascular interface in transparent zebrafish.* Proceedings of the National Academy of Sciences, 104:17406-17411.

Park SW DJ, Rhee J, Hruban RH, Maitra A, Leach SD. (2008) *Oncogenic KRAS induces progenitor cell expansion and malignant transformation in zebrafish exocrine pancreas.* Gastroenterology, 134:2080-90.

Nicoli S, Ribatti D, Cotelli F, Presta M. (2007) *Mammalian Tumor Xenografts Induce Neovascularization in Zebrafish Embryos.* Cancer Research, 67:2927-2931.

Topczewska JM, Postovit L-M, Margaryan NV, Sam A, Hess AR, Wheaton WW, Nickoloff BJ, Topczewski J, Hendrix MJC. (2006*) Embryonic and tumorigenic pathways converge via Nodal signaling: role in melanoma aggressiveness.* Nature Medicine, 12:925-932.

Nicoli S, Presta M. (2007) *The zebrafish/tumor xenograft angiogenesis assay.* Nature Protocols, 2:2918-2923.

Lee, Seftor EA, Bonde G, Cornell RA, Hendrix MJC. (2005) *The fate of human malignant melanoma cells transplanted into zebrafish embryos: Assessment of migration and cell division in the absence of tumor formation.* Developmental Dynamics, 233:1560-1570.

Haldi M, Ton C, Seng W, McGrath P. (2006) *Human melanoma cells transplanted into zebrafish proliferate, migrate, produce melanin, form masses and stimulate angiogenesis in zebrafish.* Angiogenesis, 9:139-151.

Gould A, Itasaki N, Krumlauf R. (1998) *Initiation of Rhombomeric Hoxb4 Expression Requires Induction by Somites and a Retinoid Pathway*. Neuron, 21:39-51.

Jeanes A, Gottardi CJ, Yap AS.(2008) Cadherins and cancer: how does cadherin dysfunction promote tumor progression? Oncogene, 27:6920-6929.

Nasevicius A, Ekker SC. (2000) Effective targeted gene /`knockdown/' in zebrafish. Nature Genetics, 26:216-220.

Lam SH, Chua HL, Gong Z, Lam TJ, Sin YM. (2004) *Development and maturation of the immune system in zebrafish, Danio rerio: a gene expression profiling, in situ hybridization and immunological study.* Developmental & Comparative Immunology, 28:9-28.

Lowenfels AB, Maisonneuve P, Cavallini G, Ammann RW, Lankisch PG, Andersen JR, Dimagno EP, Andren-Sandberg A, Domellof L. (1993)*The International Pancreatitis Study G. Pancreatitis and the Risk of Pancreatic Cancer*. New England Journal of Medicine, 328:1433-1437.

CHAPTER 5

SUMMARY AND DISCUSSION

Animal models have long been used in scientific research, some longer than others. Although in human disease studies, such as cancer, most research is usually done using mouse models, in the last decade a new vertebrate model has emerged. The zebrafish has proved to be very valuable in developmental studies, where its use has been mostly applied. Having a genome 98% similar to humans this small fish from the Indian rivers is nowadays a very common tool to study vertebrate development. In more recent years, the zebrafish started to be used as an animal model to help us better understand several human diseases, from hypoxia to cancer studies, or even immunological studies. In all these studies embryos and larvae, as well as the adult animal, have been used. The advantages of using such a model in human disease studies is becoming more clear as the number of research articles referring to this model increases: the large amount of eggs obtained from a single cross allows for larger sample to be used; the fast development from egg to adulthood (about three months) overcomes the long waiting periods to obtain results that other animal models, such as the mouse, have; the transparency of its embryos and larvae has proven very useful to follow the appearance and development of the disease in real time; finally, the absence of an adaptive immune system, in the early stages of development, circumvents the need to use immunosuppressor drugs, allowing the xenotransplantation of foreign bodies without the risk of rejection.

Along this thesis we demonstrated the value of the zebrafish model in the study of human diseases. We started on **chapter 2** by analyzing what changes occur in the zebrafish heart under chronic constant hypoxia (CCH). It has long been demonstrated that tissue hypoxia may be the result of insufficient blood supply and chronic ischemia. Understanding how teleost fish can withstand chronic

constant hypoxia may prove very valuable to prevent any permanent damage that such condition may cause. In our research we have demonstrated that although zebrafish can survive under CCH, its heart will have morphological and genetic alterations. Such modification may explain how fish adapt to low oxygen levels and how these changes can be used to improve survival and decrease long term effects of hypoxia in mammals. We showed that CCH of zebrafish caused smaller ventricular outflow tract, reduced lacunae and increased cardiac myocyte densities in the heart. Comparatively, in mammals the same type of exposure to hypoxia results in chronic heart failure and loss of cardiac myocytes. If the zebrafish heart responds to hypoxia in a similar manner as to mechanical dissection, this may demonstrate to be very useful in preventing apoptosis of cardiac myocytes, which will help prevent the development of anoxic cores in the cardiac myocytes. But besides the morphological changes that occurs in the heart of the zebrafish under chronic constant hypoxia, we were also interested in the underlying gene expression changes of these adaptations. Through a transcriptome analysis we found several genes were up- or down-regulated under CCH. We found gene regulations in a transcriptional network of the serum response element that were opposed to the ones described in mammals. For example, while c-fos was down-regulated in the zebrafish heart, in mammal studies it has been demonstrated to be up-regulated by hypoxia. We also uncovered novel gene expression changes induced by CCH, such has two notch receptors, whose expression was induced by CCH. Several genes linked to human heart pathology were also found to be up-regulated in this study. An example is the complement component C9 and haptoglobin, two markers for myocardial infarction. We also observed up-regulation of fetuin-α. Low levels of this gene

have been associated with heart failure in mice. Its higher expression levels in the zebrafish heart may help to better tolerate CCH. The changes identified in this study may add to the ability of teleosts to adapt to severe hypoxia. The better we understand how certain animals tolerate hypoxia, the better we can prevent its long term effects, or even use it to cure or control diseases linked to it. With this first study we demonstrated the versatility and resistance of the zebrafish model to withstand extreme conditions.

From the hypoxia study, we then demonstrated, on **chapter 3,** that the zebrafish is a useful *in vivo* animal model for rapid analysis of invasion and metastatic behavior of primary human tumor specimen. We used small explants from gastrointestinal human tumors, which were fluorescently labeled, and investigated their metastatic behavior after transplantation into zebrafish embryos. Using this model, we successfully followed the process of invasion, migration and micro-metastasis formation in real time. We started by implanting two sister human pancreatic cancer cell lines, one with invasive characteristics (PaTu8988t) and the other with a non-invasive behavior (PaTu8988s) into the yolk of the two day old zebrafish. We then followed these cell lines and observed that the cell line with invasive properties did, in fact, dislocate from the site of implantation, intravasated into the blood flow and latter extravasated and invaded distant tissues. These initial experiments validated the worth of our model to study the metastatic properties of human cancer cell lines. We then proceeded to use our model to test whether human tumors transplanted into the zebrafish also displayed metastatic behavior. We were able to establish that the early embryos and larvae used did not reject the primary tumor xenografts, and that cells would come loose from the implanted xenografts, enter the fish

circulation and, within 24h, would appear in distant tissues and organs, forming some micrometastasis, which were observed in histological sections. Furthermore, we investigated the effects of protease inhibitors on the invasiveness of implanted tumor cells and tumor tissue fragments and verified that two different protease inhibitors were able to inhibit invasiveness of the implanted cells and tissues. The panel of experiments performed along this work provided us with valid information for the future development of a screening methodology of drugs to prevent invasion and metastasis formation of human tumors.

We demonstrated here the usefulness of the zebrafish embryos as an *in vivo* model for the analysis of metastatic behavior of human tumor cells. We further established a novel assay in which resected human tumor tissue was successfully implanted into the zebrafish embryo, preserving its intrinsic metastatic ability. We followed *in vivo* and in real time the formation of micrometastasis, without the need to sacrifice the test animal, as it occurs with other mammalian models. And, above all, all of our experimental results could be obtained in a short period of time, avoiding the time consuming experiments that other animal models require. In conclusion, the zebrafish provides us with an advantageous short term model for cancer studies that could complement well established longer term tumor models, such as mouse models, which might be valuable and efficient tools to evaluate novel therapeutic strategies to fight cancer.

After validating the usefulness of the zebrafish model in cancer research, we then applied our model to two real case studies.

On **chapter 4** we used the zebrafish model to demonstrate the effect of retinoic acid receptor antagonists in pancreatic cancer. We identified microsRNA-10a as

an important mediator of metastasis formation in pancreatic tumor cells and proposed a model for its regulatory mechanisms. In a Northern blot analysis we verified that miR-10a expression is increased in pancreatic tumor cells lines and in chronic pancreatitis and pancreatic tumor tissue. Afterwards we implanted our samples of human pancreatic cell lines and human pancreatic tissue (tumor tissue, chronic pancreatitis and normal pancreatic tissue) into the zebrafish embryo to study the invasiveness and metastatic behavior of our samples. After assessing the cancerous properties of our material we investigated what role miR-10a played in the metastatic behavior of our cell lines and tissues. We verified that overexpression of miR-10a siRNA was sufficient for noninvasive cell lines to acquire invasiveness and metastatic behavior. On the other hand, blocking of miR-10a with morpholinos was enough to prevent the metastatic behavior characteristic of some of our cell lines and primary human tumors. Once we proved that miR-10a did indeed play a role in invasion and metastasis in pancreatic cancer, we proceeded to identify its regulators. Upstream, we discovered that miR-10a is regulated by RA signaling in pancreatic cancer cells. It had already been demonstrated that retinoids could be used as anticancer agents due to their pleiotropic regulatory function in cell differentiation, growth, proliferation and apoptosis. In our research we show that RARα antagonists have anti-metastatic properties and that it down-regulates miR-10a, demonstrating its potential as anti-metastatic drugs, at least in the case of pancreatic cancer.

We also found that miR-10a expression was up-regulated in conditions of chronic pancreatitis. It is however well known that chronic conditions of pancreatitis are a risk factor for the development of pancreatic cancer, which could possibly explain the higher expression of miR-10a in these cases. Although, at this time

we could not precise the role of miR-10a in the progression from chronic pancreatitis to pancreatic cancer, we theorized that miR-10a expression could be involved in more complex regulation mechanisms that control or counterparts the malignant transformation of a cell. To better understand the specific role of miR-10a in the formation of pancreatic cancer from chronic pancreatitis and the identification of miR-10a targets in chronic pancreatitis and pancreatic carcinoma, future experiments are required.

Downstream, we found that HOXB1 and HOXB3, as well as the cadherin/catenin complex proteins E-cadherin, α-catenin and β-catenin are targets for miR-10a. Using siRNAs to specifically knockdown HOXB1 and HOXB3, we found that suppression of these genes turned our non-metastatic cell line, Patu8988s, into an invasive and metastatic cell line, demonstrating that these genes function as metastasis suppressor genes. Similar results were previously observed, showing inhibition of metastatic behavior by miR-10b (154).

In view of our results we proposed a model in which suppression of HOXB1 and HOXB3 confers invasiveness and metastatic behavior to pancreatic cancer cell lines: on the one hand, RA stimulates the dimerization of RAR/RXR retinoid receptors, which bind to RAREs, triggering the increased miR-10a expression. This, in turn, suppresses HOXB1 and HOXB3, promoting invasion and metastatic behavior. On the other hand, transcriptional repression of miR-10a by a selective RARα inhibitor, releases the suppression of HOXB1 and HOX3, preventing invasiveness and metastatic behavior. Considering our findings, both RAR antagonists, as well as miR-10a inhibitors could be used as promising anti-metastatic compounds, as part of anti-metastatic therapy.

In conclusion, animals have long been used as models in scientific research, either as test subjects for new therapies against human diseases, or as models to help us better understand disease formation and progression. Vertebrates are the preferred animal model for research associated with human diseases due to their evolutionary proximity to us. The most commonly used animal model is probably the mouse, but in recent years a new model, the zebrafish, started to be used and is becoming more widely accepted as a research model in human disease studies. Through this thesis we demonstrated the usefulness of the zebrafish as a disease model in vertebrates. From its capacity to withstand and survive under hypoxia, which can help us to find newer therapies to revert this condition in humans and, as such, avert its harmful consequences. To the usefulness of the zebrafish in cancer studies, as a time saving model to complement well established models, such as the mouse, which can be rather valuable in evaluating novel therapies to fight tumor formation, progression and metastasis formation. And finally we used our vertebrate model in a case study, where we analyzed the role played by miR-10a in pancreatic cancer.

CHAPTER 6

SAMMENVATING

Proefdieren worden al sinds lange tijd in wetenschappelijk onderzoek gebruikt. Hoewel in studies van menselijke ziekten zoals kanker het meeste onderzoek gewoonlijk wordt gedaan met muismodellen, is er in het laatste decennium een nieuw model opgedoken voor gewervelde dieren, de zebravis. Dit organisme heeft inmiddels een belangrijke plaats gekregen als model in ontwikkelingsstudies. Meer onlangs is dit diermodel een werktuig geworden om een aantal menselijke ziekten te begrijpen zoals kanker of studies aan hypoxia en het immuun systeem. In deze studies worden zowel embryo's, larven en volwassen dieren gebruikt. De voordelen om dit model in menselijke ziektestudies te gebruiken zijn de grote hoeveelheden eieren die te verkrijgen zijn van een enkele kruising dat de mogelijkheid geeft op grotere schaal experimenten uit voeren; de snelle ontwikkeling van ei naar larve verkort de lange wachttijden tijdens experimenten; de doorzichtigheid van embryo's en larven zijn zeer nuttig om de symptomen en ontwikkeling van een ziekte direct te volgen; ten slotte, de afwezigheid van een adaptief immuunsysteem in de vroege stadia van ontwikkeling maakt het mogelijk om, zonder immunosuppressor medicijnen te gebruiken, xenotransplantatie van tumor cellen toe te passen zonder het risico van directe afstoting.

In dit proefschrift is de de waarde van het zebravis model in de studie van menselijke ziekten gedemonstreerd. In hoofdstuk 2 beschrijf ik een analyse van de veranderingen in het zebravis hart onder chronische voortdurende hypoxia (CCH). Een begrip van hoe in een teleost vis chronische voortdurende hypoxia kan worden weerstaan kan mechanismen aantonen die permanente schade als gevolg hiervan voorkomen. Wij hebben gedemonstreerd dat hoewel zebravis onder CCH kan overleven, het hart morfologische en genetische veranderingen

ondergaat. Wij toonden aan dat CCH in zebravis kleinere ventriculaire uitloop zones, verminderde lacunes en toegenomen hartmyocyt dichtheden in het hart veroorzaakt. Vergelijkend in zoogdieren resulteerd hetzelfde soort blootstelling aan hypoxia in chronische hartstilstand en verlies van hartmyocyten. Maar behalve de morfologische veranderingen die in het hart van de zebravis onder chronische voortdurende hypoxia gebeuren, waren wij ook in de onderliggende genexpressieveranderingen van deze aanpassingen geïnteresseerd. Door een transcriptoom analyse vonden wij diverse genen die geïnduceerd of gerepresseerd zijn onder CCH condities. Wij vonden genregulatie in een transcriptioneel netwerk van het serumreactieonderdeel die in tegenstelling zijn zoals beschreven in zoogdieren. Wij onthulden ook veranderingen van genexpressie die door CCH zijn aangezet die nog niet eerder zijn beschreven, bijvoorbeeld de verandering van expressie van twee notch receptoren. Enkele genen verbonden met menselijke hartpathologie bleken ook geïnduceerd in deze studie te zijn. Een voorbeeld is het complement component C9 en haptoglobin, twee kenmerkenvoor myocardiaal infarct. Wij hebben ook een inductie van fetuin- α waargenomen. Lage niveaus van dit gen zijn geassocieerd met hartstilstand in muizen . Het hogere expressie niveau van fetuin- α in het zebravis hart kan mogelijk een hoger tolerantie niveau van CCH bewerkstelligen. De veranderingen die we in deze studie hebben geïdentificeerd zijn mogelijk belangrijk voor het vermogen van teleosten om zich aan strenge hypoxia aan te passen. Hoe beter wij begrijpen hoe bepaalde dieren zich aan hypoxia aan kunnen passen des te beter kunnen wij strategieën ontwikkelen om de lange termijn effecten te voorkomen of om hiermee gerelateerde ziekten te genezen.

Met deze eerste studie demonstreerden wij de veelzijdigheid en weerstand van het zebravis model om extreme hypoxia omstandigheden te weerstaan.

Vervolgens demonstreerden wij in hoofdstuk 3, dat de zebravis een nuttig in vivo diermodel is voor de snelle analyse van invasie en metastatisch gedrag van menselijke tumor monsters. Van kleine explantaten van menselijke tumoren uit de maag, die fluorescerend gemerkt waren, hebben wij het metastatisch gedrag na transplantatie in zebravis embryo's onderzocht. Wij volgden met succes het proces van invasie, migratie en micro-metastaseformatie direct tijdens het plaatsvinden van dit proces. Wij zijn begonnen met het implanteren van twee verwante menselijke pancreas kankercellijnen, één met invasieve kenmerken (PaTu8988t) en de andere met een niet-invasief gedrag (PaTu8988s), in de dooier van de twee dagen oude zebravis larven. De geïmplanteerde cellen werden dan gevolgd voor drie dagen. Wij merkten op dat de cellijn met invasieve eigenschappen inderdaad verplaatst van de positie van implantatie, intravaseerd in de bloedstroom en binnendringt in afgelegen weefsels. Deze eerste experimenten valideerden ons model als een nuttig werktuig om de metastatische eigenschappen van menselijke kankercellijnen te bestuderen. We hebben vervolgens ons model gebruikt om te testen of menselijke tumors die in de zebravis zijn getransplanteerd ook metastatisch gedrag vertoonden. Wij konden bevestigen dat de vroege embryo's en gebruikte larven de voornaamste tumor xeno-implantaten niet hadden afgestoten, en dat die cellen van de geïmplanteerde xeno-implantaten waren losgekomen, de vis bloedsomloop binnen zijn gegaan en binnen 24 uur in afgelegen weefsels en organen zijn verschenen De micrometastase van een aantal van deze cellen kon op histologisch niveau worden waargenomen. Verder hebben wij de resultaten van

toediening van protease remmers op de indringing van implanteerde tumorcellen en tumorweefselfragmenten onderzocht en dit bevestigde dat twee verschillende protease remmers invasie van de geïmplanteerde cellen en weefsels konden voorkomen. Het scala van experimenten die uitgevoerd zijn met dit xeno-transplantatie systeem heeft ons voorzien van belangrijke informatie die kan worden gebruikt voor het opzetten van een snelle testmethode voor medicijnen die invasie en metastaseformatie van menselijke tumors kunnen voorkomen. Wij demonstreerden hier het nut van de zebravis embryo's als een *in vivo* model voor de analyse van metastatisch gedrag van menselijke tumorcellen. De kracht van dit model is onder andere dat we direct de formatie van micrometastase kunnen onderzoeken zonder de noodzaak om het testdier te offeren, zoals vaak met zoogdiermodellen gebeurt. Bovenal kunnen experimentele resultaten in een korte tijdsperiode worden verkregen en is daarmee tijdsbesparend vergeleken met andere diermodellen.

In hoofdstuk 4 gebruikten wij het zebravis model om het effect van retinoic acid receptorantagonisten in pancreaskanker te demonstreren. Wij hebben microRNA 10a geidentificeerd als een belangrijke bemiddelaar van metastaseformatie in pancreastumorcellen en hebben een model voor zijn regulerende mechanisme opgesteld. Wij bevestigden dat miR-10a expressie in pancreastumorcellijnen en in chronische pancreatitis en pancreastumorweefsel is toegenomen. Daarna implanteerden wij onze monsters van menselijke pancreascellijnen en menselijke pancreasweefsels (tumorweefsel, chronische pancreatitis en normaal pancreasweefsel) in de zebravis embryo's om de invasie en metastatisch gedrag van onze monsters te bestuderen. Nadat we de kankervormende eigenschappen van ons materiaal hadden bepaald, onderzochten wij wat voor rol miR -10a in

het metastatische gedrag van onze cellijnen en weefsels speelde. Wij bevestigden dat overexpressie van miR-10a siRNA voldoende was voor niet invasieve cellijnen om invasief en metastatisch gedrag te verwerven. In een tegenovergestelde aanpak bleek het belemmeren van miR-10a met morpholino's voldoende om het metastatische gedragkenmerk van een aantal van de cellijnen en voornaamste menselijke tumors te voorkomen. Zodra wij hadden bewezen dat miR-10a inderdaad een rol in invasie en metastase in pancreaskanker kan spelen, hebben wij ons vervolgens gericht op de identificatie van regulators van dit microRNA. Stroomopwaarts ontdekten wij dat miR-10a door een retinoic acid signaal in pancreaskankercellen geregeld wordt. Er was reeds gedemonstreerd dat retinoic acid derivaten als antikanker middelen zouden kunnen worden gebruikt, ten gevolge van hun pleiotrope regulerende functie in celdifferentiatie, groei, vermenigvuldiging en apoptose. In ons onderzoek tonen wij aan dat RARα antagonisten anti-metastatische eigenschappen hebben en dat het miR-10a expressie represseerd, daarmee zijn potentieel als anti-metastatisch medicijn demonstrerend, tenminste met betrekking tot pancreaskanker.

Wij vonden ook dat miR-10a expressie geïnduceerd was onder condities van chronische pancreatitis. Het is echter goed bekend dat chronische omstandigheden van pancreatitis een risicofactor voor de ontwikkeling van pancreaskanker zijn, en dit zou daarom misschien de hogere expressie van miR-10a in deze gevallen kunnen verklaren. Hoewel, wij momenteel niet de nauwkeurige de rol van miR-10a in de vooruitgang van chronische pancreatitis naar pancreaskanker kunnen analyseren, bediscussieerden wij dat miR-10a expressie betrokken is bij complexe regelmechanismen die de kwaadaardige transformatie van een cel controleren.

Stroomafwaarts vonden wij dat HOXB1 en HOXB3 evenals de cadherin/catenin complex eiwitten E-cadherin , α-catenin en β-catenin doelen voor miR-10a zijn. Met behulp van siRNAs om specifiek HOXB1 en HOXB3 uit te schakelen, vonden wij dat onderdrukking van deze genen in de gebruikte niet-metastatisch cellijn, Patu8988s, resulteerde in een invasieve en metastatische cellijn. Dit demonstreert dat deze genen als metastase suppressor genen functioneren. Soortgelijke resultaten zijn al in eerdere studies opgemerkt, die ook de remming van metastatisch gedrag door miR-10b aangetoond hebben (referentie 154).

Dankzij onze resultaten konden wij een model opstellen waarin onderdrukking van HOXB1 en HOXB3 invasief en metastatisch gedrag verleent aan pancreaskankercellijnen: retinoic acid stimuleert de dimerisatie van RAR/RXR retinoid receptoren, die aan RAREs binden, en daarmee een toename vanmiR-10a expressie bewerkstelligen. Dit onderdrukt op zijn beurt HOXB1 en HOXB3, die invasie en metastatisch gedrag bevorderen. Aan de andere kant zorgt transcriptionele repressie van miR-10a door een selectieve remmer ervoor dat de onderdrukking van HOXB1 en HOX3 wordt opgeheven en voorkomt hierdoor invasief en metastatisch gedrag. Als conclusie van dit onderzoek kunnen we vaststellen dat beide RAR antagonisten evenals miR-10a remmers als veelbelovende anti-metastatische stoffen gebruikt kunnen worden, als deel van een anti-metastatische therapie.

Ter afronding, proefdieren zijn lang als modellen in wetenschappelijk onderzoek of als testonderwerpen voor nieuwe therapieën tegen menselijke ziekten gebruikt om ons beter te helpen om ziekteontwikkeling en ziekteprogressie te begrijpen. Gewervelde dieren zijn het meest geschikte diermodel voor onderzoek aan menselijke ziekten omdat zij sterker verwant zijn aan de mens

dan bijvoorbeeld insecten en wormen die ook voor biologisch onderzoek gebruikt worden. Het meest gebruikelijke diermodel is vermoedelijk de muis, maar in recente jaren heeft een nieuw model, de zebravis zijn intrede gedaan en dit wordt inmiddels ruim erkend als een belangrijk onderzoeksmodel in menselijke ziektestudies. In dit proefschrift heb ik het nut gedemonstreerd van de zebravis als een ziektemodel voor gewervelde dieren. We hebben gebruik gemaakt van zijn capaciteit om extreme condities van hypoxia te doorstaan en te overleven, en dit kan ons helpen om nieuwe therapieën te vinden om in mensen de schadelijke gevolgen af te weren. Vervolgens is de aandacht gegaan naar het nut van de zebrafish in kankerstudies als een tijdsbesparend model om goed gevestigde modellen, zoals de muis, aan te vullen en dat zeer waardevol kan zijn in het ontwikkelen van nieuwe therapieën om tumorformatie, vooruitgang en metastaseformatie te bestrijden. Ten slotte gebruikten wij ons gewerveld model in een casestudy, waar wij de rol analyseerden die door miR-10a in pancreaskanker wordt gespeeld.

PUBLICATIONS AND CURRICULUM VITAE

Publications

Weiss FU, **Marques IJ**, Woltering JM, Vlecken DH, Aghdassi A, Partecke LI, Heidecke CD, Lerch MM, Bagowski CP. 2009. *Retinoic acid receptor antagonists inhibit miR-10a expression and block metastatic behavior of pancreatic cancer.* Gastroenterology. 137(6):2136-45

Marques IJ, Weiss FU, Vlecken DH, Nitsche C, Bakkers J, Lagendijk AK, Partecke LI, Heidecke CD, Lerch MM, Bagowski CP. 2009*. Metastatic behaviour of primary human tumours in a zebrafish xenotransplantation model.* BMC Cancer. 9:128

Ott I, Qian X, Xu Y, Vlecken DH, **Marques IJ**, Kubutat D, Will J, Sheldrick WS, Jesse P, Prokop A, Bagowski CP.2009*. A gold(I) phosphine complex containing a naphthalimide ligand functions as a TrxR inhibiting antiproliferative agent and angiogenesis inhibitor.* J Med Chem52(3):763-70

Marques IJ, Leito JT, Spaink HP, Testerink J, Jaspers RT, Witte F, van den Berg S, Bagowski CP. 2008*. Transcriptome analysis of the response to chronic constant hypoxia in zebrafish hearts*. J Comp Physiol B178(1):77-92.

Ott EB, Sakalis PA**, Marques IJ**, Bagowski CP.2007*. Characterization of the Enigma family in zebrafish*. Dev Dyn. 236(11):3144-54

te Velthuis AJ, Ott EB**, Marques IJ**, Bagowski CP.2007*. Gene expression patterns of the ALP family during zebrafish development*. Gene Expr Patterns. 7(3):297-305

van der Meer DL**, Marques IJ**, Leito JT, Besser J, Bakkers J, Schoonheere E, Bagowski CP.2006. *Zebrafish cypher is important for somite formation and heart development.* Dev Biol; 299(2):356-72

Curriculum vitae

Inês João dos Santos Marques was born on July 8, 1980 in Lisboa, Portugal. She attended high school in Escola Secundária do Pragal. In 1998 she started the study of Biology at Faculdade de Ciências da Universidade de Lisboa (FCUL). From October 2002 to May 2003 she did a research internship on the response of red fox to feral cat presence, in the wood of Valdelatas, under the supervision of Dr. Javier de Miguel, at Universidad Autonoma de Madrid (UAM). In July 2003 she obtained her Licenciatura in Biology. She entered the Master program of Animal Biology at Leiden University in January 2005. Her first master project focused on the role of PDZ proteins in zebrafish development. The second master project focused on the effects of chronic constant hypoxia on zebrafish. Both projects were supervised by Dr. Christoph Bagowski. On September 2006 she obtained her MSc diploma *cum laude*. From October 2006 until December 2010 she worked as a PhD student under the initial supervision of Dr. Christoph Bagowski and afterwards of Prof. Michael Richardson and Prof. Herman Spaink.